International Journal of Engineering Research and Applications (IJERA) ISSN: 2248-9622
National Conference on Advances in Engineering and Technology
(AET- 29th March 2014)

RESEARCH ARTICLE OPEN ACCESS

Critical Gap Comparison between HARDERS and "INAFOGA" Methods for U-Turn Median Openings

Suprabeet Datta*
*(Department of Civil Engineering, National Institute of Technology Rourkela, Odisha-769008
Email: dattasuprabeet@gmail.com)

ABSTRACT
Unsignalized median openings are been installed every day on divided arterials at most of the developing cities in India during the past few years because of the non-accommodation of U-turn movements at unsignalized intersections. Studies of U-turn Gap Acceptance had been neglected under Indian traffic. In this paper, Critical gap has been used as the sole parameter for gap acceptance. Estimation of critical gaps for U-turns at median openings under mixed traffic conditions have not been addressed till today due to the complex and risky traffic interactions at these facilities. Video image processing of 4 U-turn median openings were done to extract the decision variables of the study. For the first time a new concept of merging behaviour of U-turn vehicles for evaluation of gaps by drivers has been introduced here. Two empirical methods namely Harders and Satish et al. "INAFOGA" are used for estimating critical gap considering four motorized modes of transport for all the four sections. Bar comparison plots for all four sections are drawn to compare the methods considering the four motorized modes. A paired sample T-test was done in IBM SPSS 22.0 which revealed that "INAFOGA" method yield critical gap values 28-41% more than those obtained by Harders method. This explained the effectiveness of "INAFOGA" method in judging mixed traffic conditions for U-turns at median openings**.**
Keywords **-** critical gap, gap acceptance, Indian traffic, median openings, SPSS, U-turns, unsignalize

I. INTRODUCTION

For the few years there has been increased installation of non-traversable & directional medians all over India particularly in sub-urban cities on arterial highways. As a part of traffic management to improve intersection operation, some traffic movements are not permitted at selected intersection locations, especially along divided arterials. In most cases, such minor movements are accommodated at separate U-turn median openings. This increased installation reflects the much needed attention towards Access Management [1] [2]. One of the best ways of accessing roads is by installing non-traversable and un-signalized median openings [1] [3]. The purpose of using non-traversable and directional median openings is to eliminate problems associated with left-turns and crossing movements at intersections on multi-lane highways [2] [3] [4]. At un-signalized median openings vehicular interactions are extremely complex [5] [6]. Thus, a U-turning vehicle driver needs to accept a gap or time span between the arrivals of successive vehicles on the through street after it has arrived at a close vicinity of the median opening. This defines the phenomenon of "Gap Acceptance" for median openings. Conventionally, Gap is defined as the time or space headway between two successive vehicles in the through traffic stream [7] [8] [9]. Gap differs from headway in the fact that the latter is measured as a time span between front bumpers of two successive vehicles whiles the former as the time length between back bumpers/wheel bases. "Gap acceptance" analysis forms the prime objective for safe operation of U-turning vehicles at Median Openings under heterogeneous traffic situations.

Critical gap is an important parameter in "gap acceptance" study. The definition of critical gap has undergone certain modifications over the past decades [10]. In [11], authors defined the critical gap as the size of the gap whose number of accepted gaps shorter than it is equal to the number of rejected gaps longer than it. In [12], authors presented critical gaps as "Critical Headway" and defines "as the minimum time interval in the major street traffic stream that allows intersection entry for one minor-street vehicle". Regarding the above definition we tried to define "Critical Gap" for U-turns at median openings as "the minimum time interval in between two through/conflicting traffic vehicles that allows complete merging manoeuvre for one U-turn vehicle at a median opening". Critical gap is difficult to measure directly in field. The measurement varies for different drivers and with time instants depending upon manoeuvres of the U-turn vehicles under mixed traffic conditions prevailing on the median openings [10] [11] [13]. There are a bunch of useful estimation procedures for determination of critical gap

corresponding to homogeneous traffic conditions. Some of the estimation procedures are empirical whereas rest have a strong theoretical background [11] [16]. In this paper some of the previous estimation techniques are used to estimate critical gaps for various modes of U-turning vehicles willing to merge with the through traffic stream at un-signalized median openings.

Bhubaneshwar is the capital of the Indian state Odisha. It constitutes of an average population of 1.2-1.4 million people as per the 2011 census [14]. The city of Bhubaneswar comprises of wide roads in grid form inside the central city. Bhubaneswar has approximately 1,600 kilometres (990 mi) of roads, with average road density of 11.82 square kilometres (4.56 sq. m) [15]. Due to the presence of a wide stretch of divided highways, the city consists of a fair amount of unsignalized median openings which focused our attention towards this area for our study

Gap acceptance analysis for median openings under heterogeneous traffic conditions has not been given proper attention in the previous years. Neither the global traffic engineering manual HCM even in its recent issue of 2010 had addressed the gap acceptance study for median openings. The obvious reason being the complex and haphazard behaviour caused by U-turn vehicles under mixed traffic situations compared to other movements like right turns/left turns at intersections [10] [17]. In this paper, an effort has been made to estimate critical gaps for different U-turning modes prevailing on the median openings in India which would further instigate to understand the gap acceptance concept under mixed traffic conditions.

II. STUDIES IN THE PAST

A large population of researchers have worked on "gap acceptance" during the past few decades, but majority of them considered homogeneous traffic flow conditions. Several techniques or models have been established since the year of 1947 in literatures to estimate "critical gap" as closely as possible [10] [11] [16]. Thus, it is clear that literatures regarding gap acceptance phenomenon is rich. Majority of literatures normally consider the accepted and rejected gaps as the key parameters in estimation of critical gaps [7] [16] [18]. "HCM 2010" states that critical headway/gap can be estimated on the basis of observations of the largest rejected and smallest accepted gap corresponding to a given transportation facility [12].

In [16], author proposed the term "critical lag" as an important parameter in the determination of "gap acceptance" for a minor street driver willing to take a directional movement in an "un-signalized intersection". Author also defined it as the gap/lag for which the number of accepted lags shorter than it is equal to the number of rejected lags longer than it and proposed a graphical model in which two cumulative distribution curves related to the no. of accepted and rejected gaps intersect to yield the value of Critical Lag (Tl). In [19], author corrected the Raff's model and concluded that it gave suitable results for light-to-medium traffic but is not acceptable in heavy traffic conditions. The author also verified that the model gives satisfactory results for "gaps" as that obtained for "lags". This means "critical gap" can also be obtained by the method. Simulation study was used to generate artificial data and comparison was based on the central value estimated by each method. They found that Ashworth's method and maximum likelihood technique gave satisfactory results [16] [19]. A model of estimated length of time gap needed by a U-turn driver based on driver's Age, Gender and the elapsed time between arriving and experiencing the gap is proposed in [5]. The study related driver-related factors on critical gap acceptance whose data were obtained by analysing 4 Median U-turn openings.

In [16], authors estimated the average Critical Gap (Tc,avg) from the Mean and Standard Deviation of gaps accepted by a driver through an empirical mathematical relation with the through traffic volume in vehicles per second assuming exponential distribution of accepted gaps. In [11] [19] 20], authors estimated the critical gap (Tc) by the expectation of the cumulative frequency distribution curve [Fc (t)] for the proportion of accepted gaps of size i, provided to all U-turning vehicles. A more precise form of Maximum Likelihood Method with a satisfactory mathematical derivation and used Log-Normal distribution for finding the critical gaps (Tc) [17] [21].

In [10], authors used some of the existing methods like HARDER, Logit, Probit, Modified Raff and Hewitt methods for estimation of critical gap at un-signalized intersections [10]. There was significant variation (12-38%) among the values which highlighted the incapability of the methods to address mixed traffic situations. Thus, they came up with an alternate procedure making use of clearing behaviour of vehicles in conjunction with gap acceptance data [10]. The "clearing behaviour" was converted to "merging behaviour" in case of U-turns at median openings in this study.

This critical review of the previous literatures instigates the need for evaluation of critical gaps for U-turning vehicles at median openings under heterogeneous traffic situations prevailing in Indian states.

III. MIXED TRAFFIC PROBLEMS IN INDIA

Estimation of critical gap under mixed or heterogeneous traffic situations is more complex than

that under homogeneous traffic conditions. The different types of vehicles found in India and many other developing countries have varying operational characteristics such as speed, maneuverability, effective dimensions, power-weight ratio and response to the presence of other vehicles in the traffic stream [10]. Smaller size vehicles often squeeze through any available gap between large size vehicles and move into the influence area in haphazard manner [5] [6]. A single gap in the through traffic stream can be accepted by more than one vehicle moving parallel to each other and after crossing the conflicting traffic these vehicles move in a single file, after one another [10]. The combined effect of all these factors makes the estimation of critical gap a more challenging task. These situations require a re-look into the concept of critical gap & conflict area near median openings and method of data extraction.

IV. STUDY AREA DETAILS

The area of study can be broadly classified based on the necessity of data for analyzing "Critical Gap" and comparing the same between different modes of transport as shown in Fig 2. Two types of median openings prevail in INDIA. First one being on a typical 4-lane divided highway and the second one on a 6-lane divided street. Median openings are provided in urban areas for minimum major street flow of 500 vehicles/day having a maximum speed limit of 70-80 kmph (40 miles/hr.).

Bhubaneswar being the capital of Odisha consists of a broad network of roadways on which mixed traffic is dominant. Some of the motorized modes include 3 wheelers like four-stroke Auto-rickshaws and pick-up vans, light commercial vehicles which includes 4 wheeler tempos, variable categories of cars namely Sedans and Hatchbacks, Sports utility or Multi-utility vehicles (SUVs/ MUVs). About 4 different sections of median openings on 4-lane divided highways having 75-90 % of U-turning vehicles were selected for the study. All the sections involved with the case study for Bhubaneswar varied in their geometry. Assumptions were made regarding the geometrical variations for individual sections. Each median opening selected for the study were spaced about 600-700 feet apart from their near unsignalized intersections as per the stipulations in HCM 2010.

4.2. Data Collection Details

Data collection primarily comprised of video recording of the selected median openings by a Sony Handycam capable of playing videos at a frame rate of 30 frames/second during the months of January, March, April and September. Peak hours of U-turns were surveyed and video shooting was done for the morning, noon and afternoon sessions depending on the importance of the days. Shooting was done only during weekdays. Weekends and public holidays were generally neglected due to variation of U-turning traffic at median openings. Video recording of all the 4 sections resulted in an average proportion of U – turning and through traffic of 70-90% and 65-85% respectively. All of these 4 sections are median openings on 4-lane divided roads. Through traffic volume comprised of all types of vehicles including HVs, LCVs excluding non-motorized vehicles and pedestrians. Classes of U-turning vehicles considered are as pointed below:

1. Motorized 4 Wheelers (Including Sedan and Hatch Backs)
2. Motorized 2 Wheelers (Driver: Male / Female , Motor-bikes , Scooters)
3. Motorized 3 Wheelers (4-stroke-Auto-rickshaws , 3W Pick-up vans)
4. Sports utility vehicles / multi utility vehicles (SUVs)

The variation of U-turning flow with respect to through or conflicting traffic volume can graphically represented as a cumulative distribution in PCU/hr. The conversion from no. of vehicles to their corresponding Passenger car equivalents was done according to Table 1 adopted from IRC: 86-1983 (Geometric Design Standards for Urban Roads on Plains). Fig 1 shows the distribution of U-turn flow for the 4 different sections with respect to the increasing through traffic volume in PCU/hr. with increase in through traffic volume there is an exponential or power decrease in U-turn traffic gap acceptance.

Table 1: Passenger Car Equivalents (PCU) for Flow Calculation as per IRC: 86-1983

Serial Nos.	Vehicle Types	PCU Equivalents
1.	Car, LCV,3W,SUV	1.0
2.	HV like truck,bus,lorry	3.0
3.	2W(motor-bikes, scooters)	0.5

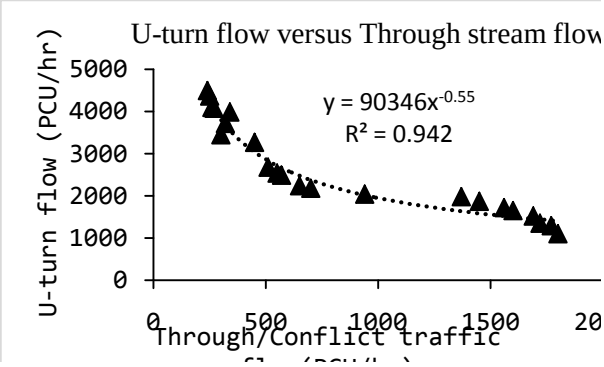

Fig 1: U-turn flow versus through traffic volume in PCU/hr.

4.3 Gap Acceptance Concept by "INAFOGA"

After video shooting of the median openings, extraction of necessary decision variables for estimation of critical gap was done as per Satish et al "INAFOGA" method. The video data collected from the field was converted to .AVI format from .MPG file type. All necessary decision variables were extracted by playing the .AVI videos in a demuxer software named as AVIDEMUX Version 2.6 capable of running videos at a frame rate of 25 frames/second. The time frames chosen for data extraction were based on the concept of "INAFOGA" as given by Satish et al in his theory of gap acceptance under mixed traffic conditions in India in 2011. Fig 3 represents the schematic diagram of a median opening on a 4-lane divided carriageway in AUTOCAD 2009 representing the "INAFOGA"method. The influence area for gap acceptance (INAFOGA) of a U-turning vehicle is the rectangular area bounded by the Red, Green and Blue lines. "Red" line represents the stop line of the U-turn vehicle after approaching the median opening while the "Yellow" and "Blue" lines form the upstream and downstream ends of "INAFOGA". The length (L) of the area measures {(d/2) + 2.2 m} while the breadth (W) as {a + (c/2)}. All these measurements have been experimentally proved in general for all the 4 sections. The U-shaped and the straight arrows show the directions of the U-turning and through traffic respectively. Here, 'a' represents the distance between inner lanes while 'b', 'c' &'d' are dimensions of the median openings. The "Green" line is at d/2 distance horizontally from the face of the median.

Fig 2: Pictorial representation of the Study Area

The time frames chosen during extraction of data with the aid of AVIDEMUX software are as follows:

1. T_0 = time instant front bumper of through traffic vehicle preceding the subject vehicle touches the U/S end of INAFOGA
2. T_1 = time instant front bumper of the subject vehicle touches the stop line in b/w the median opening
3. T_2 = time instant front bumper of the first through traffic vehicle after arrival of the subject vehicle touches the U/S end of "INAFOGA"
4. T_3, T_4, T_n = corresponding time instants for arrival of through traffic vehicles on the U/S end of "INAFOGA"
5. T_w = time instant at which back bumper of the subject vehicle touches the stop line
6. T_m = time instant back bumper of the subject vehicle touches the D/S end of "INAFOGA"

V. METHODS COMPARED

A conclusion section must be included and should indicate clearly the advantages, limitations, and possible applications of the paper. Although a conclusion may review the main points of the paper, do not replicate the abstract as the conclusion. A conclusion might elaborate on the importance of the work or suggest applications and extensions.

The time frames extracted from the raw video data were then represented in an MS-Excel spreadsheet and the following decision variables or inputs were found out to estimate the critical gaps using the existing methods as described earlier in section 4 of this paper:

1. LAG (only accepted) = time interval b/w arrival of U-turn vehicle on opening and arrival of first through traffic vehicle= T_2-T_1
2. GAP (accepted & rejected) = difference b/w arrivals of consecutive through traffic vehicles at U/S end of "INAFOGA" = $T_{n+1} - T_n$
3. Merging Time Of U-turning Vehicle = $T_m - T_w$

5.1 Harders Method

Harders (1968) have developed a method for t_c estimation that has become rather popular in GERMANY. The method only makes use of gaps. For Harder's method, lags should not be used in the sample. The time scale is divided into intervals of constant duration, e.g. $\Delta t = 0.5$ secs. The center of each time interval i is denoted by ti. For each vehicle queuing on the minor street, we have to observe all major stream gaps that are presented to the driver and, in addition, the accepted gap. From these observations we calculate the following frequencies and relative values:

Ni = number of all gaps of size i, that are provide to minor street vehicle; Ai = number of accepted gaps of size i; ai = Ai / Ni

Now, these ai values can be plotted over ti. The curve generated by doing this has the form of a cumulative distribution function of critical gaps. It is treated as the function Fc (t). However, nobody has provided any conclusive mathematical concept that this function ai= function (ti) has real properties of Fc (t) [19, 21].

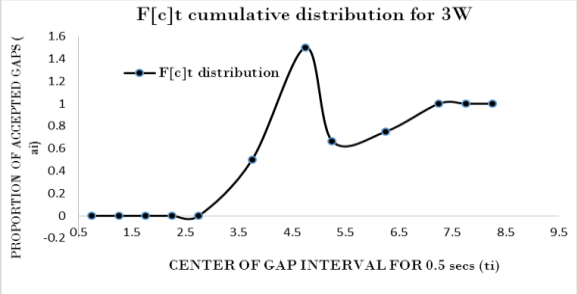

Fig 3: Critical Gap for 3W by Harders Method

Decision variables or inputs used are no. of accepted gaps along with total no. of all gaps. A cumulative distribution curve showing variation of critical gap with time is plotted between the proportions of accepted gaps (ai) {ratio of no. of accepted to total no. of all gaps} and time elapsed divided into constant durations of 0.25 seconds. Fig 3 and Fig 4 shows the F[c]t distribution of critical gaps for 3 wheelers and SUVs respectively.

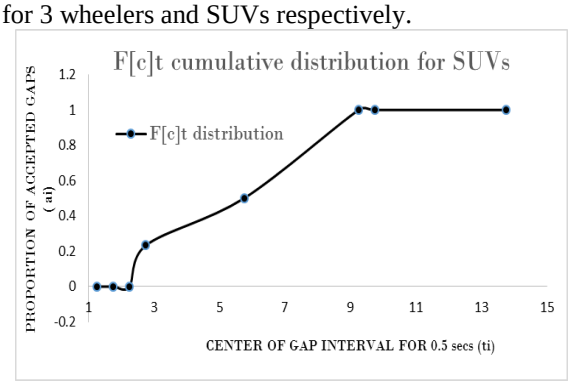

Fig 4: Critical Gap for SUVs by Harders Method

5.2 "INAFOGA" Method

In [10], author introduced a new concept for measuring critical gap making use of clearing behaviour of vehicles in conjunction with gap acceptance data. He proposed an area named as INAFOGA (Influence Area for Gap Acceptance) which had a dimension of L*W, where L= 3.5 m (lane width) & W= 1.5 times width of crossing /merging vehicle. It takes into account the clearing behaviour of a vehicle (clearing time is the time taken by the minor street vehicle to clear the influence area) & gap acceptance behaviour. Following are the characteristics of "INAFOGA":

- A vehicle taking right turn from Minor Street waits at the stop line near INAFOGA & is said to clear the intersection when its tail end crosses the stop line in the major street.
- Difference between the arrivals of consecutive major street Vehicles at the upstream end of the INAFOGA is considered as 'Gap'
- In this method, a typical cumulative frequency distribution curve for clearing time of a minor street vehicle against its corresponding Lag & Gap Acceptance curve is plotted having a common point of intersection. This point of intersection indicates the minimum/critical gap sufficient for the vehicle to enter the INAFOGA keeping in mind the SAFETY aspect.

Both accepted lags and gaps are used in this method to determine critical gaps. Cumulative frequency percentages of lags and gaps are plotted against merging time expressed as frequency distribution. Fig 5 and Fig 6 predicts the critical gap of U-turning 3 wheelers and SUVs using "INAFOGA" method.

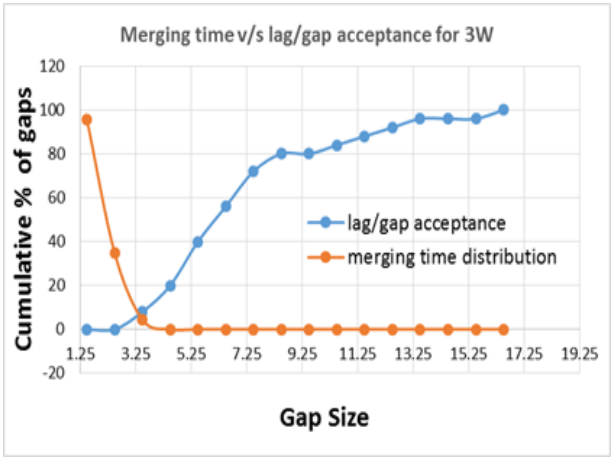

Fig 5: Critical gap by "INAFOGA" method for three wheelers (3W)

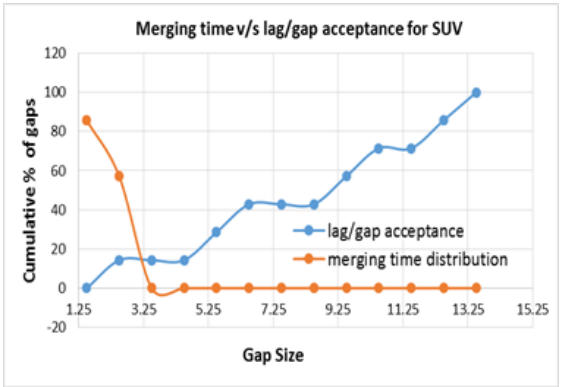

Fig 6: Critical gap by "INAFOGA"method for Sport utility vehicles (SUVs)

VI. RESULTS AND ANALYSIS

Table 2: Critical gap Values for Various Modes Estimated Using Harders Method

Median Opening Section no.	Vehicle Type	Critical Gap (secs) for U-turn vehicles by HARDERS Method
1	CAR	3.38
	2-WHEELER	3.95
	3-WHEELER	4.50
	SUVs/MUV	4.25
2	CAR	3.75
	2-WHEELER	3.25
	3-WHEELER	3.75
	SUVs/MUV	4.15
3	CAR	4.25
	2-WHEELER	3.25
	3-WHEELER	4.25
	SUVs/MUV	4.25
4	CAR	3.45
	2-WHEELER	4.15
	3-WHEELER	3.75
	SUVs/MUV	3.75

Tables 2 and Table 3 displays the critical gap values for 4 different sections of median openings on 4-lane divided roads of Bhubaneshwar. Four different categories of vehicles namely cars (4W), 2-wheelers, 3-wheelers and Sport utility vehicles have been considered in this study. Table 3 gives the critical gap values as obtained by applying "INAFOGA" method while Table 2 shows the same for Harders method. Values in parenthesis for Table 3 indicate the sample sizes and the symbol ** indicates either low or nil sample size. Cluster plots are shown to compare the critical gap values between different sections based on the values represented in tables 2 and Table 3. Referring to the cluster plots in Fig 8, for Harders method, critical gap values obtained for 2 wheelers were more than that of other modes except for section 1 where it contradicted for SUVs {2W(4.75s)<SUVs(5.75s)}. So, Harders method fail to optimize critical gap values for section 1. On the other hand, it can be concluded that Harders method is well efficient and best suited in determining critical gap values for cars (4W) and 2 wheelers respectively.

Table 3: Critical gap Values for Various Modes Estimated Using "INAFOGA" Concept

Median Opening Section No.	Mode/Vehicle Type	Critical Gap (secs) by "INAFOGA"
1	CAR	4.78(65)
	2-WHEELER	4.75(90)
	3-WHEELER	4.65(125)
	SPORTS UTILITY VEHICLES	5.15(35)
2	CAR	5.40(84)
	2-WHEELER	5.80(42)
	3-WHEELER	5.50(33)
	SPORTS UTILITY VEHICLES	5.70(20)
3	CAR	5.55(34)
	2-WHEELER	6.00(26)
	3-WHEELER	5.85(22)
	SPORTS UTILITY VEHICLES	**
4	CAR	5.15(43)
	2-WHEELER	4.75(52)
	3-WHEELER	4.80(21)
	SPORTS UTILITY VEHICLES	5.75(20)

A paired sample T-test was done for the critical gap values obtained for Harders and "INAFOGA" method to find out the difference in means of the values in IBM SPSS (Statistical Package for Social Sciences) software version 22.0. The results indicated a significance value of 0.044 which was lower than (p = 0.050) which in turn signified that the critical gap values for the two methods can indeed be compared. After a manual calculation it was certified that the critical gap values obtained using Merging behaviour concept of U-turn vehicles inspired from Satish et al "INAFOGA" method shown in Fig 7, are found to be higher by 28-41% as compared to those obtained by Harders method which has been used normally under uniform traffic conditions. Reason being the abrupt vehicular interactions in mixed traffic conditions. This indicates that the "INAFOGA" concept is successful than Harders method in gap acceptance analysis under mixed traffic.

Paired Samples Statistics					
		Mean	**N**	**Std. Deviation**	**Std. Error Mean**
Pair	Harders	4.8163	32	.90157	.31875
	"INAFOGA"	4.031250	32	.4292331	.1517568

Paired Samples Correlations				
		N	**Correlation**	**Significance**
Pair	Harders & "INAFOGA"	32	.872	.005

Paired Samples Test									
		Paired Differences					**t-statistic**	**D.f**	**Sig.(2-tailed)**
		Mean	**Std. deviation**	**Std. Error Mean**	**95% Confidence Interval of the Difference**				
					Lower	**Upper**			
Pair	Harders–"INAFOGA"	.4850000	.5676518	.2006952	.0104312	.9595688	-2.417	31	.0444

Fig 7: Statistical Details of The Paired sample T-test Between Harders & "INAFOGA" methods for Critical Gaps

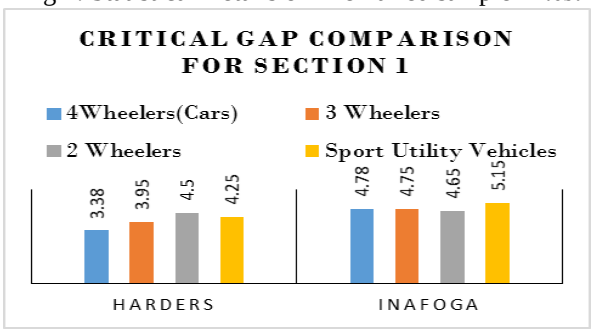

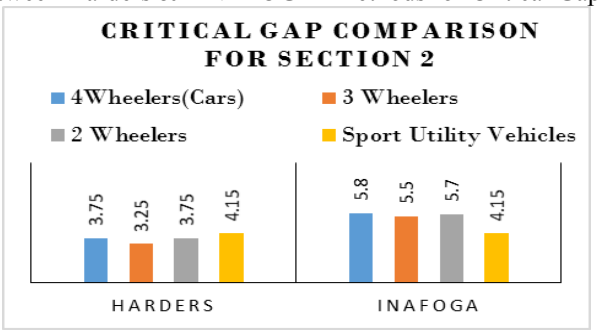

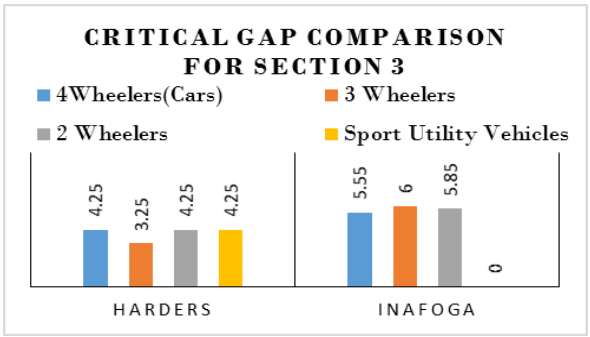

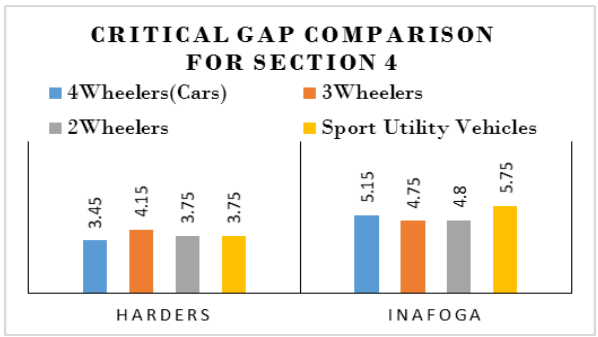

Fig 8: Cluster Plots of critical gap comparison for 4 different sections under mixed traffic conditions

VII. CONCLUSIONS

A general estimation and comparison of critical gaps between four types of motorized modes has been shown in this paper for four different median opening sections under mixed traffic conditions. Data involved video recording of median openings of Bhubaneshwar city in the state of Odisha. Two existing methods available in previous literatures were used to estimate the critical gap values. Using the "INAFOGA' concept for data extraction, estimation of critical gaps for U-turns at median openings under mixed traffic conditions have been done in this paper. The only limitation found while studying gap acceptance is the inefficiency of Harders method in predicting appropriate critical gap values under mixed traffic conditions. The reason being the use of this method by previous researchers under uniform traffic conditions only. A paired sample T-test between critical gap values for Harders and "INAFOGA" method was performed to find out the difference in means of the values. The values were found to be 28-41% lesser as compared to the values obtained using form Satish et al "INAFOGA" method. A new concept of merging time inspired from Satish et al "INAFOGA" method for U-turn vehicles at median openings is introduced in this paper. Merging time indicates the complete merging maneuver of a U-turn vehicle at a median opening. Cluster diagrams plotted gives the comparison of critical gap values for the four different modes considered in this study for all the four sections. The new concept used for finding critical gaps of U-turns has never been used previously and is simple and easy. Thus, the concept introduced for critical gap estimation for U-turns at unsignalized median openings will definitely serve as a handy tool for traffic engineers working on median openings.

REFERENCES

[1] Pavani Boddapati, "Comparative study of Type 2 Median Crossovers and median U-turns", *Technical Report, University of Missouri, Columbia, 2010.*

[2] Pan Liu, Evaluation of Operational Effects of U-turn Movements, *Technical Report, University of Florida*, 2006.

[3] Pan Liu, Jian Liu, Fengxuan Hu, "Headway Acceptance Characteristics Of U-turning Vehicles On 4-lane Divided Roadways", *86th Annual Meeting of TRB, 2007.*

[4] Pan Liu, Jian John Liu, Fengxuan Hu, Gary Sokolow, "Capacity Of U-turning Movement at Median Openings on Multi-lane Highways", *Journal of Transportation Engg. , ASCE, 134 (4), 2008, 147-154.*

[5] Turki I. Al – Suleiman Obaidat , Muhammad S. Elayan, "Gap Acceptance Behavior At U-turn Median Openings – Case study in Jordan", *Jordan Journal of Civil Engg., 7 (3) , 2013, 332-341.*

[6] Abdul Khalik Al-Taei, "Gap Acceptance and Traffic Safety Analysis on U-turn Median Openings of Arterial Roads, *Al-Rafidain Engg., 18 (6), 2010, 42-53.*

[7] P.Solberg, J.C. Oppenlander, "Lag and Gap Acceptances At Stop-controlled Intersections: Technical Paper", *Joint Highway Research Programme (JHRP), Purdue University, Purdue-e-Pubs, 1964, 1-58.*

[8] C.B.Uber, "Driver Gap Acceptance Phenomenon", *Doctoral diss., J. Transportation Engg. M.ASCE, 110 (1), 1984, 145-147.*

[9] Rui-Jun Guo, Bo-liang Lin, "Gap Acceptance at Priority Controlled Intersections", *Journal of Transportation Engg. ASCE, 137(1), 2011, 296-276.*

[10] Ashalatha R., Satish Chandra, "Critical Gap through Clearing Behavior at Un-signalized Intersections", *KSCE Journal of Civil Engineers, Springer Publications, 15(2), 2011, 413-425.*

[11] R.H.Hewitt, "Measuring Critical Gap", *Transportation Science, 17(1), 1983, 87-109.*

[12] "Highway Capacity Manual", *Transportation Research Board, Washington D.C., 2010.*

[13] Tomer Toledo, Haneen Fareh, "Alternative definition of Passing Critical Gaps", *TRR, Journal of the Transportation Research Board, 2260(09), 2011, 76-82.*

[14] City Development Plan: Bhubaneswar, *JNNURM, Government of India, Retrieved 2012.*

[15] "Preface of Comprehensive Development Plan for the Bhubaneswar-Cuttack Urban Complex", 2011.

[16] W. Brilon, R. Koenig and R.J. Troutbeck, "Useful Estimation Procedures for Critical Gaps", *Transportation Research, 33(3), 1999, 161-186.*

[17] Ashalatha R, Satish Chandra and K.Prasanth, "Critical Gap at Un-signalized Intersection Using Maximum Likelihood Technique", *Technical Paper, Indian Highways, India, 2005.*

[18] Antje Weinert, "Estimation of Critical Gaps and Follow –up Times at Rural Un-signalized Intersections in Germany", *Transportation Research Circular E-C018:*

4th International Symposium on Highway Capacity, Bochum, Germany, 2001

[19] Adrea Gavulova, "Use of Statistical Techniques for Critical Gap Estimation", *12th International Conference on "Reliability and Statistics in Transportation and Communication-2012", Riga. Liva. , 2012, 20-26.*

[20] L.Vasconceles, A.B.Silva, A.Seco and G.Rouxinol, "Estimation of Critical headways at un-signalized intersections- a microscopic approach", *Journal of Advances in Transportation Studies, 29, 2012, 59-72.*

[21] Z.Tian , Mark Vandehey , Bruce W. Robinson , Wayne Kittelson , Michael Kyte , Rod Troutbeck , Werner Brilon and Ning Wu , 'Implementing the maximum likelihood methodology to measure a driver's Critical Gap", *Transportation Research Part A , Elsevier Ltd., 33 (3-4), 1999, 187-199.*

[22] Ning Wu, 2006, "A New Model for Estimating Critical Gap and its Distribution at Un-Signalized Intersections Based on the Equilibrium of Probabilities", *5th International Symposium on Highway Capacity and Quality Of service, 2006-7, 517-526.*

International Journal of Engineering Research and Applications (IJERA) ISSN: 2248-9622
National Conference on Advances in Engineering and Technology
(AET- 29th March 2014)

RESEARCH ARTICLE OPEN ACCESS

Seismic Behaviour Of A Soft Storey Building With & Without Viscous Dampers

Yuvraj Bisht*, Saraswati Setia**
*(Department of Civil Engineering, NIT Kurukshetra, Haryana, INDIA
Email: yuvraj.bisht89@gmail.com)
** (Department of Civil Engineering, NIT Kurukshetra, Haryana, INDIA
Email: ss_ts97@gmail.com)

ABSTRACT
During january 2001 Bhuj Earthquake in India, many multi-storeyed buildings in urban areas collapsed and suffered wide spread damages. Post earthquake observations revealed many deficiencies in these structures including non-adoption of seismic engineering practices and lack of seismic resistant features. The seismic performance of a building can be improved by using energy absorbing devices, which may be active or passive in nature. Active control techniques have not found much appreciation due to its high cost and large instrumentation set up. Whereas, passive control systems such as base isolation, dampers, bracing systems etc are found to be easy to install and cost effective as compared to previous one. Use of dampers is now becoming cost effective solution to improve seismic performance of existing as well as new buildings. This paper deals with use of viscous dampers in the building. A five storey building with a open ground storey is analysed with and without braced type viscous dampers placed at soft storey. Non-linear time history analysis is carried out using SAP2000 software and comparisons are shown in a tabular and graphical format.
Keywords - Energy dissipation, Seiemic retrofitting, Soft storey, time history analysis, Viscous dampers.

I. INTRODUCTION

Over the past few decades world has experienced numerous devastating earthquakes, resulting in increased loss of human life due to collapse of buildings and severe structural damages. In recent years, much attention has been paid to the research and development of structural control techniques such as passive control system, active control system, and semi active control system giving special importance on improvement of wind and seismic responses of buildings. Passive control systems do not require any power supply. In conventional construction Earth quake-induced energy is dissipated in Components of the gravity resisting system .the action of dissipating energy in framing, such as beam and column in a moment-resisting frame produces damage in those components. Repair of such damage after an earth quake is typically expensive and often requires evacuation of the building. The objective of adding damping hardware to new and existing construction is to dissipate much of the earth quake-induced energy. The philosophy is limiting the damage to the gravity-load-resisting system. Although testing and Perhaps replacement of all supplemental damping devices in a building should be anticipated after a design earth quake, evacuation of the building for repair might not be necessary and hence the total cost of repair will likely be less as compared with the cost associated with repair in a conventional building.

II. VARIOUS PASSIVE ENERGY DEVICES

The main reason to use passive energy dissipation devices in a structure is to limit damaging deformations in structural components. The degree to which a certain device is able to accomplish this goal depends on the inherent properties of the basic structure, the properties of the device and its connecting elements, the characteristics of the ground motion. Device that have most commonly been used for seismic protection of structures include viscous fluid dampers, viscoelastic solid dampers, friction dampers and metallic dampers. Semi-active dampers have also been used for seismic response control in other countries, notably Japan, but not within the United States (Soong and Spencer, 2002) [1].

2.1 Viscous Fluid Damper

Viscous fluid dampers are commonly used as passive energy dissipation devices for seismic protection of structures. Such dampers consist of a hollow cylinder filled with fluid as shown in Fig 1, the fluid typically being silicone based. As the damper piston rod and piston head are stroked, fluid

is forced to flow through orifices either around or through the piston head. The resulting differential in pressure across the piston head (very high pressure on the upstream side and very low pressure on the downstream side) can produce very large forces that resist the relative motion of the damper (Lee and Taylor 2001)[2]. The fluid flows at high velocities, resulting in the development of friction between fluid particles and the piston head. The friction forces give rise to energy dissipation in the form of heat. The fluid typically has a relatively low viscosity (e.g., silicone oil with a kinematic viscosity on the order of 0.001 m^2/s at 20°C). Note that the fluid damper - shown in Fig 2 includes a double-ended piston rod. Such configurations are useful for minimizing the development of restoring forces due to fluid compression.

2.2 Viscous Elastic Damper

Viscoelastic solid dampers generally consist of solid elastomeric pads viscoelastic material bonded to steel plates as shown in Fig 1. The steel plates are attached to the structure within chevron or diagonal bracing. As one end of the damper displaces with respect to the other, the viscoelastic material is sheared resulting in the development of heat which is dissipated to the environment. By their very nature, viscoelastic solids exhibit both elasticity and viscosity. For viscoelastic materials, the mechanical behavior is typically presented in terms of shear stresses and strains rather than forces and

	Viscous Fluid Damper	Viscoelastic Solid Damper	Metallic Damper	Friction Damper
Basic Construction			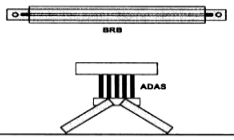	
Idealized Hysteretic Behavior	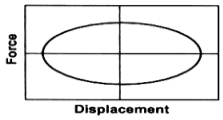	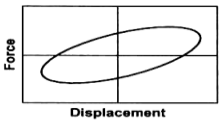	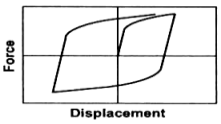	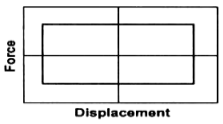
Idealized Physical Model	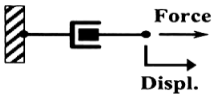	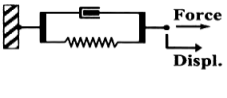	Idealized Model Not Available	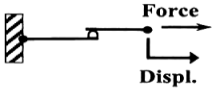
Advantages	- Activated at low displacements - Minimal restoring force - For linear damper, modeling of damper is simplified. - Properties largely frequency and temperature-independent - Proven record of performance in military applications	- Activated at low displacements - Provides restoring force - Linear behavior, therefore simplified modeling of damper	- Stable hysteretic behavior - Long-term reliability - Insensitivity to ambient temperature - Materials and behavior familiar to practicing engineers	- Large energy dissipation per cycle - Insensitivity to ambient temperature
Disadvantages	- Possible fluid seal leakage (reliability concern)	- Limited deformation capacity - Properties are frequency and temperature-dependent - Possible debonding and tearing of VE material (reliability concern)	- Device damaged after earthquake; may require replacement - Nonlinear behavior; may require nonlinear analysis	- Sliding interface conditions may change with time (reliability concern) - Strongly nonlinear behavior; may excite higher modes and require nonlinear analysis - Permanent displacements if no restoring force mechanism provided

Fig 1: Summary of construction, models, advantages, and disadvantages of Dampers [8]

displacements. The mechanical properties then become the storage and loss moduli that define the properties of the viscoelastic material rather than properties of the damper. In general, the storage and loss moduli are dependent on frequency of motion, strain amplitude, and temperature.

2.3 Metallic Damper

Two major types of metallic dampers are buckling-restrained brace dampers and added damping and stiffness dampers. A BRB damper consists of a steel brace with a cruciform cross section that is surrounded by a stiff steel tube. The region between the tube and brace is filled with a concrete-like material and a special coating is applied to the brace to prevent it from bonding to the concrete. Thus, the brace can slide with respect to the concrete-filled tube. The confinement provided by the concrete-filled tube allows the brace to be subjected to compressive loads without buckling. Under compressive loads, the damper behavior is essentially identical to its behavior in tension. Since buckling is prevented, significant energy dissipation can occur over a cycle of motion. Additional details on the behavior of BRB dampers are provided [3].

2.4 Friction Damper

Friction dampers dissipate energy via sliding friction across the interface between two solid bodies. Examples of such dampers include slotted-bolted dampers are available wherein a series of steel plates are bolted together with a specified clamping force as shown in Fig 1. The clamping force is such that slip occurs at a pre-specified friction force. At the sliding interface between the steel plates, special materials may be utilized to promote stable coefficients of friction. An alternate configuration, known as the Pall cross-bracing friction damper, consists of cross-bracing that connects in the center to a rectangular damper [4]. Other configurations include a cylindrical friction damper in which the damper dissipates energy via sliding friction between copper friction pads and a steel cylinder [5]. The idealized hysteretic response of a friction damper for cyclic loading reveals that the force output is bounded and has the same value for each direction of sliding as shown in Fig 1. The hysteresis loops are rectangular, indicating that significant energy can be dissipated per cycle of motion. However, the rectangular shape of the hysteresis loops indicates that the cyclic behavior of friction dampers is strongly nonlinear. The deformations of the structural framing are largely restricted.

III. MODELLING OF BUILDING FRAME WITH VISCOUS DAMPERS

A five storey reinforced concrete building frame with open ground storey is modeled. Sudden reduction in lateral strength and stiffness of ground storey due to absence of masonary wall at ground storey results in excessive inelastic deformation on the ground story columns leading to the soft-story collapse of the building under the seismic loading conditions. Here, viscous dampers are provided to check the seismic performance of the structure. In this example, non-linear time history analysis is carried out using SAP 2000 version 14 software. Modelling procedure is summarized in following steps.

1. Create a five storey model using file menu.
2. Define materials to be used, here we will define concrete, steel and strut material using define section properties menu.
3. Assign properties to all the framed sections and struts which are used to incorporate the masonary wall effect.
4. Dampers are added into the model by defining link/support properties in the SAP. Input appropriate value of stiffness, damping coefficient and damping exponent in the data sheet.
5. Assign the joint masses/forces using Assign menu.
6. Define and apply time history analysis using past earthquake data. A time history data of 31.2 seconds ‘el centro earth-quake’ at 0 degree is considered for the analysis. This is given in the form of text file having 1560 points of acceleration data equally spaced at .020 second as is shown in Fig 2. Define menu select the function option and apply time history.

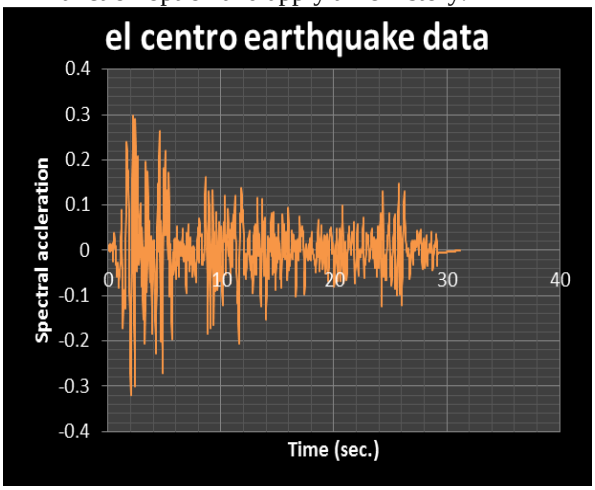

Fig 2: El centro earthquake data

7. Assign the load cases using assign menu. Non-linear time history cases are considered for analysing the given model.
8. At last Analyze menu activates analysis of the frame. SAP is capable of doing different types of analysis. In this problem, nonlinear time history analysis is carried out to compare the response of building with or without dampers.

IV. MODEL DETAILS & SPECIFICATIONS

The model represents a five storey building with open ground storey considerations. Fig 3 shows the building model without Dampers while Fig 4 shows the building model with viscous Damper considerations.

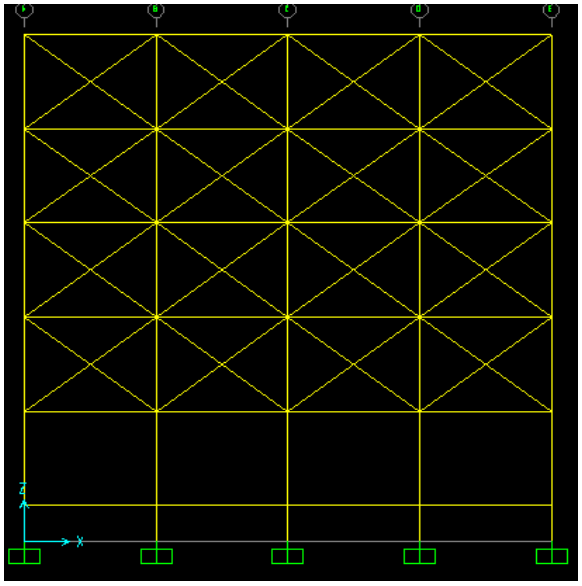

Figure 3: Five storey building Model without Damper

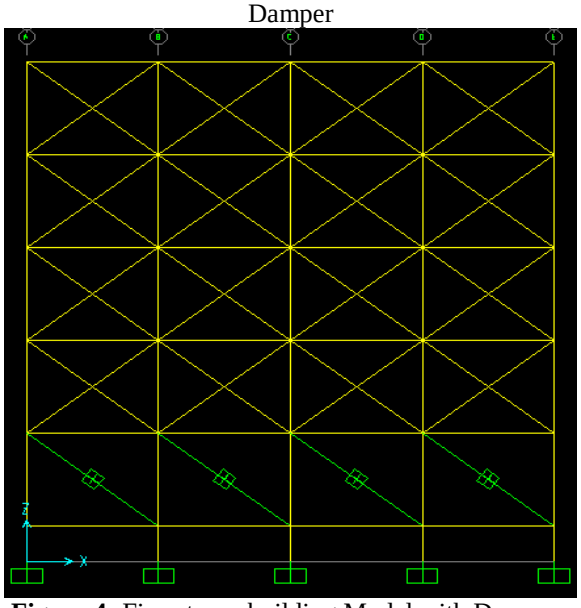

Figure 4: Five storey building Model with Dampers

Fig 5 shows the complete three dimensional model structure of the analyzed frame. Open ground storey at the ground level is also clearly highlighted.

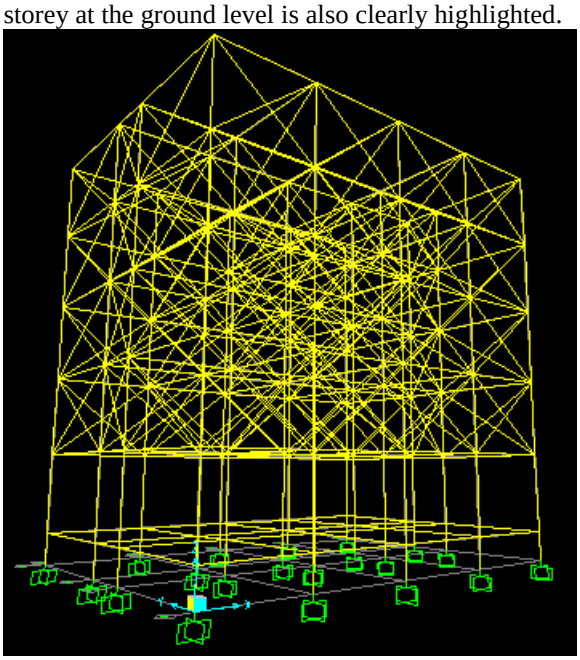

Figure 5: 3-Dimensional Model of building frame

Effects of masonary provided in the structures are considered in the form of struts provided which take compression forces only with the help of SAP 2000. Specifications of Dampers and Struts have been provided in Table.1 . A constant Damping coefficient is considered for analyzing given model. Struts are provided of three different types depending upon dimensions of Bays , a uniform width equal to wall width of 230 mm is considered and accordingly strut width are calculated using equivalent strut width formula and there values are tabulated in Table.1. Here, strut2, strut4, strut5 refers to struts provided in Bays with length of 2m, 4m and 5m respectively.

Table 1: Properties of Dampers

PROPERTIES OF DAMPERS	
Damping coefficient	40000
Damping exponent	1
Stiffness	0
Strut 2 width	0.795m
Strut 4 width	0.767m
Strut 5 width	1.07m

Following Table 2 shows the various specifications and properties of member, materials used in the given model. Three values of bays width are provided for three different bay lengths.

Table 2: Specifications of Building

SPECIFICATIONS OF BUILDING	
Items	Properties
Density of concrete	25 KN/m^3
Height of the floor	3.1 m
Bay width	2m, 4m, 5m
Poisson's ratio (concrete)	0.2
Elasticity of concrete	25000 N/mm^2
Density of Masonary	20000 N/mm^2
Live load	3 KN/m^2
Beam size	450 x 300
Column size	450 x 300

Table 3 shows the calculations and values of various types of loads considered in the given building model. All results and conclusions are obtained with respect to these load value and all loads are applied as line loads , floors loads are converted to line loads format using trapeziodal and triangular load distribution patterns.

Table 3: Load Calculations

Load Calculations		
Load Type	Calculations	Magnitudes
External Wall	0.23x(3.1-.45) x20	12.19 KN/m
Internal Wall	0.15x (3.1-.45) x20	7.95 KN/m
Parapet Wall	0.23 x 1.5 x 20	6.9 KN/m
Slab	0.15 x 1 x 1 x 25	3.75KN/m
Floor finish	1 x 1	1 KN/m
Roof treatment	1.5 x 1	1.5 KN/m
Live	3 x 1	3 KN/m
Live roof	1.5x 1	1.5 KN/m

V. ANALYSIS AND RESULTS

A viscous damper provides a damping force of F = C Vu, where C is the damping coefficient, V is the velocity and u is the damping exponent. Damping exponent is generally in the range of 0.4 to 1.0 and in this paper it is taken as 1.0 for all cases. The value of damping coefficient C is taken as 40000(KN.s/m). The response of structure is determined for five storey building with open ground storey (without damper) and same soft storey building frame with dampers provided up to specific storey and the results are given in the various tables below.

Table 4: Drift of different storey

Drift of different storey (mm)		
	Normal Frame	With Damper
Storey 1	10.98	6.21
Storey 2	573.50	133.3
Storey 3	10.94	3.981
Storey 4	8.92	3.542
Storey 5	8.314	3.325

In Fig 6, the analysis results show that there is a sudden rise in drift and displacements at storey 2 due to loss of stiffness at the ground storey. Thus, the building can undergo soft storey failure if exposed to seismic conditions. Also, it can be interpreted from the results that the use of Viscous Dampers has improved the performance of the building to great extent.

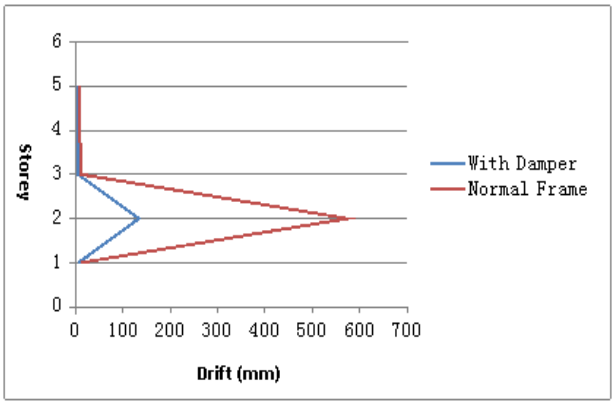

Fig 6: Plot of Drift vs Storey

Sudden change in red plot at storey 2 indicates sharp change in stiffness due to soft storey. Blue plot represents the drift behavior of soft storey with viscous Damper and shows considerable reduction in this soft storey problem of excessive drift. Also the maximum drift of building is checked within the maximum permissible limits.

Table 5: Displacements of different storey

Displacements of different storey (mm)		
	Normal Frame	With Damper
Storey 1	10.98	6.12
Storey 2	584.48	139.42
Storey 3	595.42	143.40
Storey 4	604.34	146.94
Storey 5	612.66	150.27

VI. CONCLUSIONS

- With the deployment of viscous damper in the structure maximum response and drift reduces in structure during seismic loading.
- The performance of building structure in seismic loading is improved to great extent. By the provision of viscous dampers up to five stories, maximum drift is reduced from 3.7 % to 0.86 %.
- Main factors for reduction of response of the structure are parameters associated with Dampers and the dissipation of energy produced during earthquake by the mean of viscous Dampers.
- The maximum acceleration decreases from 2.2% to 0.4% and base shear increased from 0.8% to 1.67% by providing dampers.

REFERENCES

[1] Soong, T. T., and Spencer, Jr. B. F.. "Supplemental energy dissipation: State-of-the-art and state-of-the-practice", *Engineering Structure*, 24 (3), 2002, 243–259.

[2] Lee, D., and Taylor, D. P. "Viscous damper development and future trends", *Struct. Des. Tall Build.*, 10(5), 2001, 311–320.

[3] Black, C. J., Makris, N., and Aiken, I. "Component testing, seismic evaluation and characterization of buckling-restrained braces", *J. Struct. Eng.*, 130(6), 2004, 880–894,

[4] Pall, A. S., and Marsh, C. "Seismic response of friction damped braced frames", *J. Struct. Div.*, 108(6), 1982, 1313–1323,

[5] Soong, T. T., and Dargush, G. F. "Passive energy dissipation systems in structural engineering", *Wiley, Chichester*, U.K, 1997

[6] Symans, M. D., and Constantinou, M. C. "Passive fluid viscous damping systems for seismic energy dissipation", *J. of Earthquake Technology*, 35(4), 1998, 185–206.

[7] Symans, M. D., Charney, F. A., Whittaker, A. S., Constantinou, M. C., Kircher C. A., Johnson M. W., McNamara R. J., "Energy Dissipation systems for Seismic Application: Current Practice and Recent Developments", *J. of Structural Engineering, ASCE*, 134(1), 2008, 3-21.

International Journal of Engineering Research and Applications (IJERA) ISSN: 2248-9622
National Conference on Advances in Engineering and Technology
(AET- 29th March 2014)

RESEARCH ARTICLE OPEN ACCESS

Effect Of Inclination On Boundary Layer In A Low Speed Wind Tunnel On Different Roughness'

Vivek Gupta*, Awadhesh Kumar**
*(Department of Civil Engineering, NIT Rourkela, India
Email: vivek4656112@gmail.com)
** (Department of Civil Engineering, NIT Rourkela, India
Email: akumar@nitrkl.ac.in)

ABSTRACT
The boundary layer of a flowing fluid is the thin layer close to the wall. For the basic understanding of flow characteristics over a flat plate, the experiment was carried out in the laboratory using a low speed wind tunnel. In a flow field viscous stresses are very prominent within this layer due to existence of velocity gradient. Velocity reading at 21 locations over the flat plate (wood surface with stacked on a 40 grade and 60 grade emery paper) with a free stream velocity (U) and with the concept of 0.99U velocity profile is plotted at different locations of working section length. The inclination of flat plate gives a better idea of free steam bodies for the purpose of design. The boundary layer thickness of the boundary layer ranges from 2.2mm to 59.2mm.The boundary layer growth over the rough flat plate was found out with the help of velocity profiles at different locations. The boundary layer growth gives a brief idea of fluid flow over a flat surface. Comparison of rough flat plates with different inclination gives a better understanding of boundary layer.
Keywords **-** boundary layer, roughness, flat plate, velocity profile, inclination of plate.

I. INTRODUCTION

Boundary layer is a layer adjacent to the surface where viscous effects are important. When real fluid flows past a solid body or a solid wall, the fluid particles adhere to the boundary and condition of no slip occurs. This means that the velocity of fluid close to the boundary will be same as that of boundary. If the boundary is not moving the velocity of fluid at the boundary will be zero. Further away from the boundary, the velocity will be increase gradually and as a result of this variation of velocity, the velocity gradient will exist. The velocity of fluid increases from zero velocity on the stationary boundary to the free stream velocity of the fluid in the direction normal to the boundary. The extent of atmospheric boundary layer (ABL) thickness is quite high and all types of structures lies with atmospheric boundary layer thickness. To conduct wind tunnel experiments on the small scale replica of a structure (civil, mechanical or any), it is necessary that the models should lie within boundary layer zone. But in wind tunnel the boundary layer thickness is very small and hence constant attempts have been made by different researchers to increase boundary layer thickness by different means.

In the first part of experiment the study was based on the fact that reading was taken with some obstruction like 40 grade in approaching flow with 0 degree (horizontal position) and 5 degree inclination. With these reading velocity profile were plotted and then growth of boundary layer were also drawn. In the second part of experiment reading were taken in presence of less rough flat plates and the thickness of boundary layer is decreased in comparison to previous cases. This is because obstruction helps in the generation of vortex formation and consequent turbulence.

Boundary layer study is of utmost importance for stability and design point of view. Much work has been done by many researchers in this field out of which those related to the present work has been described as follows. In [1], author analyzed the laminar boundary layer oscillation and stability of flow by mathematical model.

In [2], author measured the boundary layer on smooth flat plate in supersonic flow. In [3], author proposed a boundary flow near the trailing edge of a flat plate. in [4], author placed an elliptic wedge in front of air flow i.e. roughness and barriers are placed in wind tunnel. In [5], authors suggested a three dimensional steep hill model in wind tunnel and studied the velocity profile in all three planes. In [6], authors studied turbulent boundary layer in a flat plate. In [7], author analyzed transition to turbulent flow in boundary layer on a flat plate in presence of negative pressure gradient. In [8], authors put aerodynamically different position of the cyclist and did analysis in CFD. They put full scale model in the wind tunnel. In [9], authors developed a numerical

simulation technique for unsteady turbulent dispersion over a complicated terrain. In [10], authors developed mathematical model in heat and mass transfer in a flat plate and put an inclined plate in the viscous medium.

II. EXPERIMENTAL SETUP

For carrying out research on boundary layer study a Low Speed Wind Tunnel is built in the Hydrodynamics Laboratory of NIT Rourkela as shown in Fig 1. The speed of air in this wind tunnel can be varied from 10 to 25 m/s.

Fig 1: Photograph of Low Speed Wind Tunnel

The wind tunnel consists of a testing section somewhere in the central region where the velocity variation in the air stream is nearly uniform. The dimensions of the various components of the wind tunnel are given in Table 1.

Experimental models are placed here to carry out studies done on the objects to find the effect of the air stream on them. The photograph of the testing section is shown in Fig 2.

Table 1: Dimensions of Wind Tunnel Components

Components	Length	Inlet (m)	Outlet (m)
Effuser	1.3 m	2.1 X 2.1	2.1 X 2.1
Test Section	8 m	0.6 X 0.6	0.6 X 0.6
Diffuser	5m	0.6	1.3

To study the effect of boundary layer flat plates of length 100cm and width 50cm with different surface roughness is considered. Two different surface roughnesses are taken in the current study, namely 40 and 60 Grade. The value of the grain size in 40 and 60 Grade is 375 µm and 290 µm respectively. For the current study; 21 positions along the length of the plate are considered for velocity measurement in the vertical direction. However data for 8 such sections at 15 cm interval from the leading edge are considered in this paper Fig 4. At each such section, velocity data is taken initially at 1mm interval and later the interval is increased to 5mm when the free surface velocity is achieved.

Measurements are taken with a Telescopic Pitot Tube which is connected to a Digital Veloci Manometer shown in Fig 3. The pitot-tube is moved across the testing section throughout the length of the flat plate. The pitot-tube is held in the appropriate position and the corresponding velocity is taken directly by the digital manometer. Some wedges are used to give the inclination of rough flat plate.

Fig 2: Photograph of the Test Section

Fig 3: Photographs of Digital Veloci Manometer

III. DISCUSSION AND RESULT

For a given free stream velocity, velocity profiles data are taken throughout the testing section where the rough flat plates are positioned. Speed of the low speed wind tunnel used here is less than 25 m/s. The boundary layer thickness is in the range of 2.2-59.2 mm (of 40 grade and 60grade rough emery paper) with 0 and 5 degree inclination which was expected for rough flat plate at some fixed velocity in the low speed wind tunnel.

Here two different types of roughnesses with two different inclinations have been used. It means the boundary layer thickness is also different in these roughnesses. These plates are put horizontally and with 5 degree inclination with respect to bed. There is no variation in the magnitude of the velocity in the lateral direction at a particular section and at the same level. The readings have been taken for the lateral side at the distance of 50 cm on the leading edge. The boundary layer of the rough flat plate grows as the length is increased and tends to have great tangent as the velocity increases. Velocity profile changes along the length of the flat plate. Initially the velocity

profiles has steeper gradient compared to the velocity profiles at end ones. Tangent at each and every point of the boundary layer will be different from others.

Velocity profiles have been plotted according to the velocity readings as obtained from digital veloci manometer in m/s. Here 8 sections have been used in the longitudinal direction as shown in Fig 4. With the help of these velocity profiles, boundary layer of 40 grade roughness emery paper has been plotted in horizontal position as shown in Fig 4. As 40 grade boundary layer has been plotted in 0 degree, similarly 40 grade with 5 degree of inclination has been plotted using some wedges in Fig 5. With the help of velocity profile of 40 grades with 0 degree and 5 degree, boundary layers has been plotted as shown in Fig. 6. Similar plots have been obtained for 60 grade rough flat plate in 0 degree and 5 degree of inclinations as shown in Fig 7, Fig 8 and Fig 9. Finally for the comparison of all four boundary layers a graph has been plotted in Fig 10.

As the roughness of the emery paper is decreased, the grain size diameter decreases. Therefore main stream flow faces less resistance and thickness of the boundary also decreases. As we increase the inclination of the flat plate the boundary layer thickness also increases.

Velocity profile in the longitudinal direction has been carried out to measure the velocity at different sections.

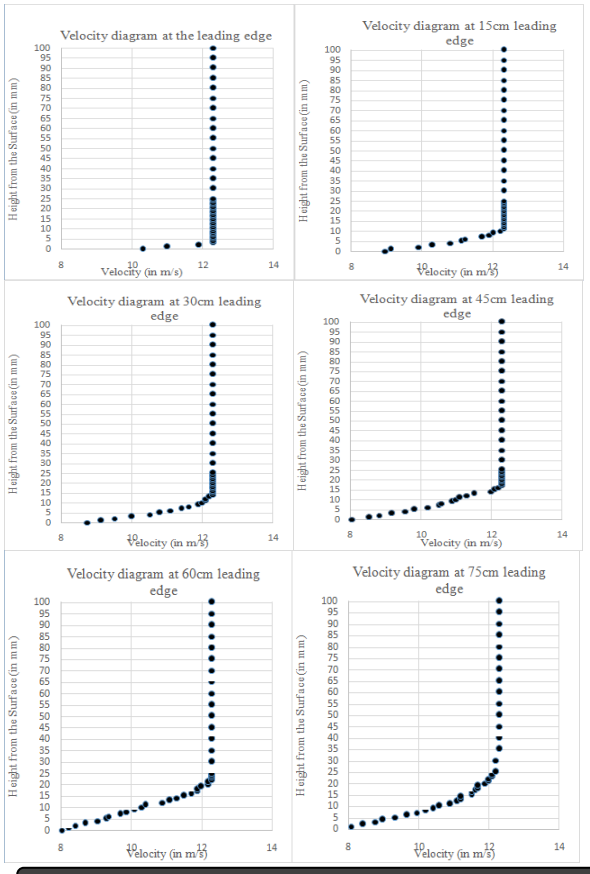

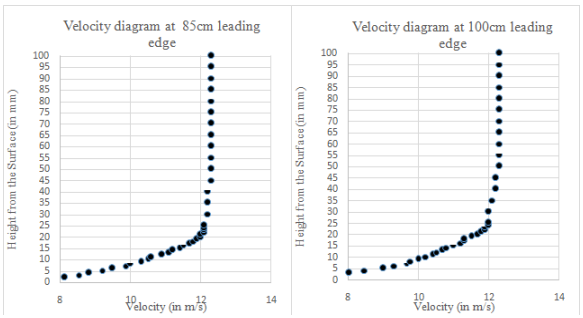

Fig 4: Velocity Profile Plots for 40 Grade at horizontal level.

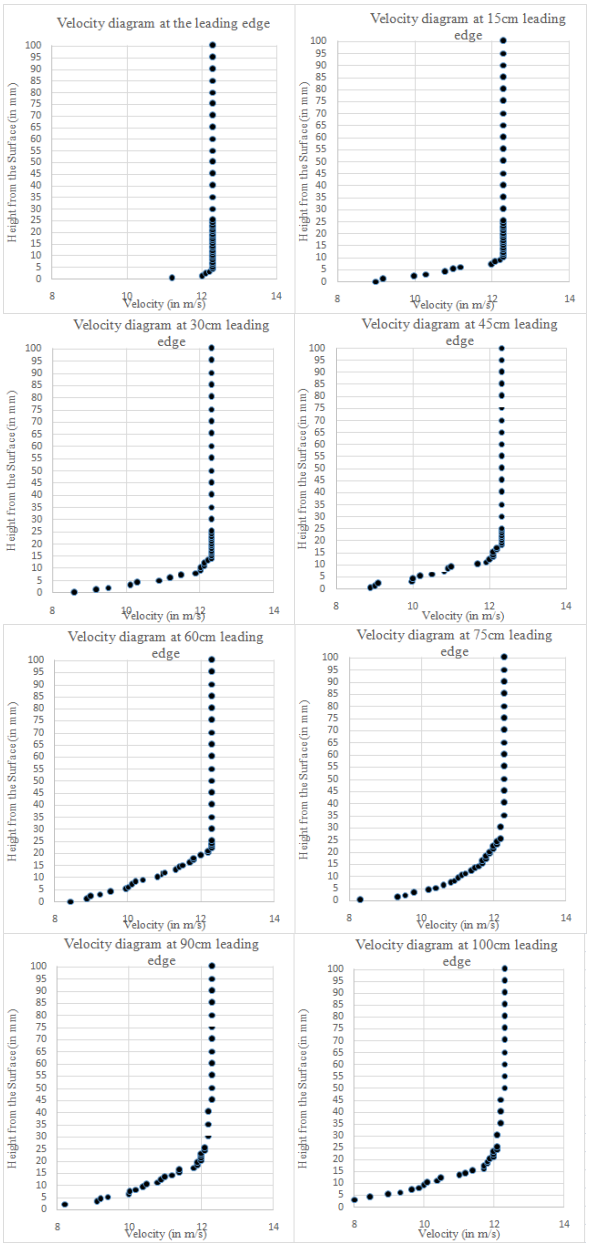

Fig 5: Velocity Profile Plots for 40 Grade at 5° inclination

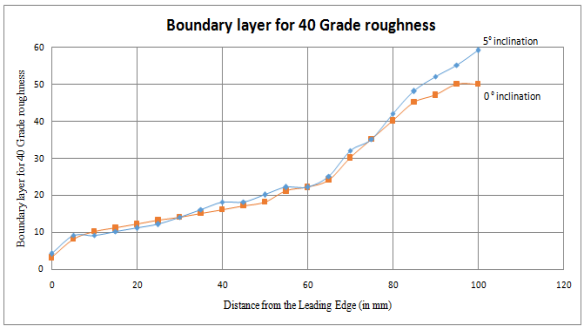

Fig 6: Boundary Layer Graph for 40 Grades

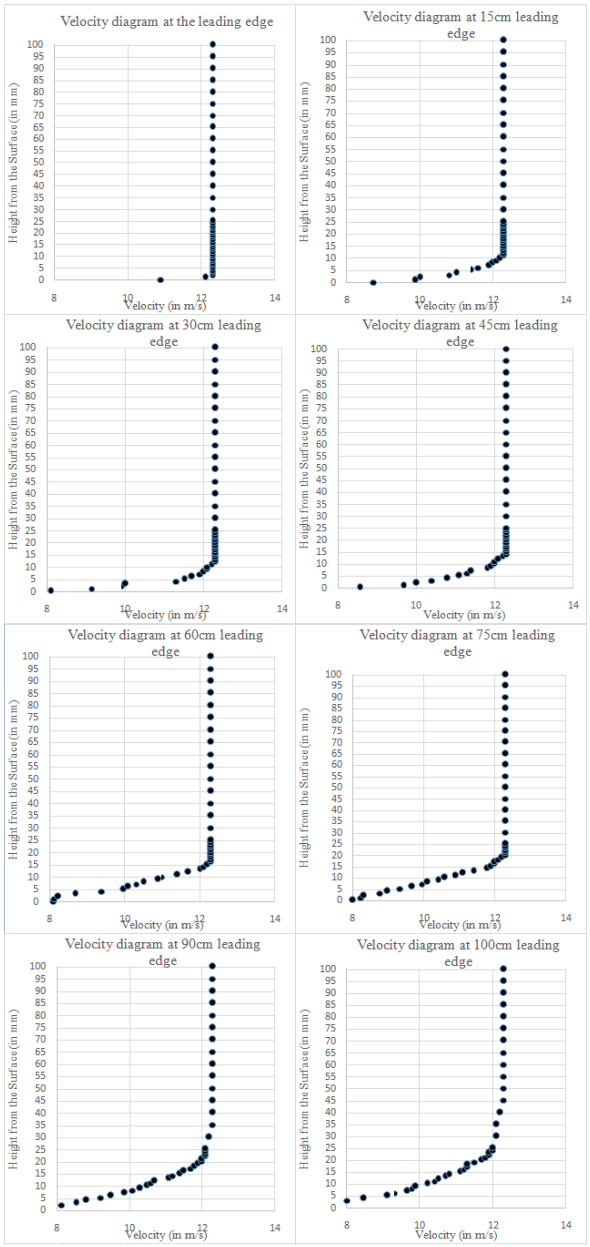

Fig 7: Velocity Profile Plots for 60 Grade at horizontal level

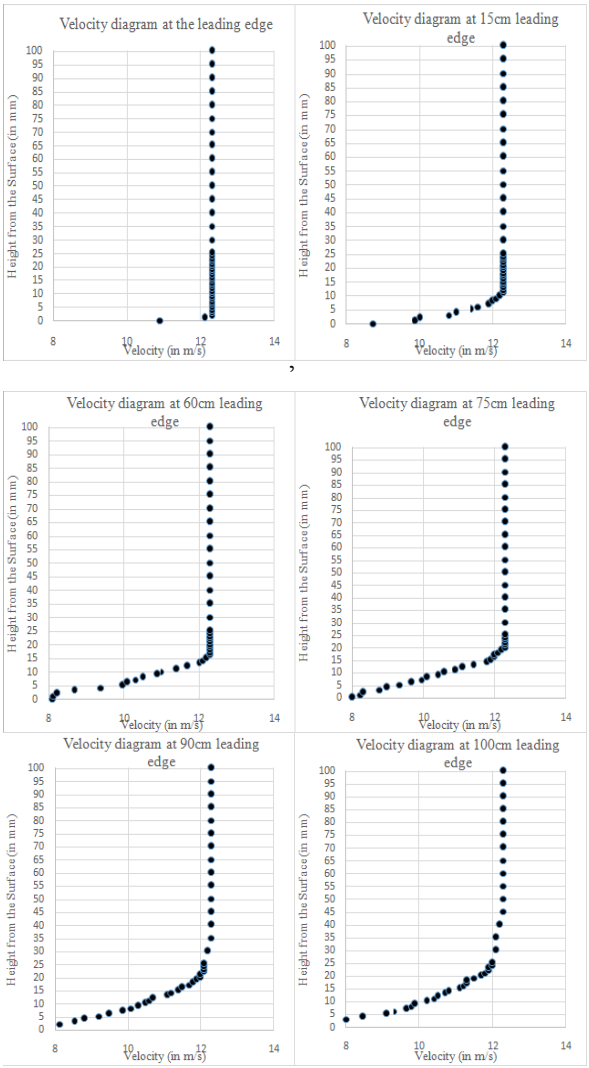

Fig 8: Velocity Profile Plots for 60 Grade at 5° inclination

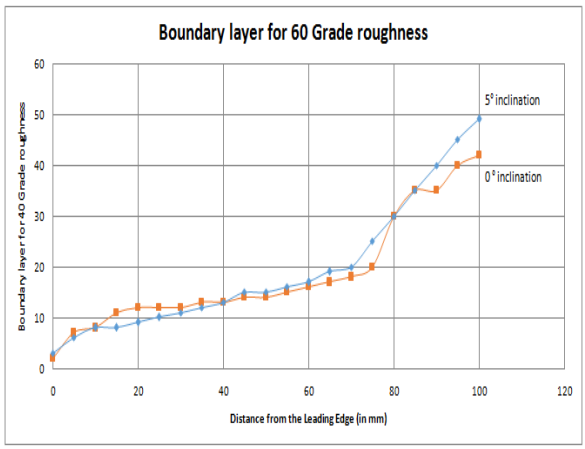

Fig 9: Boundary Layer Graph for 60 Grades

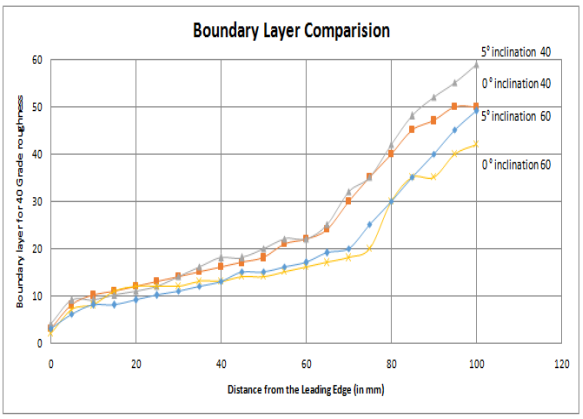

Fig 10: Boundary Layer Graphs

IV. CONCLUSION

The following conclusions can be presented by this work:

- From the velocity profile graphs, it is observed that profiles have steeper gradient near the leading edge as to the profiles generated in the latter section.
- Tests conducted on different rough flat plates gave a better understanding of boundary layers and the design. Study of Comparison between boundary layers of different – different roughness is easy.
- The velocity profiles gave a clear view of variation which took place along the length of the rough flat plate.
- There is no variation in the velocity magnitude in the lateral direction at a particular section and at the same level.
- By increasing the inclination from the horizontal; boundary layer thickness also increases.
- Tangent at each and every point of the boundary layer will be different from others.
- Uses of different grades 40, 60 and inclinations give a clear picture of boundary layer thickness close to each-other.

REFERENCES

[1] Schubauer, G. B. "Laminar boundary-layer oscillations and stability of laminar flow", *Journal of the Aeronautical Science*, 14(2), 1947, 69-78.

[2] Coles, Donald Earl. "Measurements in the boundary layer on a smooth flat plate in supersonic flow", *PhD diss.*, California Institute of Technology, 1953.

[3] Messiter, A. F. "Boundary-layer flow near the trailing edge of a flat plate", *SIAM Journal on Applied Mathematics, 18(1),* 1970, 241-257.

[4] Cook, N. J. "Wind-tunnel simulation of the adiabatic atmospheric boundary layer by roughness, barrier and mixing-device methods", *Journal of Wind Engineering and Industrial Aerodynamics 3(2),* 1978, 157-176.

[5] Ishihara, Takeshi, Kazuki Hibi, and Susumu Oikawa. "A wind tunnel study of turbulent flow over a three-dimensional steep hill", *Journal of Wind Engineering and Industrial Aerodynamics, 83(1)* 1999, 95-107.

[6] Osterlund, Jens M., "Experimental studies of zero pressure-gradient turbulent boundary layer flow," Ph.D Thesis, *Royal Institute of Technology, Department of Mechanics*, 1999.

[7] Lushchik, V. G., A. A. Pavel'Ev, and A. E. Yakubenko, "Transition to turbulence in the boundary layer on a plate in the presence of a negative free-stream pressure gradient", *Fluid Dynamics 39 (2)* 2004, 250-259.

[8] Defraeye, Thijs, Bert Blocken, Erwin Koninckx, Peter Hespel, and Jan Carmeliet, "Computational fluid dynamics analysis of cyclist aerodynamics: Performance of different turbulence-modelling and boundary-layer modelling approaches", *Journal of biomechanics 43(12)* 2010, 2281-2287.

[9] Okabayashi, Kazuki, Yoshinori Nagayama, Tomohiro Hara, Eiichi Hori, Yuji Ohya, and Takanori Uchida,"Development of Numerical Simulation Technique for Unsteady Turbulent Dispersion over Complicated Terrain-As an Alternative to Wind Tunnel Experiments", *Mitsubishi Heavy Industries Technical Review* 49(1) , 2012, 98-104.

[10] Mahmoudi, A. H., Shahi, M., & Talebi, F. "Entropy generation due to natural convection in a partially open cavity with a thin heat source subjected to a nanofluid", *Numerical Heat Transfer*, Part A: Applications, 61(4), 2012, 283-305.

International Journal of Engineering Research and Applications (IJERA) ISSN: 2248-9622
National Conference on Advances in Engineering and Technology
(AET- 29th March 2014)

RESEARCH ARTICLE OPEN ACCESS

Effect on Strength of Concrete after Adding Rice Husk Ash

Parvinder Singh[*], Balwinder Lallotra[**] and Vandana Patyal[***]
[*] Civil Engineering Department, Maharishi Markandeshwar University, Ambala.
(Email: singhparvinder270@gmail.com)
[**] Civil Engineering Department, Maharishi Markandeshwar University, Ambala.
(Email: balwinder.com@gmail.com)
[***] Civil Engineering Department, Maharishi Markandeshwar University, Ambala.
(Email: vandanapatyal2009@gmail.com)

ABSTRACT
The rice husk is one of the agriculture waste products which are creating health hazard and other environmental problems in our society. In India, there are large numbers of food plant which produces about the million tonnes of Rice Husk Ash (RHA) annually. As India is a fast growing country and need huge infrastructure, so there is an urgent need to utilize this waste to produce an economical and eco friendly concrete for infrastructural development. IS 456:2000 (Indian Standard: Plain and Reinforced Concrete – Code of practice) marked M15 and M20 grade of concrete as Ordinary concrete and the concrete grade above M15 are suitable for making RCC. This paper is based on the possibilities of using Rice Husk Ash (RHA) to replace cement partially. A comprehensive study on the properties of concrete (include workability of fresh concrete, compressive strength, modulus of elasticity for hardened concrete) containing rice husk ash is carried out. The results show that the strength of concrete grade M15 and M20 is maximum when 12.5% of cement content is replaced with Rice husk ash.

Key Words: Cement, Compressive strength, Pozzolanic reaction, Rice husk ash.

I. INTRODUCTION

Rice is one of the major food crops in the world. Its production generates an equally great amount of waste in the world, namely rice husk (RH), a by-product of the multistage processing of rice. The chemical composition of RH has been found to vary from sample to sample. Any of the differences in type of paddy, crop year, climatic and geographical conditions, soil chemistry, sample preparation, or method of analysis could be a reason for this variation. In many smaller towns and villages in southern parts of India, materials result in the form of fibers and granular materials as waste [1]. RH is an excellent source of high-grade silica. Rice husk has recently been recognized as pozzolona. A pozzolona is a siliceous/ aluminous material which in itself has little or no cementitious value. Addition of rice husk ash to Portland cement does not only improve the early strength of concrete, but also forms a calcium silicate hydrate (CSH) gel around the cement particles which is highly dense and less porous, and increase the strength of concrete against cracking. It was revealed that the structural nature of the silica produced from rice husk is independent of the purification methods but largely dependent on the incineration temperature used in the production process. Recycling of waste components contribute to energy savings in cement production, to conservation of natural resources, and to protection of the environment. Furthermore, the use of certain components with potentially pozzolanic reactivity can significantly improve the properties of concrete. One of the most suitable sources of pozzolanic material among agricultural waste components is rice husk, as it is available in large quantities and contains a relatively large amount of silica. Unlike natural pozzolana, the ash is an annually renewable source of silica. It is worth to mention that the use of RHA in concrete may lead to the improved workability, the reduced heat evolution, the reduced permeability, and the increased strength at longer ages.

II. OBJECTIVE

The objective of this study is to find out the various properties of concrete after adding various percentage of rise husk ash by weight of cement content in M15 and M20 concrete. In this study, rice husk ash in varying percentages (15%, 20%, 25%, 30% etc) by weight of cement is added and compressive strength of different concrete samples is determined.

III. MATERIALS

3.1 Rice Husk Ash

Rice Husk Ash is a major agricultural product obtained from paddy. The high percentage of

siliceous material present in rice husk ash indicated that it has pozzolanic properties.

3.2 Cement

Ordinary Portland cement (43 grades) available in local market is used in the investigation.

3.3 Fine Aggregate

River sand is used as fine aggregates and its specific gravity is 3.22. Table 1 shows the grading of fine aggregate.

Table 1: Grading of fine aggregate

IS sieve (mm)	% Retained	% Cumulative Retained	Cumulative % passing	Requirement of cum. % passing for Zone-II sand As per IS 383
10	0	0	100	100
4.75	2	2	98	90-100
2.36	13	15	85	75-100
1.18	20	35	65	55-90
600 micron	20	55	45	35-59
300 micron	24	79	21	8-30
150 micron	18	97	3	0-10
Residual	13	100	0	-

Fineness modulus: E_F= Cumulative % passing/100
=417/100
= 4.17

3.4 Coarse Aggregates

Crushed angular 20 mm size stones are used as coarse aggregates and its specific gravity is 4.17. Table 2 shows the grading of coarse aggregate.

Table 2: Grading of coarse aggregate

IS sieve (mm)	% Retained	% Cumulative Retained	Cumulative % passing	Requirement of cum. % passing for 20mm graded coarse agg. As per IS 383
40	0	0	100	100
20	4	4	96	95-100
16	36	40	60	-
12.5	24	64	36	-
10	10	74	26	25-55
4.75	22	96	4	0-10

Fineness modulus: E_C= Cumulative % passing/100
=322/100
= 3.22

IV. RESULTS

4.1 Cube Compressive Strength

Compressive strength tests are carried out on cube specimens of the age of 7 and 28 days curing. The test set up for compression strength on cube is shown in Fig 1 and Fig 2.

Fig 1: Compression Testing Machine

Fig 2: Cube Compressive Strength

4.2 Compressive Strength Results

Compressive strength tests are carried out on specimen size 150mm*150mm*150mm on 2000 KN capacity compression testing machine. Compressive strength results for M15 grade concrete is shown in the Table 4 and Fig 3. Table 3 shows the nomenclature of material used.

Table 3: Nomenclature

Symbol	M15 grade of concrete with	Symbol	M20 grade of concrete with
M15	No replacement	M20	No replacement
M15-R5	5% replacement	M20-R5	5% replacement
M15-R10	10% replacement	M20-R10	10% replacement
M15-R15	15% replacement	M20-R15	15% replacement
M15-R20	20% replacement	M20-R20	20% replacement

Table 4: Compressive Strength Result for M15 Concrete

SAMPLE	7DAYS STRENGTH N/mm^2	28 DAYS STRENGTH N/mm^2
M15	12.63	18.65
M15-R5	12.94	19.87
M15-R10	13.76	22.75
M15-R12.5	14.43	24.09
M15-R15	13.44	22.01
M15-R20	12.35	20.73
M15-R21	11.75	18.97
M15-R22	10.23	17.13

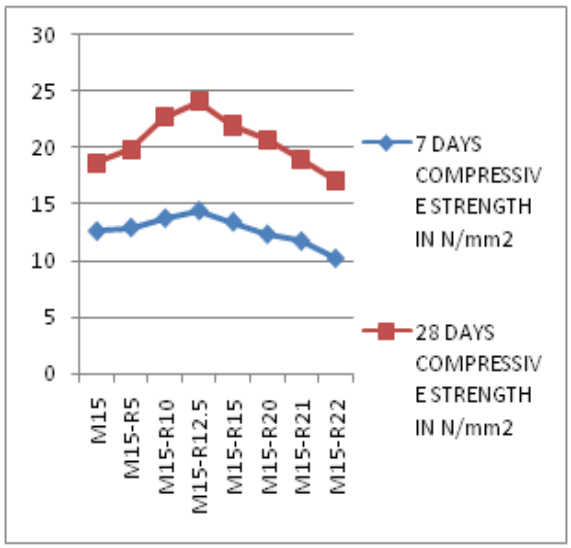

Fig 3: Graph for M15 Grade Concrete for 7 and 28 Days

Compressive strength results for M20 grade concrete is shown in the table 4 and the same is illustrated with the help of Fig 5.

Table 5: Compressive Strength Results for M20 Concrete

SAMPLE	7DAYS STRENGTH N/mm^2	28 DAYS STRENGTH N/mm^2
M20	16.70	23.72
M20-R5	17.94	25.20
M20-R10	18.87	27.89
M20-R12.5	19.04	28.13
M20-R15	17.02	27.02
M20-R20	16.54	23.79

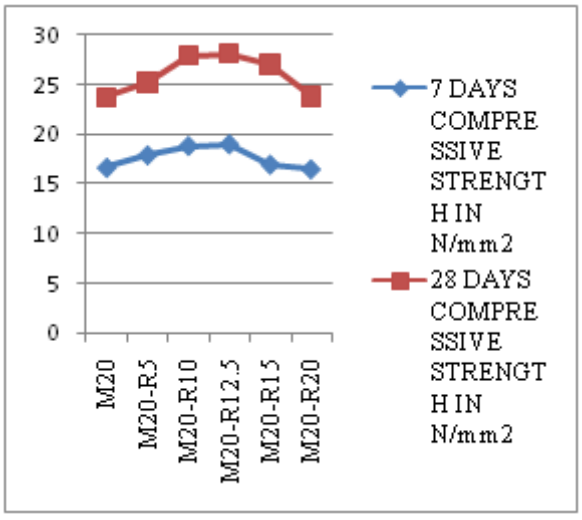

Figure 4: Graph Showing Results for M20 Grade Concrete for 7 and 28 Days

V. COST ANALYSIS AND COMPARISION

The cost comparisons for M15 Concrete and M20 Concrete are shown in Table 5 and Table 6.

Table 5: Cost Comparison for M15 Concrete

GRADE OF CONCRETE	CEMENT REPLACEMENT %AGE	CEMENT IN KG	PRICE PER KG	RHA IN KG	PRICE PER KG	COARSE AGGREGATE IN KG	PRICE PER KG	FINE AGGREGATE IN KG	PRICE PER KG	MIXING AND PLACING COST PER CUM (RS)	TOTAL COST PER CUMEC OF CONCRETE (Rs)
M15	NIL	300	6	-	1	1502.58	2	1118.36	2	600	7641
	5%	285	6	15	1	1502.58	2	1118.36	2	600	7567
	10%	270	6	30	1	1502.58	2	1118.36	2	600	7492
	12.5	262.5	6	37.5	1	1502.58	2	1118.36	2	600	7455
	15%	255	6	45	1	1502.58	2	1118.36	2	600	7417
	20%	240	6	60	1	1502.58	2	1118.36	2	600	7342
	21%	237	6	63	1	1502.58	2	1118.36	2	600	7327
	22%	234	6	66	1	1502.58	2	1118.36	2	600	7312

Table 6: Cost Comparison for M20 Concrete

GRADE OF CONCRETE	CEMENT REPLACEMENT %AGE	CEMENT IN KG	PRICE PER KG	RHA IN KG	PRICE PER KG	COARSE AGGREGATE IN KG	PRICE PER KG	FINE AGGREGATE IN KG	PRICE PER KG	MIXING AND PLACING COST PER CUM (RS)	TOTAL COST PER CUMEC OF CONCRETE (Rs)
M20	NIL	380	6	-	1	1407.699	2	1017.47	2	600	7730
	5%	361	6	19	1	1407.699	2	1017.47	2	600	7635
	10%	342	6	38	1	1407.699	2	1017.47	2	600	7540
	12.5%	332.5	6	47.5	1	1407.699	2	1017.47	2	600	7493
	15%	323	6	57	1	1407.699	2	1017.47	2	600	7445
	20%	304	6	76	1	1407.699	2	1017.47	2	600	7350

VI. CONCLUSION

Based on the experimental work, it can be concluded that RHA mixed cubes has equal or somewhere gives more strength with that of conventional concrete cubes. For M15 grade concrete, load carrying capacity is increased by 15 to 30 percent for certain percentages of Rice Husk and for M20 concrete, load carrying capacity is increased by 15 to 20 percent for certain percentages of Rice Husk.

Rice husk ash concrete proves to be eco friendly as it protects environment by utilization of waste products. By referring the cost comparison table, it can easily estimated that for the same strength, as in case of no replacement, we can save up to 22 percent of cement by replacing it by rice husk ash, hence it proves economical too.

REFERENCES

[1] M. Sivaraja and S. Kandasamy "Potential reuse of waste rice husk as fibre composites in concrete", *Asian journal of Civil Engineering (Building and housing),* 12(2), 2011, 205-217.

[2] Iyenagbe B. Ugheoke and Othman Mamat "A critical assessment and new research directions of rice husk silica processing methods and properties", *Maejo Int. J. Sci. Technol*., 6(3), 2012, 430-448.

[3] Ezzat Rafiee, Shabnam Shahebrahimi, Mostafa Feyzi1 and Mahdi Shaterzadeh, "Optimization of synthesis and characterization of nanosilica produced from rice husk (a common waste material)" , *International Nano Letters*, 29(2), 2012.

[4] M.U Dabai, C. Muhammad,B.U. Bagudo and A. Musa "Studies on the Effect of Rice Husk Ash as Cement Admixture", *Nigerian Journal of Basic and Applied Science*, 17(2), 2009, 252-256.

[5] Fernanda Giannotti da Silva, Jefferson B. L. Liborio, Paulo Helene ,"Improvement of physical and chemical properties of concrete with brazilian silica rice husk (SRH)", *Fecha de recepción*, 23(1), 2008,18 – 25.

[6] A. A. Ramezanianpour, M. Mahdi khani, Gh. Ahmadibeni "The Effect of Rice Husk Ash on Mechanical Properties and Durability of Sustainable Concretes", 7(2), 2009, 83-91.

[7] C.Marthong, "Effect of Rice Husk Ash (RHA) as Partial Replacement of Cement on Concrete Properties" *International Journal of Engineering Research & Technology (IJERT),* 1(6), 2012, 1-7.

[8] V. Ramasamy, "Compressive Strength and Durability Properties of Rice Husk Ash Concrete", 16(1), 2012, 93-102.

[9] IS:456-2000 *code of practice of design of concrete structures*.

[10] M.L. Gambhir, " Concrete Technology*", TMH Pub.*,2004.

[11] A.K. Goyal & I.C. Syal, "Design of concrete structures*", S.Chand Pub*., 2008.

[12] A.K. Jain, "Design of concrete structures", *Nem Chand & Bros*., 2002.

International Journal of Engineering Research and Applications (IJERA) ISSN: 2248-9622
National Conference on Advances in Engineering and Technology
(AET- 29th March 2014)

RESEARCH ARTICLE OPEN ACCESS

Experimental Investigation Of Flow Past A Rough Surfaced Cylinder

Monalisa Mallick[1], A. Kumar[2]
[1](Department of Civil Engineering, National Institute of Technology Rourkela, Odisha
Email: monalisa4489@gmail.com)
[2] (Department of Civil Engineering, National Institute of Technology Rourkela, Odisha
Email: akumar@nitrkl.ac.in)

ABSTRACT
The present work is the result of extensive experimentation on cylindrical bodies with varying cylinder diameters, surface roughness and air velocity. The experimental variables include cylinders of diameters as 12.5mm, 15 mm, 20 mm, and 25 mm, air velocity as 24.10, 24.45 and26.14 m/s andsurface roughness as 325 micron, 260 micron, 200 micron and 160 micron. The drag coefficient of flow in each case was calculated from data obtained by performing tests on an air flow bench (AF12). A comparison for the drag co-efficient and pressure distribution between the smooth and rough surfaces of the cylinders are extensively presented. In case of smooth surface cylinder, the separation angles for different diameter of cylinder calculation are found to be around 80^0~90° on either side of the cylinder from the upstream stagnation point. The drag coefficients for smooth surface of different diameter cylinders are calculated by experimentation and subsequent changes in drag due to introducing surface roughness are demonstrated. The surface roughness is found by experimentation of different drag coefficient.
Keywords-Cylinder, Drag coefficient, Drag force, Pressure distribution, Surface roughness.

I. Introduction

The resistance of a body as it moves through a fluid is of great technical importance in hydrodynamics and aerodynamics. The study of the performance of bodies in moving airstreams is called aerodynamics. Reduced drag force lowers fuel consumption, larger operational range and higher achievable speeds. Different flow phenomena such as flow separation, pressure distribution over the surface, drag, etc. are also studied at different diameter of cylinder.

Simplicity of geometric and widespread applications in real life, the flow past a circular cylinder has been a subject for studies. Drag coefficient is a function of speed, flow direction, object position, object shape and size, fluid density and fluid viscosity. Theoretical flow over a cylinder is considered to be in viscous, incompressible and irrotational; known as 'Potential Flow' in which the reattachment of streamlines is considered to be complete and symmetrical to detachment at the upstream resulting in zero drag force. In real life, more or less, drag is present in case of flow over the body. There is presence of viscosity and the flow is neither incompressible nor irrotational. This paper is subjected to experimental investigation of air flow over a circular cylinder of different diameter. Experimental procedure is carried out in an airflow bench with a circular cylinder of different diameter having a pressure distribution and drag force on the surface. separation angle on both the top and bottom surfaces at zero relative roughness by predicting the instability of coefficient of pressure C_P at the surface of the cylinder as C_P tends to fluctuate frequently within the separated zone. Coefficient of drag C_D is another important dimensionless parameter whose relative fluctuation is observed under different surface roughness which can be used to predict the critical relative roughness for flow over the cylinder. Experimental procedure is to measure C_P at different angular position on the surface of the cylinder to predict the overall drag coefficient and separation angle of the cylinder. Many researches had been carried out to predict the variation of Co-efficient of drag vs. Reynolds number for circular cylinder.

Effect of relative roughness on drag for the flow over circular cylinder was observed [1], in the range of Reynolds number 6×10^3 to 5×10^6. Authors investigated vortex shedding phenomena in this range. In [2], authors described the effect of three dimensionality on the lift and drag of nominally two-dimensional cylinders which is useful to describe the variation of numerical results between two dimensional and three dimensional analysis. Authors also described the effect of surface

roughness for flow over a body at high Reynolds number using wind tunnel. In [3], authors presented comprehensive description of flow phenomena at different Reynolds number and in [4], authors studied that drag reduction of a circular cylinder in an air-stream is studied the flow characteristics of a bluff body cut from a circular cylinder. Two types of test models were employed in their study. In [5], authors discussed flow past a circular cylinder for Re= 10^0 to 10^7numerically by solving the unsteady incompressible two dimensional Navier-Stokes equations. In [6], authors used I-type small cylinder with a cutting angle of θs =65º as passive control at a stagger angle of α=0 and it is most effective in reducing the drag of the large circular cylinder, among the passive control cylinders used in this investigation. In [7], authors described separation angle for flow over the cylinder at low Reynolds number. In [8], authors presented the result of an investigation on the effect of wind turbulence for the reduction of drag for a speed skater. A speed skater competing in an indoor oval is subjected to turbulent flow condition. The goal of the research is to calculate drag coefficients for different Reynolds numbers. The goal of the report is to identify the characteristics of different drag coefficient on bluff body aerodynamics and to show the need of slender bodies through the drag values. In [9], authors presented that a circular cylinder produces large drag due to pressure difference between upstream and downstream. The difference in pressure is caused by the periodic separation of flow over surface of the cylinder.

II. Experimentation

Hydraulic mechanics Lab facilities of National Institute of Technology (NIT) was used to study the flow over the cylinder experimentally. The set-up air flow bench as shown in Fig 1, consists of two types of attachments: (i) for drag force by direct weighing method as shown in Fig 2, and (ii) drag co-efficient by pressure distribution method as shown in Fig 3.The setup consists of adjusting lever to control flow, a multitube manometer for pressure measurement. A circular cylinder has been placed with its axis normal to the direction of airstream and resistance (drag) has been measured by two methods: (i) by direct weighing method, and (ii) by pressure distribution method.

In Direct weighing method, drag force due to air flow was balanced by applying suitable load on the lever of the set up. Similarly, the pressure data have been noted for the varying angular position (0^0-180^0 and 180^0 to 360^0) with respect to the direction of flow. The same procedure for the measurement of drag force and pressure distribution has been repeated for varying diameter of cylinders, velocity of air flow and surface roughness.

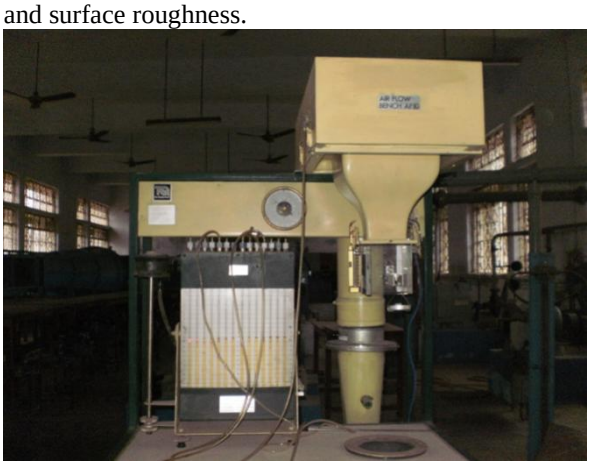

Fig 1: Experimental setup

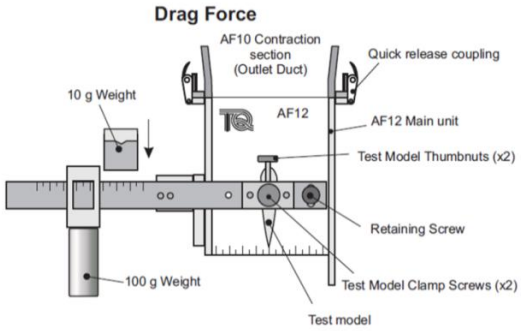

Fig 2: Drag Force by Direct weighing method

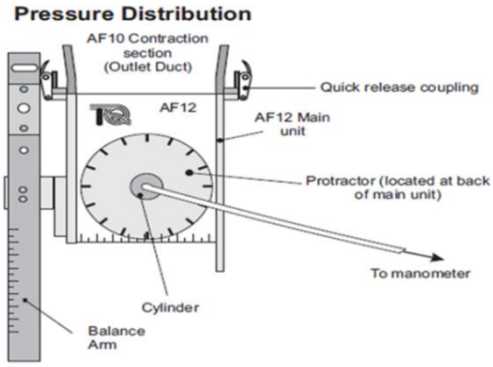

Fig 3: Drag Coefficient by Pressure Distribution method

III. Results and Discussion

Fig 4, Fig 5 and Fig 6 represent variation of drag coefficients as obtained from direct measurement method with cylinder diameters of varying surface roughness. The variation of drag co-efficient with air flow velocity for the cylinders of varying roughness have been shown in Fig 7, Fig 8, and Fig 9. Similary the variation of drag co-efficient with velocity for the same roughness of cylinders of

different diameters have been presented in Figures 10 to 12. A typicalplot shown in Fig 13, Fig 14, Fig 15 and Fig 16, has been shown for pressure distribution at varying location for the cylinder of same roughness and varying diameters.

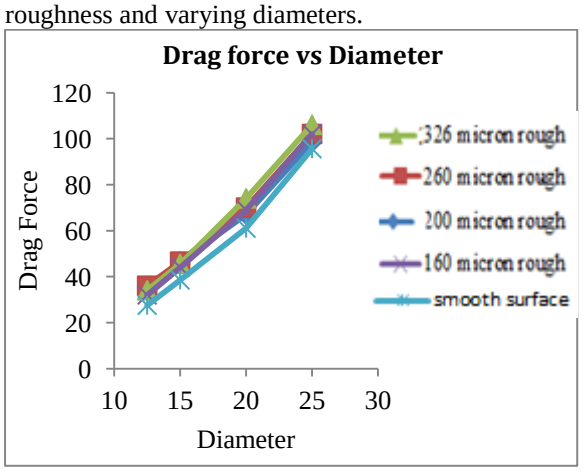

Fig.4 Drag force for Different diameter of cylinder at velocity=26.14 m/sec

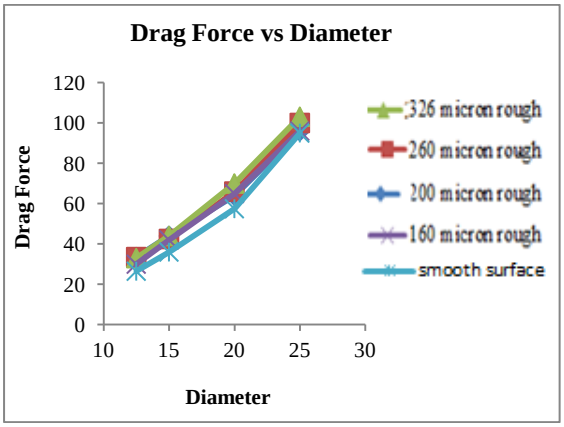

Fig.5 Drag force for Different diameter of cylinder at velocity=24.45 m/sec

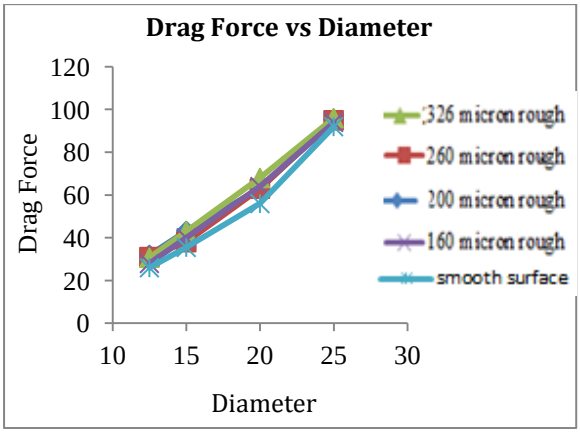

Fig.6 Drag force for Different diameter of cylinder at velocity=24.10 m/sec.

The experimental data of drag force obtained under varying conditions of flow velocity and constant diameter of the cylinder have been plotted in Fig 4 to Fig 6. In this case diameter is constant, velocity increase and drag force increase. In smooth surface drag force is less when roughness increases drag force will increases.

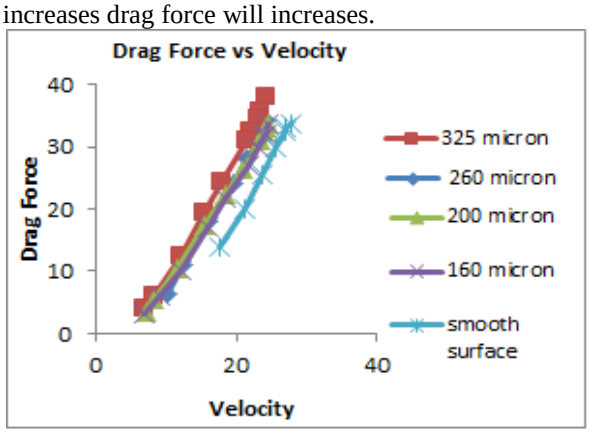

Fig.7 Drag force for 12.5mm diameter of cylinder at different roughness.

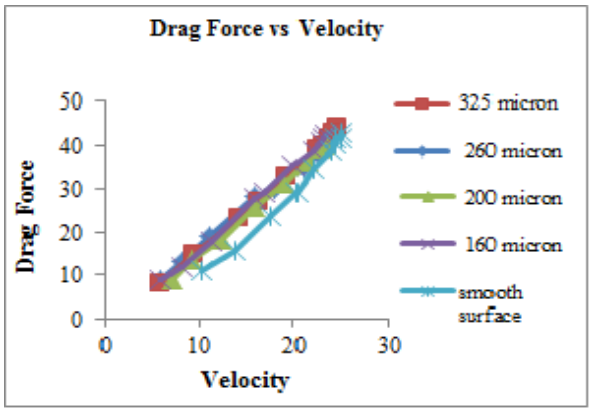

Fig.8 Drag force for 15mm diameter of cylinder at different roughness.

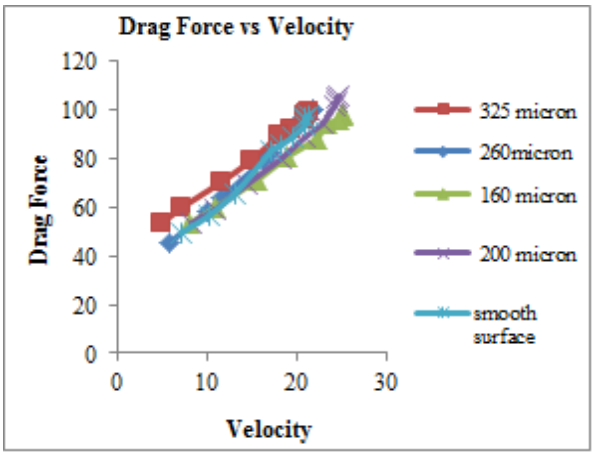

Fig.9 Drag force for 25mm diameter of cylinder at different roughness.

In this above graph to show the effect of diameter and velocity together, drag force versus velocity plot is presented for different diameters of the cylinder in Fig 7 to 9.

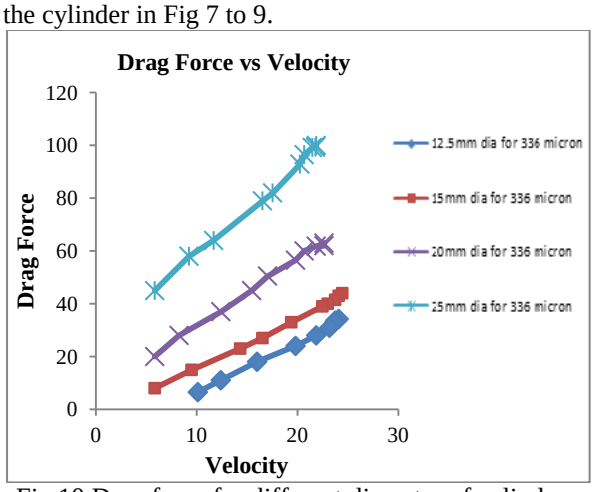

Fig.10 Drag force for different diameter of cylinder having roughness 336 micron.

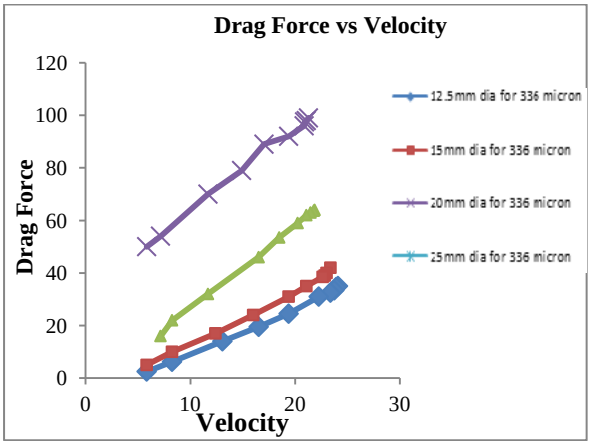

Fig.11 Drag force for different diameter of cylinder having roughness 260 micron.

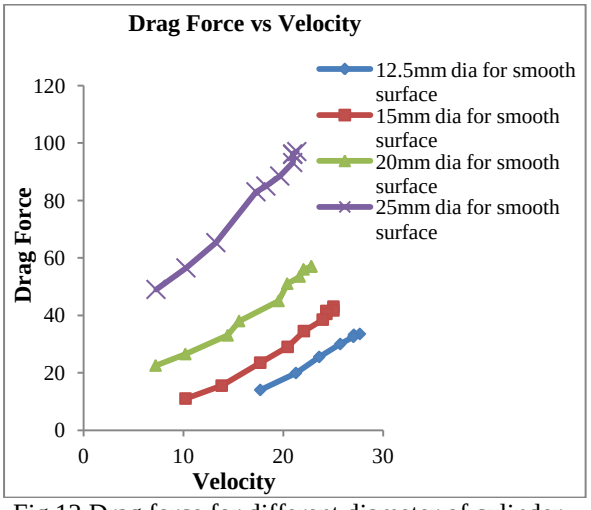

Fig.12 Drag force for different diameter of cylinder for smooth surface.

The above experimental data of pressure coefficient obtained under varying angles of incidence for the different conditions with velocity constant and diameter of the cylinder have been plotted in Fig 13 & Fig 14. Pressure distribution between smooth and rough surface of the cylinder calculation are found to be around 80^0-90^0 on either side of the cylinder from the upstream stagnation point.

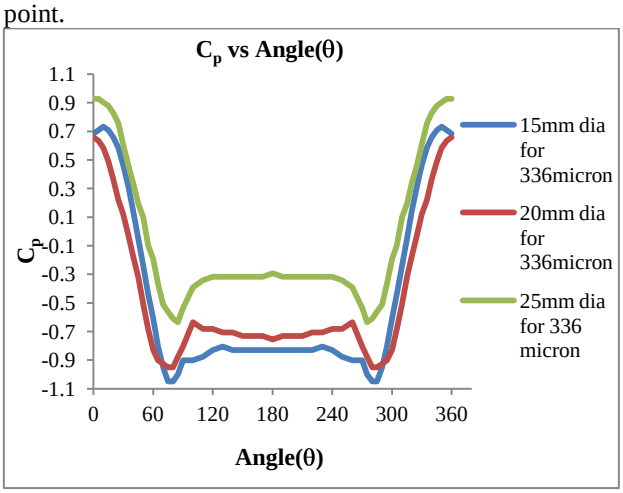

Fig.13At constant velocity 26.50 m/s distribution of $C_p$for different diameter of rough cylinder.

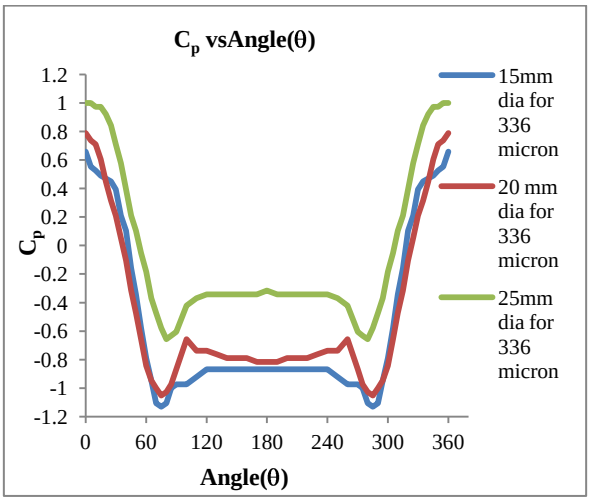

Fig.14At constant velocity 25.51 m/s distribution of C_p for different diameter of rough cylinder.

To show the effect of pressure coefficient and angle of incidence together, $C_p\cos\theta$ versus degree (θ) plot is presented for different diameters of the cylinder Fig 15 & Fig 16. Now C_D for experimental results derived from the area under the curve C_P Vs. $\cos\theta$ Fig 15 is 1.04 and Fig 16 is 1.02.

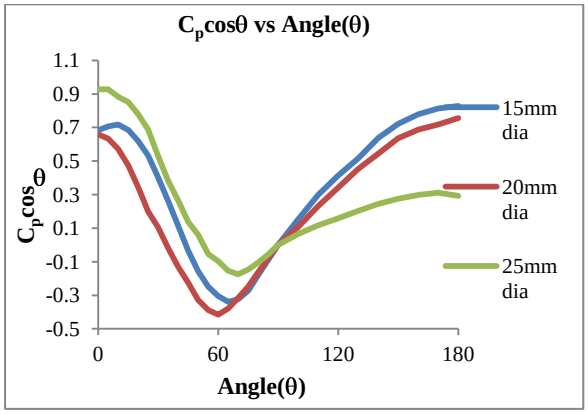

Fig.15 Pressure Distribution for different diameter of cylinder for roughness 336 micron and $C_p\cos\theta$.

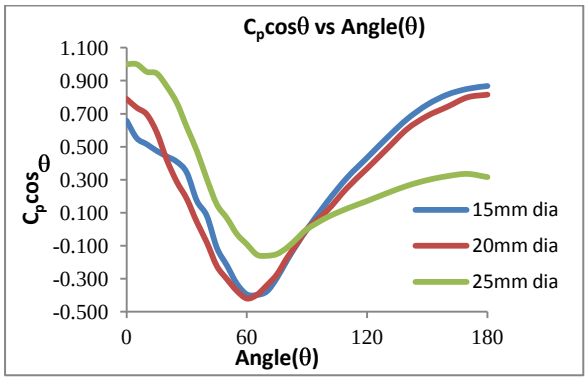

Fig.16 Pressure Distribution for different diameter of cylinder for roughness 336 micron and $C_p\cos\theta$.

IV. Conclusion

From the experimental findings and different plots shown above, the following conclusions can be derived:

- The drag force increases with increase in diameter of the cylinder.
- For a cylinder of particular diameter and roughness, drag force has been found to increase with increase in air velocity.
- Also, for a cylinder of given diameter and velocity, the drag force increases with surface roughness.
- As compare to both methods of drag force, the direct measurement method gives more reliable than the pressure distribution method. The drag co-efficient in earlier case has been found close to unity.
- The results of pressure distribution profiles clearly showthat the flow separates at around 80^0-90^0 on either side of the cylinder from the upstream stagnation point.
- The present study under taken can be further extended to studythe effect ofsurface roughness on flow parametersfor different shape and configuration of objects.
- The effect of surface roughness on the separation angle can be another centre of interest for future researchers.

References

[1] Achenbach, E., and Heinecke, E., "On vortex shedding from smooth and rough cylinders in the range of Reynolds numbers 6×10^3 to 5 $\times10^{6}$", *Journal of Fluid Mechanics*, 109, 1981,239-251.

[2] Mittal, R.andBalachander, S., "Effect of three-dimensionality on the lift and drag of nominally two-dimensional cylinders", Physics of Fluids, 7, 1995, 1841- 1865.

[3] Williamson, C.H.K. , "Vortex Dynamics in the Cylinder Wake", *Annual Review of Fluid Mechanics*, 28, 1996, 477-539

[4] T. Tsutsui and T. Igarashi, "Drag reduction of a circular cylinder in an air-stream," *Journal of Wind Engineering and Industrial Aerodynamics*, 90, 2002, 527-541,

[5] Singh, S.P.,and Mittal, S., "Flow Past a Cylinder: Shear Layer Instability and Drag Crisis" ,*International Journal for Numerical Methods in Fluids*, 47, 2005, 75-98.

[6] Y Triyogi, D Suprayogi, and E Spirda, " Reducing the drag on a circular cylinder by upstream installation of an I-type bluff body as passive control", *J.Mech.Engg. & Sci. 10.* 223, 2009, 2291-2296.

[7] Sen, S., Mittal, S., and Biswas, G., "Numerical Simulation of Steady Flow Past a Circular Cylinder", *Proceedings of the 37th National & 4th International Conference on Fluid Mechanics and Fluid Power, IIT Madras*, 2010, 16-18.

[8] Annick D., Auteuiln, Guy L., Larose, Steve J., Zan J., "Wind turbulence in speed skating Measurement, simulation and its effect on aerodynamic drag", Wind Eng. *Ind. Aerodyn*.104-106, 2012, 585–593.

[9] U. Butt and C. Egbers, "Aerodynamic Characteristics of Flow over Circular Cylinders with Patterned Surface," *International Journal of Materials, Mechanics and Manufacturing*, 1(2), 2013, 121-125.

International Journal of Engineering Research and Applications (IJERA) ISSN: 2248-9622
National Conference on Advances in Engineering and Technology
(AET- 29th March 2014)

RESEARCH ARTICLE OPEN ACCESS

Identification of Accident Prone Locations Using Accident Severity Value on a Selected Stretch of NH-1

Gourav Goel *, S.N. Sachdeva **
*(Department of Civil Engineering, M. M. Engineering College, Mullana-133207, Haryana, India
Email: gouravgoelshinu@gmail.com)
** (Department of Civil Engineering, NIT, Kurukshetra, India
Email: snsachdeva@yahoo.co.in)

ABSTRACT
Growing number of road accidents needs to be controlled by identifying the accident prone locations on road stretches. In this paper a study has been carried out on road accident data of a selected stretch of NH-1 (Delhi-Ambala-Amritsar Road). A 50 km road stretch between RD 98 km to 148 km was selected and road accident data of four years (2007-2010) was collected. The 6-laning work of NH-1 is in progress during the selected period so the study considers the effect of widening project on road accidents also. To identify the accident prone locations the total stretch was divided into smaller sections of 5 km each. Total accidents and accident severity value has been used to rank the accident prone locations. The stretch of the road 140-144 km is found to be the most accident prone followed by the stretch 98-104 km and the stretch 145-148 km. A field study has been conducted to compare the analysis with field results.

Keywords **-** Road Accidents, Accident Prone Location, Accident Severity Value.

I. INTRODUCTION

Road transportation provides benefits to everybody by facilitating the movement of goods and people. It enables increased access to jobs, economic markets, education and health care, which in turn have direct and indirect positive impacts on the health of population of the country. However, increase in road transportation has considerably increased the number of road accidents also. A number of studies on road accident study pattern have been carried in India in the past. In [2], authors used accident prone index to identify black spots on roads. In [1], authors ranked accident prone locations by calculating accident rates. In India we have only 2% of road length of national highways out of total road length to accommodate 40% of the total traffic on Indian roads. This has resulted in a steep increase in number of road accidents fatalities in India which is alarming. Between 1970 to 2009, the number of road accidents increased by 4.3 times with more than 7 fold increase in injuries and about 8.7 times increase in fatalities in the backdrop of about 3 fold increase in road network. Around 56 road accidents take place every hour in which 14 deaths occurs on roads in India. There is a great need to take up measures that can help improve road safety in the country. Safety on roads has become a major area of concern. The number of persons killed in road accidents has increased considerably from during in the last decade. The road accident data in India during 2002-2009 has been given in Table 1, [4].

Table 1: Numbers of Accidents during 2002-2009 in India

Year	Number of Accidents	Number of Persons Killed
2002	4,07,497	84,674
2003	4,06,726	85,998
2004	4,29,910	92,618
2005	4,39,255	94,968
2006	4,60,920	1,05,749
2007	4,79,216	1,14,444
2008	4,84,704	1,19,860
2009	4,86,384	1,25,660

As NHs are responsible for causing about 40% of fatalities on Indian roads. The present study has been undertaken to identify and suggest remedies for the accident prone locations on road stretch RD 98km-148km of NH-1.

II. DATA COLLECTION

The accident data is collected for four years from 2007 to 2010 from National Highway Authority of India (NHAI) and SOMA Isolux. NHAI is associated with maintenance and construction of NHs in the country. The SOMA Isolux construction

company is presently engaged in widening project of NH-1 from Panipat to Jalandhar. The study also evaluates the impact of 6-laning widening project on road accidents which started in May, 2009. The accident data includes that data also. The accident data contain the information like date, time and location of accidents. The data also include type of accident (fatal / minor or serious injury), number of persons dead / injured, vehicles involved in accident, probable cause of accident and the jurisdiction of the police station.

III. METHODOLOGY OF STUDY

The study aims at identifying and improving the accident prone locations on a given stretch of NH-1. With this objective in view, the accident data of the selected road stretch for the study, 98km-148km of NH-1, were collected from different sources. The collected data of the year 2007 to 2010 has been analyzed by dividing the selected stretch of NH-1 from 98 km to 148 km into smaller stretches of approximately 5 km each. After analysis of the data, the results are summarized. The effect of 6-laning work on road accidents has been evaluated by dividing total number of accidents into two groups before construction and after construction work started. The accident prone locations are identified using the concept of Accident Severity Value (ASV) and field visits are made to check the real time locations conditions.

IV. EFFECT OF 6-LANING PROJECT

The data of accidents is analyzed with reference to location of occurrence of accident. Table 2 shows the total number of accidents per year that occurred on different locations in the period 2007-10. It is clear that the number of accidents in every stretch increased considerably after construction work. It is worth noticing that in 2009 construction work started in May only. The maximum number of accidents takes place between 98-104 km followed by 105-109 km and 109-114 km.

It shows that construction activity has led to significant increase in accidents on the road. The increase in accidents can very well be attributed to non-compliance of safety measures in the construction zones and increased congestion on the road due to lesser carriageway available for the movement of traffic.

Table 2: Total Number of Accidents during 2007-2010

Year / Stretch	Before Construction			After construction Work Started	
	2007	2008	2009	2009	2010
98-104	6	2	0	60	123
105-109	3	1	0	32	103
110-114	5	0	2	42	100
115-119	5	4	0	29	63
120-124	10	7	1	37	51
125-129	7	13	1	37	69
130-134	13	11	4	40	69
135-139	6	15	3	41	77
140-144	7	19	5	48	82
145-148	11	10	5	36	69

V. IDENTIFICATION OF ACCIDENT PRONE LOCATIONS

Accident prone locations are identified by using the concept of Accident Severity Value (ASV).

a. Accident Severity Value:

The Accident Severity Value measures the severity or injury level of an accident. In this concept different injury levels are given some values based on their severity. For this study, following values have been given to different types of accidents.

- Fatal Accident: It is a serious accident in which death occurs either at the spot or later provided the cause of death is the injury received in the accidents. The severity value given to the fatal accident is 10.
- Serious Injury Accident: It is an accident in which a person is injured badly or severity is more but no death occurs. The severity value given to the serious injury accident is 5.
- Minor Injury Accident: It is an accident in which a person suffers minor injury. The value given to this type of accident is 3.
- Non Injury Accident: It is an accident in which no injury takes place. The severity value given to this type of accident is 2.

By using the values assigned to each type of injury level, Accident Severity Value has been calculated various locations of the studied stretch and tabulated in Table 3.

Table 3 Accident Prone Locations by ASV

Sr. No.	Stretch (km)	Fatal Injury	Serious Injury	Minor Injury	Non Injury	Total No. of Accident	Accident Severity Value	Ranking of Stretch
1.	98-104	10	36	40	115	191	630	2
2.	105-109	7	47	23	78	139	581	6
3.	110-114	4	27	18	96	149	487	7
4.	115-119	6	27	15	58	101	431	9
5.	120-124	4	25	10	72	110	429	10
6.	125-129	2	37	20	67	127	459	8
7.	130-134	8	50	31	67	137	584	5
8.	135-139	12	45	37	67	142	599	4
9.	140-144	10	61	37	62	161	649	1
10.	145-148	10	70	24	44	131	658	3

It is observed from the table that maximum number of accidents take place on 98-104 km stretch followed by 140-144 km and 110-114 km. However, when we take severity of accident into consideration, stretch 140-144 km comes out to be the most critical followed by 98-104 km and 145-148 km.

b. Field Visits

In order to understand the location specific causes, field visits were taken up. The photographs of various locations of the road have been given from Fig 2, Fig 3, Fig 4, and Fig 5.

Fig 2: Lack of Proper Diverging Lane (RD 143.400 Km)

Fig 3: Sharp Diversion (RD 140.000 Km)

Fig 4: Wrong Signage near Toll Barrier (RD 145.000 Km)

Fig. 5 Road Side Development on Y- Junction (RD 129.030 Km)

VI. IMPROVEMENT MEASURES

Over speeding/ driver's fault and lack proper control measures are found to be main reason for most of accidents taking place on the road, effective speed regulation measure need to be taken on the road. This results in high speed driving even through

these stretches leading to more accidents in these areas. It is suggested that:

1. Rational speed safe limits should be determined based upon 85th percentile speed of vehicles on the road.
2. Proper signage should be put in place and violators be punished by the enforcement agencies.
3. Proper diverging lane should be provided.
4. Road side development should be discouraged.
5. It is observed through analysis of collected road accident data that accident increased tremendously after construction work for widening of 6-laning started in May, 2009. Field study of various sits of the studied stretch indicated that proper safety measures have not been taken in the construction zones. A layout plan of signs and control devices for a typical road with a diversion as recommended by IRC-SP-55 is shown in Fig 6. It is seen that nowhere in the studied stretch of the road the guidelines of IRC-SP-55 have been followed which is one of the main reasons for increase in number of accidents after start of construction of widening project.

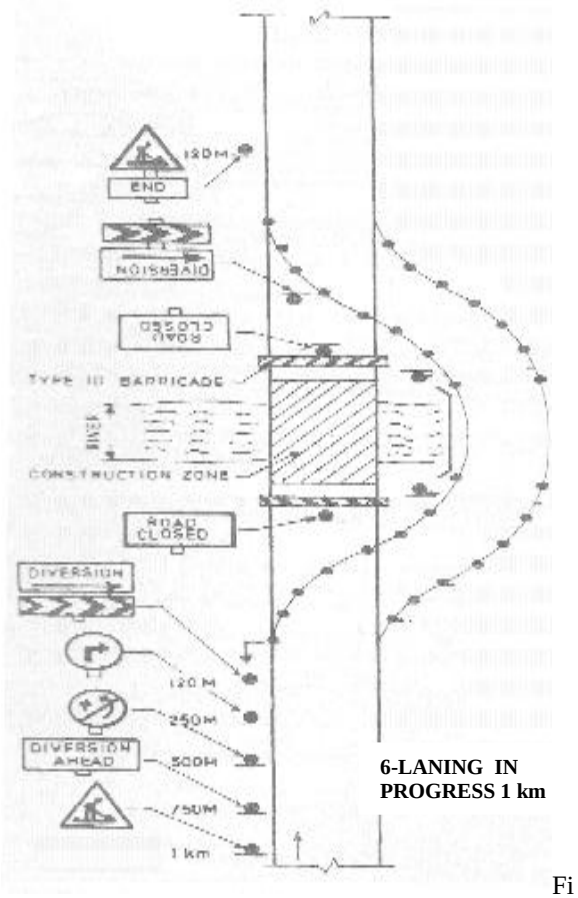

Fig 6: Layout of signs and control devices for road closed with diversion

VII. CONCLUSIONS

The study presented in the dissertation has been conducted to identify the accident prone locations on the selected stretch (98-148 km) of NH-1 and suggest the improvements. The following are the main conclusions drawn from the study:

1. The road accident data for the year 2007-10 for the stretch 98-148 km of NH-1 was collected from NHAI and Soma Isolux, the agency involved in widening project of NH-1.
2. The number of accidents increases tremendously after the start of construction work in May, 2009 for widening of NH-1.
3. The concept of accident severity value has been used to identify more accident prone locations on the studied stretch of the road. The selected 50 km stretch of the road is further divided into sub-stretches of length about 5 km each. Using the concept of accident severity value these sub-stretches have been ranked 1 to 10 in order of their decreasing accident severity value.
4. The stretch of the road 140-144 km is found to be the most accident prone followed by the stretch 98-104 km and the stretch 145-148 km.

REFERENCES

[1] A. Anne Rosaline, B. Sathya Naraynan and S. Shanmuga Sundara Boopathy, "Comparison of Accident Rate Using Accident Ranking", Indian Highways, 2010.
[2] A. Ramesh and M. Kumar, "Road Accident Models for Hyderabad Metropolitan City of India", Indian Highways, 2011.
[3] IRC-SP-55-2001, "Guidelines on Safety in Road Construction Zones".
[4] Sensarma Kuntal, Balani Nimmi, Rawat S S, "Road Accidents in India, 2009", 2011.

International Journal of Engineering Research and Applications (IJERA) ISSN: 2248-9622
National Conference on Advances in Engineering and Technology
(AET- 29th March 2014)

RESEARCH ARTICLE OPEN ACCESS

Review Of Algorithms For Control Systems For Civil Engineering Structures

Pratyush Malaviya*, Sandeep Lamba*, Anil Kumar*
*(Department of Civil Engineering, Jaypee University of Information Technology
Waknaghat, Solan (H.P.) – 173234
Email: pratyushmalaviya@gmail.com
Lamba5550@gmail.com

ABSTRACT
One of the most significant technological innovations in the structural engineering field is the practical application of active and semi-active control to civil structures. A number of structures integrating active, hybrid, and semi-active response control technologies have been constructed in Japan, China and USA. Any control system whether it is in aircraft, spaceship or building; it needs an algorithm to be run by the computer installed in the structure. A state-of-the-art review on algorithms for response-triggered structural control systems is presented. The review focuses on the active control of structures for earthquake excitations, and covers theoretical backgrounds of different active control schemes, important parametric observations on active structural control, limitations and difficulties of their practical implementation, and brief descriptions of three actively controlled tall buildings in Japan. A brief introduction of more promising semi-active control of structures is also presented. This study focuses on the development of an active control algorithm based on several performance levels anticipated from an isolated building during different levels of ground shaking corresponding to various earthquake hazard levels. The proposed active control algorithms change the control gain depending on the level of shaking imposed on the structure. These active control systems have been evaluated using a series of analyses performed on ground motion records. Simulation results show that the newly proposed algorithms are effective in improving the structural as well as nonstructural performance of the building for selected earthquakes.
Keywords **–** Active Control, Algorithms, Control-theories, Structure Control-System.

I. INTRODUCTION

The most important task of civil engineering structures is to design them such that they can withstand the forces and accommodate the deformations without major damage or a collapse. The response of the system can always be limited by providing stiffer structural members but in general the system would become uneconomical. So it has been a common practice to generate more ductile designs, providing the means for adequate energy dissipation through the yielding of individual members and generation of localized plastic hinges. The occurrence of damage during a seismic event is unavoidable in this design philosophy. Further, the permanent deformations in the structure surviving the seismic events may seriously affect its service life. Recently the attention of the civil engineering community has moved on reducing forces and deformations in structures through the methods of the structural control in which information is fed into the controller which processes the measured quantities and structural properties to generate the corresponding control signal, which is then input to the actuators which may be driven by a power source to produce the control action, as shown in Fig 1. These method of response reduction can address not only the prevention of total failure or the limitation of damages but also they can be designed to provide comfort to the occupants of the structure on the basis of mode of operation of these special devices the structural response control methods can be broadly classified as passive, active and semi-active control approaches.

A passive control system does not require an external power source for operation and utilizes the motion of the structure to develop the control forces. Control forces are developed as a function of the response of the structure at the location of the passive control system. An active control system typically requires a large power source for operation of electro-hydraulic or electro-mechanical actuators which supply control forces to the structure. Control forces are developed based on feedback from sensors that measure the excitation and/or the response of the structure. The feedback from the structural response may be measured at locations remote from the location of the active control system.

A semi-active control system requires a relatively small external power source for operation (like a battery) and utilizes the motion of the structure to develop the control forces, the magnitude of which can be adjusted by the external power source. Control forces are developed based on feedback from sensors that measure the excitation and/or the response of the structure. The feedback from the structural response may be measured at locations remote from the location of the semi-active control system. Sometimes these systems are combined to form hybrid control systems.

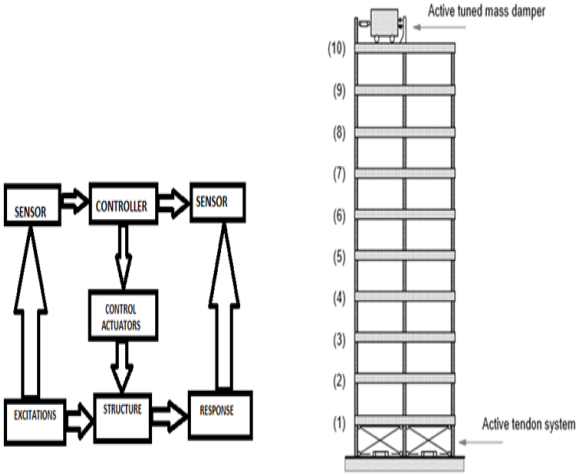

Fig 1: Control system applied on a building

Some actual applications of active control schemes for the reduction of wind-induced vibrations of tall buildings have been reported. The 11-storey building made of rigid steel frames is located at Chuo-Ku, Tokyo, with a frontage of 4 m and a total height of 33 m. Two AMDs are located at the top floor, spaced apart with masses of 4 tons and 1 ton, respectively Fig 2. The idea of providing two AMDs was to control the torsional response of the structure also. The schematic diagram of the AMD is shown to actuate the masses. Sensors are placed at the basement, 6th floor, and at the 11th floor. The computer is provided on the top floor itself. This is the world's first AMD installed on a building. Sensors are placed at the basement, 6th floor, and at the 11th floor. Other example is a Duox system on ANDO Nighikicho, Tokyo. It has 14 storeys and two basement levels, and is made of rigid steel frames. Above the ground, mass of the building is 2600 tons. Two-directional simultaneous AMD is placed on the top of a TMD which is placed on the top floor as shown in Fig 3. The damping system of the TMDs consists of oil dampers. The TMD mass is 18 tons, while the AMDs have 2-ton mass, each. The Duox system operates on the principle that if the active control system fails, the TMD will provide at least the minimum control of response.

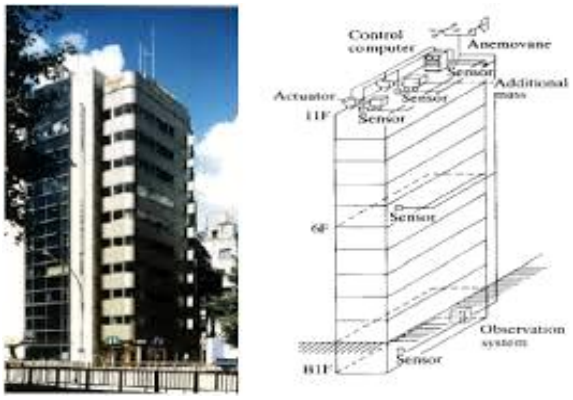

Fig 2: Building at Chuo-Ku.

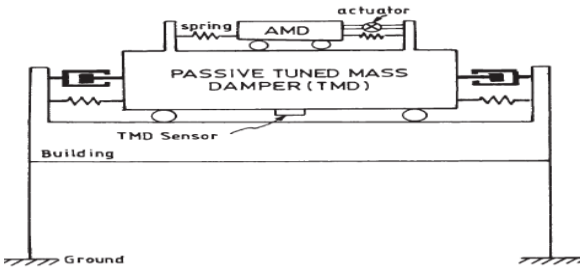

Fig 3: Duox system for ANDO building

II. CONTROL SYSTEM THEORY FOR DYNAMICS OF STRUCTURES

Most of the control theories reported in the literature are based on deterministic control system with lumped parameters and time-varying control operations. The dynamic equation of motion for all control methods is given as

$$M\ddot{x}(t) + C\dot{x}(t) + Kx(t) = Du(t) + Ef(t) \quad (1)$$

where M, C, K are mass, damping and stiffness matrices; $x(t)$ is the displacement vector; $f(t)$ is the excitation due to ground motion; D is the location matrix of control force; E is the location matrix for the excitation forces; and $u(t)$ is the control force vector. The control force vector has the following approximate form:

$$u(t) = K_1x(t) + C_1\dot{x}(t) + E\,f(t) \quad (2)$$

where K_1,C_1,and E_1 are respectively control gains which can be time-dependent. From Eqs. (1) and (2), it follows that

$$M\ddot{x}(t) + (C - DC_1)\dot{x}(t) + (K - DK_1)x(t) = (E + DE_1)f(t) \quad (3)$$

It is seen from Eq. (3) that the effect of structural control is to mathematically modify the damping the stiffness and the excitation, in such a way that the response of the system is controlled. The matrices K_1, C_1, and E_1 are called gain matrices, and can be obtained in such a way that the response, in-principle, can be totally eliminated. However, in real practice, it is not possible to reduce the response totally. Different degrees of control of response are achieved by deriving the control gain matrices K_1, C_1,

and E_1. Derivation of these matrices depends on the control algorithms selected. In general, the control algorithms have some objective functions to be minimized. Accordingly, the gain matrices are derived. Different control algorithms differ in respect of finding these gain matrices or finding the control force vector, keeping in view an objective function that reduces the structural response. The solution of the control problem and the development of control algorithm are obtained by writing the control equation of motion in state space of the form,

$$\dot{z}(t) = Az(t)+Bu(t)+Hf(t) \quad (4)$$

where, $z(t)$ is the state vector defining displacement and velocity of the structure. IN the recent years, various algorithms have been developed to process the information from ground excitation, state of the structure, as discussed below.

2.1 Linear-Quadratic Optimal Control

The most popular control algorithm is based on linear optimal control theory which has closed loop structure. In this algorithm, minimization of a Liapunov's quadratic performance index J of the following form is carried out.

$$J = \int_0^{tf} [z^T(t)Qz(t)\ u^T(t)Ru(t)]\ dt \quad (5)$$

where Q and R are called weighting matrices, and t_f is the time duration over which the control force operates. The minimization problem requires the solution of a Riccati matrix equation, leading to the control force vector given as

$$u(t) = -\frac{1}{2}R^{-1}B^T P(t)z(t) = Gz(t) \quad (6)$$

in which G is called the gain matrix. Many studies have been carried out on linear optimal control, such as those by Yang (1975), Abdel-Rohman and Leipholz (1983), Chang and Soong (1980), Chung et al. (1988), Soong (1992), and Sarbjeet and Datta (1998).

2.2 Method of Pole Assignment

Having defined $u(t)$ by Eq. (6) the control equation of motion can be written in the form:

$$\ddot{z}(t) = (A+BG)\ z(t) + Hf(t) \quad (7)$$

The modal damping ratios and frequencies obtained from the modified matrix$(A+BG)$ provide the dynamic characteristics of the system. The gain matrix G can be chosen such that the eigenvalues of the modified matrix take a set of prescribed values. Generally, the eigenvalues corresponding to the first few modes are considered. Therefore, the control scheme is useful for structures having first few modes as the predominant modes of vibration. There have been a few works in this area, like those reported by Abdel-Rohman and Leipholz (1978), Martin and Soong (1976), and Abdel-Rohman and Nayfeh (1987).

2.3 Modal Space Control Algorithm

In this control scheme, the state space equation is written in modal co-ordinates by defining a modal control force $u_j(t)$ and modal load $f_i(t)$. The equation of motion becomes decoupled, if it is assumed that the modal control force $u_j(t)$ depends only on the modal co-ordinate y_j (t). A modal quadratic performance function J_j of the form of Eq. (5) can be constructed, and a total performance function, ΣJ_j (Meirovitch and Oz, 1980; Meirovitch and Baruh, 1983; Meirovitch and Ghosh, 1987) is minimized to obtain the modal control force. Meirovitch and a few other researchers investigated the effectiveness of modal space control.

2.4 Instantaneous Control Technique

In this control algorithm, the latest values of external excitation are utilized in obtaining the improved control algorithm which makes use of the time-dependent performance function $J(t)$. The optimal control force is derived by minimizing $J(t)$ at any instant of time, t. The formulation of the problem is based on writing the state vector $z(t)$ in terms of the state vector and excitation at previous time step, which are supposed to be known by now. The performance function $J(t)$ is minimized subjected to the constraint given by the expression of the evolution of the state vector $z(t)$ subject to the constraint given by the expression of the evolution of the state vector $z(t)$ over the time-interval Δt . Some works on instantaneous control include those by Abdel-Rohman and Leipholz (1979), and Yang et al. (1987). The minimization of the cost function is carried out over the time interval.

2.5 Bounded State Control

In bounded state control, the control force is applied to keep response within an allowable range. All pulse control strategies in the literature fall into this category. The basic idea of pulse control is to apply a train of force pulses to produce responses matching that produced by a continuous loading of arbitrary nature. It is meant to destroy gradual rhythmic building up of the structural response in the case of resonance. The pulse magnitudes are determined analytically so as to minimize non-negative cost function of linear quadratic regulator form. The minimization of the cost function is carried out over the inter-pulse spacing. They may be applied every time, a zero crossing of the response variable is detected. A continuous monitoring of the system state

variable is required in this control scheme. The advantages of the bounded state control are its applicability for inelastic structures and its energy saving. The bounded state control was studied by Abdel-Rohman et al. (1993), Udwadia and Tabai (1981a, 1981b), Masri et al. (1981a, 1981b), Prucz et al. (1985), and by Reinhorn et al. (1987).

2.6 Non-linear Control Theory

In non-linear control, a higher order performance function is minimized, such that the control force becomes a non-linear function of the state variable. The idea behind determining a non-linear control strategy is to obtain a better control of response, with relatively less control force. Wu et al. (1995) developed a non-linear control strategy in the line of LQR problem by using the solution of Riccati equation. The control force was expressed in a convenient form by using a weighted non-linearity feedback parameter. By setting this parameter to zero, the control force becomes same as that of the LQR problem. Other works on non-linear active control include those of Shefer and Beakwell (1987), Suhardijo et al. (1992a), and Wu et al. (1995). Another type of non-linear control scheme is addressed in the literature for response reduction of non-linear structures. The stiffness and damping non-linearities can be included in this algorithm, and the non-linear equation of motion can be solved in time domain, with a control force derived as a non-linear function of state variable. The minimization of the non-linear performance function is achieved through the solution of Matrix-Riccati equation.

2.7 Generalized Feedback Control

In this control scheme, the dynamic equations of controller are also incorporated. As a result, absolute acceleration of the structure also becomes another feedback, apart from the displacement and velocity of the structure. The modified LQR performance function contains the acceleration feed-back vector, and therefore, the control force becomes a function of structural displacement, velocity and acceleration. Studies on active control with acceleration feed-back have been reported by Yang et al. (1991, 1994), Suhardjo et al. (1992b), Spencer et al. (1993), Rofooei and Tadjbakhsh (1993), Dyke et al. (1996a), and by Suneja and Datta (1998).

2.8 Sliding Mode Control (SMC)

Sliding mode control scheme was first developed by Utkin (1978). In the sliding mode control, a sliding surface is generated consisting of a linear combination of state variables. The sliding surface is defined such that the motion of the structure, i.e. structural response, is stable on this surface. The sliding surface is obtained by minimizing a performance function of LQR type, and thus by requiring the solution of Riccati equation. Controllers are designed such that they drive the response trajectory on to the sliding surface. This is accomplished by the Liapunov stability criterion (since the motion of the sliding surface is always stable). From this condition, the control force is estimated. A possible continuous controller which allows the response trajectory to move on to the sliding surface (even if the sliding surface is discontinuous) is obtained by allowing sliding margin. An improvement over the sliding mode control is achieved by designing a controller which provides control force based on linear feed-back system and non-linear feed-back of the state vector. The non-linear feed-back is introduced to take into consideration the uncertainties arising from the excitation. The purpose is to make the control strategy robust against all kinds of uncertainties in the system. Some of the important studies on sliding mode control include those by Yang et al. (1994), Singh and Matheu (1997), Adhikari and Yamaguchi (1997), and by Sarbjeet and Datta (2000).

2.9 Time Delay Compensation

The aforementioned control algorithms are based on the instantaneous effect, i.e. it is assumed that there exists no time delay between the response measurement and the control action. In reality, this is never achieved, and there always exists a time delay between the two. It is somewhat difficult to include the time delay effect in the control scheme and to define control force in terms of delayed state vector. The introduction of time delay parameter makes the system of equations as parametered differential equations and nonlinear. As a consequence, the stability analysis of the system becomes important. In fact, the time delay effect, if not properly compensated, may cause instability of the system. The importance of time delay compensation in structural control has been demonstrated in laboratory (Chung et al., 1988, 1995; McGreevy et al., 1988), and several compensation methods have been proposed (Hammerstrom and Gros, 1980; Abdel-Rohman, 1985; Soliman and Roy, 1992). These include modification of control gain by performing a phase shift of measured state variables in the modal domain and by methods updating the measured quantities dynamically. Some of the important works on the time delay effect were presented by Abdel-Rohman (1985, 1987, 1993), Jun-Ping and Kelly (1991), Jun-PingandDeh-Shiu (1988), Yang et al. (1990), and by Chung et al. (1995).

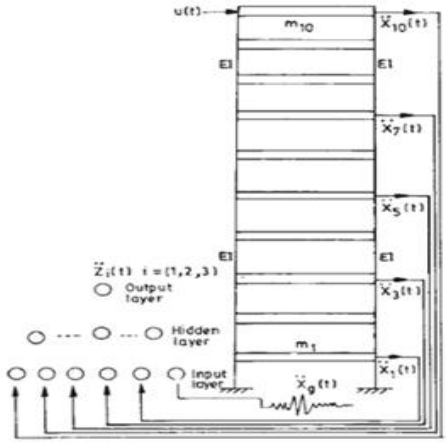

Fig 4: Active neuro fuzzy control.

2.10 Active Control Using Neural Network and Fuzzy Logic

In recent years, there has been growing application of the neural network and the theory of fuzzy logic, for controlling the structural response due to dynamic excitation. The main objective of applying this concept for structural control is to obviate the need for developing a control algorithm analytically. However, in some cases, the neural network or fuzzy logic is used, keeping in view the minimization of some objective function, which tends to reduce the structural response. These control strategies do not strictly optimally control the structural response. They are better in terms of practical applications, and are more versatile. In the active control of structures using neural network, neural nets tend to provide control forces, which would reduce the response of the structure when subjected to unknown future earthquakes. Various types of neuro-controllers have been reported in the literature (Ghaboussi and Joghataei, 1995; Chen etal., 1995; Bani-Hani and Ghaboussi, 1998; Rao and Datta, 1998). A neuro-controller is trained with the help of a trained emulator network. The purpose of emulator network is to aid the learning of the neuro SET controller in establishing the desired relation between the immediate past history of the response of the structure and the adjusted control signals of the actuator. Emulator network is essentially used to determine the error at the output of the neuro-controller, which is minimized during the training of the neuro-controller network. Further, emulator network helps in averaging out the error developed due to the time delay effect. Once the neuro-controller is trained by using the emulator network, it can be independently used for controlling the response of the structure. The neuro-controller is trained via the minimization of certain criterion. Chen et al. (1995) described a criterion in which the instantaneous error function is taken as the summation of errors between the actual and desired responses. Ghaboussi and Joghataie (1995) considered the criterion to be the average of an expected response for the future time steps to be zero. Kim et al. (2000) used the minimization of the cost function (of closed loop control scheme, LQR) as the criterion for training. This control scheme was used to control both linear and nonlinear structures. Rao and Datta (1998) developed a control scheme by using a single neural network, for a predetermined response reduction of the single mode control of building frames. This control scheme explicitly takes into account the time delay effect in the training of the neural network. This concept was further extended to the multi-mode response of building frames in which the use of emulator network was dispensed with. The method first predicts the modal response of the structure, and then obtains the required control force to be applied to the structure. A typical neural net-based control scheme is shown in Fig 4. In recent years, fuzzy control theory has drawn considerable interest of researchers for active and semi-active control of structures subjected to earthquake excitations. The advantage of this approach is its inherent robustness and its ability to handle the non-linear behavior of the structure. Moreover, the computations for driving the controller are quite simple, and can be easily implemented into a fuzzy chip. In the fuzzy control, the control equation of motion is generally solved by using the MATLAB environment with the help of Simulink and Fuzzy tool boxes. Different types of fuzzy rule bases are used to map control forces according to the levels of the structural responses. The rule bases can be constructed by considering feed-back as: (i) only velocity, (ii) velocity and displacement, and (iii) velocity, acceleration, and displacement. Generally, maximum bounds on the control forces/damping coefficients for active/semi-active control schemes are prescribed. Fuzzy control does not provide an optimal control, but has more flexibility compared to the classical control theories. Different applications of fuzzy control theory for active and semi-active control of different types of structures include those by Symansand Kelly (1999), Battaini et al. (1998), Tani et al. (1998), Kurata et al. (1999).

2.11 Other Types of Control Strategies

In line with the concept of active/semi-active control, a few other types of control strategy have been investigated, namely hybrid control, adaptive control, and stochastic control. Hybrid control is a combination of passive control and active control. Various combinations of passive and active systems have been attempted, such as base isolation and actuators, ATMD, visco-elastic dampers and actuators etc. Hybrid control is preferred when more

stringent control of one or more response quantities is desired. It is governed by a control algorithm in which the dynamic characteristics of structural system include those of passive control devices. Formulation of active control problem remains the same, except that the structural system becomes non-classically damped. An adaptive controller is a controller with adjustable parameters, incorporating a mechanism for adjusting these parameters. Adaptive control is generally used to control structures whose parameters are unknown or uncertain. It consists of choice of the controlled structure, choice of a performance function, online evaluation of the performance with respect to some desired behaviour, and online adjustment of the control parameters, to bring the performance closer to the desired behaviour. The adaptive control methods are generally divided into direct and indirect methods. Indirect methods have been experimented, and have been used by considering the direct model. The structure to be controlled is represented by:

$\dot{X}$ (t) = $A_s X_s$ (t) + $B_s u_s$(t) (8)

Y_s (t) = $C_s X_s$ (t) – observer (9)

Here, Y_s is the response of adaptive control.The reference model has the similar structure, and has response with suffix m. The adaptive controller is based on tracking the error, e (t) = Y_m (t) –Y_s(t) Both feed-forward and feed-back control are possible by the least mean-square algorithm. Stochastic active control becomes necessary when (i) uncertainty exists in both inherent nature of the structure and exogenous forces that it sees, (ii) structures are with infinite degrees of freedom, and are not completely observable from sensors located, and (iii) sensors are also contaminated with noise. Responses are modeled as random processes, and may have non-linear transfer relationships with the input. Determination of control force requires minimization of the expected values of the cost function. The problem is mathematically tractable for white noise type of disturbance by using stochastic dynamic programming. Another variation of stochastic control consists of covariance control, such that the state feed-back gain K is determined such that

E [u(t)u^T(t)] = KSK^T (10)

in which S is the covariance matrix of the stationary state.

III. FUTURE DIRECTIONS

Besides the availability of the advanced algorithms, there are a number of problems encountered in the practical implementation of the active control scheme. Because of these problems, active control of structures has not yet been widely applied. Apart from the availability of large power sources for the implementation of control schemes, there are some other real time application problems. They include modeling error, time delay, limited sensor, parameter uncertainties and system identification, reliability, cost-effectiveness and hardware requirement. These problems have gained attention of the researchers, and it is hopeful that control systems will soon be applied to a large number of structures in developing as well as developed countries.

REFERENCES

[1] Yang (1975), Abdel-Rohman and Leipholz (1983), Chang and Soong (1980), Chung et al. (1988), Soong (1992), and Sarbjeet and Datta (1998).

[2] Abdel-Rohman and Leipholz (1978), Martin and Soong (1976), and Abdel-Rohman and Nayfeh (1987).

[3] Meirovitch and Oz, (1980); Meirovitch and Baruh, (1983); Meirovitch and Ghosh, {1987).

[4] Abdel-Rohman and Leipholz (1979), and Yang et al. (1987).

[5] Abdel-Rohman et al. (1993), Udwadia and Tabai (1981a, 1981b), Masri et al. (1981a, 1981b), Prucz et al. (1985), and by Reinhorn et al. (1987).

[6] Shefer and Beakwell (1987), Suhardijo et al. (1992a), and Wu et al. (1995).

[7] Yang et al. (1991, 1994),Suhardjo et al. (1992b), Spencer et al. (1993), Rofooei and Tadjbakhsh (1993), Dyke et al. (1996a), and by Suneja and Datta (1998).

[8] (Chung et al., 1988, 1995; McGreevy et al., 1988),

[9] (Hammerstrom and Gros, 1980; Abdel-Rohman, 1985; Soliman and Roy, 1992Abdel-Rohman (1985, 1987, 1993)

[10] Symansand Kelly (1999), Battaini et al. (1998), Tani et al. (1998), Kurata et al. (1999).

[11] T.K. Datta ,Department of Civil Engineering, Indian Institute of Technology Delhi, Hauz Khas, New Delhi-110016

[12] B.F. Spencer, Jr. Department of Civil Engineering and Geological sciences, University of Notre Dame, Notre Dame, IN 46556, USA

[13] T.T. Soong, Department of Civil, Structural and Environmental Engineering, State University of New York at Buffalo, Buffalo, NY 14260, USA

[14] Michael D. Symans (1996/1997) and Michael C. Constantinou (1996/1997); Washington-University, State University of Newyork (Buffalo).

International Journal of Engineering Research and Applications (IJERA) ISSN: 2248-9622
National Conference on Advances in Engineering and Technology
(AET- 29th March 2014)

RESEARCH ARTICLE OPEN ACCESS

Review Of Algorithms For Control Systems For Civil Engineering Structures

Pratyush Malaviya*, Sandeep Lamba*, Anil Kumar*
*(Department of Civil Engineering, Jaypee University of Information Technology
Waknaghat, Solan (H.P.) – 173234
Email: pratyushmalaviya@gmail.com
Lamba5550@gmail.com

ABSTRACT
One of the most significant technological innovations in the structural engineering field is the practical application of active and semi-active control to civil structures. A number of structures integrating active, hybrid, and semi-active response control technologies have been constructed in Japan, China and USA. Any control system whether it is in aircraft, spaceship or building; it needs an algorithm to be run by the computer installed in the structure. A state-of-the-art review on algorithms for response-triggered structural control systems is presented. The review focuses on the active control of structures for earthquake excitations, and covers theoretical backgrounds of different active control schemes, important parametric observations on active structural control, limitations and difficulties of their practical implementation, and brief descriptions of three actively controlled tall buildings in Japan. A brief introduction of more promising semi-active control of structures is also presented. This study focuses on the development of an active control algorithm based on several performance levels anticipated from an isolated building during different levels of ground shaking corresponding to various earthquake hazard levels. The proposed active control algorithms change the control gain depending on the level of shaking imposed on the structure. These active control systems have been evaluated using a series of analyses performed on ground motion records. Simulation results show that the newly proposed algorithms are effective in improving the structural as well as nonstructural performance of the building for selected earthquakes.
Keywords **–** Active Control, Algorithms, Control-theories, Structure Control-System.

I. INTRODUCTION

The most important task of civil engineering structures is to design them such that they can withstand the forces and accommodate the deformations without major damage or a collapse. The response of the system can always be limited by providing stiffer structural members but in general the system would become uneconomical. So it has been a common practice to generate more ductile designs, providing the means for adequate energy dissipation through the yielding of individual members and generation of localized plastic hinges. The occurrence of damage during a seismic event is unavoidable in this design philosophy. Further, the permanent deformations in the structure surviving the seismic events may seriously affect its service life. Recently the attention of the civil engineering community has moved on reducing forces and deformations in structures through the methods of the structural control in which information is fed into the controller which processes the measured quantities and structural properties to generate the corresponding control signal, which is then input to the actuators which may be driven by a power source to produce the control action, as shown in Fig 1. These method of response reduction can address not only the prevention of total failure or the limitation of damages but also they can be designed to provide comfort to the occupants of the structure on the basis of mode of operation of these special devices the structural response control methods can be broadly classified as passive, active and semi-active control approaches.

A passive control system does not require an external power source for operation and utilizes the motion of the structure to develop the control forces. Control forces are developed as a function of the response of the structure at the location of the passive control system. An active control system typically requires a large power source for operation of electro-hydraulic or electro-mechanical actuators which supply control forces to the structure. Control forces are developed based on feedback from sensors that measure the excitation and/or the response of the structure. The feedback from the structural response may be measured at locations remote from the location of the active control system.

A semi-active control system requires a relatively small external power source for operation (like a battery) and utilizes the motion of the structure to develop the control forces, the magnitude of which can be adjusted by the external power source. Control forces are developed based on feedback from sensors that measure the excitation and/or the response of the structure. The feedback from the structural response may be measured at locations remote from the location of the semi-active control system. Sometimes these systems are combined to form hybrid control systems.

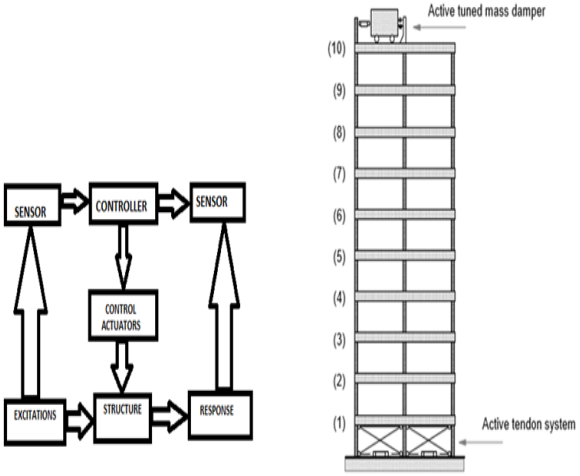

Fig 1: Control system applied on a building

Some actual applications of active control schemes for the reduction of wind-induced vibrations of tall buildings have been reported. The 11-storey building made of rigid steel frames is located at Chuo-Ku, Tokyo, with a frontage of 4 m and a total height of 33 m. Two AMDs are located at the top floor, spaced apart with masses of 4 tons and 1 ton, respectively Fig 2. The idea of providing two AMDs was to control the torsional response of the structure also. The schematic diagram of the AMD is shown to actuate the masses. Sensors are placed at the basement, 6th floor, and at the 11th floor. The computer is provided on the top floor itself. This is the world's first AMD installed on a building. Sensors are placed at the basement, 6th floor, and at the 11th floor. Other example is a Duox system on ANDO Nighikicho, Tokyo. It has 14 storeys and two basement levels, and is made of rigid steel frames. Above the ground, mass of the building is 2600 tons. Two-directional simultaneous AMD is placed on the top of a TMD which is placed on the top floor as shown in Fig 3. The damping system of the TMDs consists of oil dampers. The TMD mass is 18 tons, while the AMDs have 2-ton mass, each. The Duox system operates on the principle that if the active control system fails, the TMD will provide at least the minimum control of response.

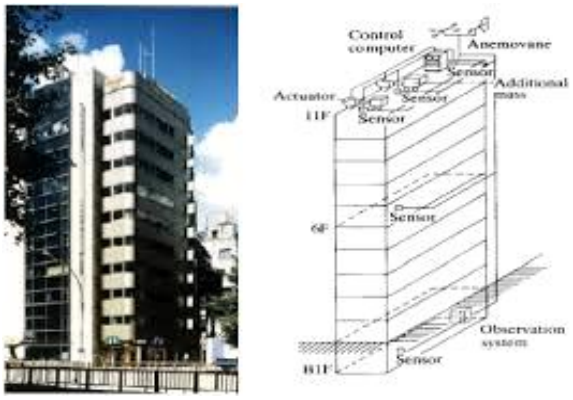

Fig 2: Building at Chuo-Ku.

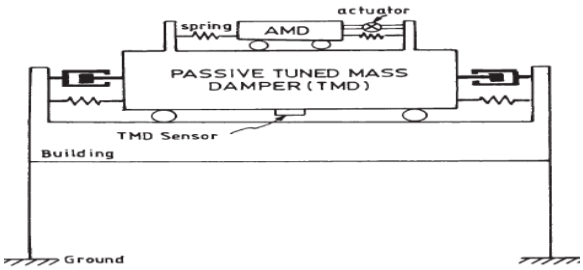

Fig 3: Duox system for ANDO building

II. CONTROL SYSTEM THEORY FOR DYNAMICS OF STRUCTURES

Most of the control theories reported in the literature are based on deterministic control system with lumped parameters and time-varying control operations. The dynamic equation of motion for all control methods is given as

$$M\ddot{x}(t) + C\dot{x}(t) + Kx(t) = Du(t) + Ef(t) \quad (1)$$

where M, C, K are mass, damping and stiffness matrices; $x(t)$ is the displacement vector; $f(t)$ is the excitation due to ground motion; D is the location matrix of control force; E is the location matrix for the excitation forces; and $u(t)$ is the control force vector. The control force vector has the following approximate form:

$$u(t) = K_1x(t) + C_1\dot{x}(t) + E\,f(t) \quad (2)$$

where K_1,C_1,and E_1 are respectively control gains which can be time-dependent. From Eqs. (1) and (2), it follows that

$$M\ddot{x}(t) + (C - DC_1)\dot{x}(t) + (K - DK_1)x(t) = (E + DE_1)f(t) \quad (3)$$

It is seen from Eq. (3) that the effect of structural control is to mathematically modify the damping the stiffness and the excitation, in such a way that the response of the system is controlled. The matrices K_1, C_1, and E_1 are called gain matrices, and can be obtained in such a way that the response, in-principle, can be totally eliminated. However, in real practice, it is not possible to reduce the response totally. Different degrees of control of response are achieved by deriving the control gain matrices K_1, C_1,

and E_1. Derivation of these matrices depends on the control algorithms selected. In general, the control algorithms have some objective functions to be minimized. Accordingly, the gain matrices are derived. Different control algorithms differ in respect of finding these gain matrices or finding the control force vector, keeping in view an objective function that reduces the structural response. The solution of the control problem and the development of control algorithm are obtained by writing the control equation of motion in state space of the form,

$$\dot{z}(t) = Az(t)+Bu(t)+Hf(t) \quad (4)$$

where, $z(t)$ is the state vector defining displacement and velocity of the structure. IN the recent years, various algorithms have been developed to process the information from ground excitation, state of the structure, as discussed below.

2.1 Linear-Quadratic Optimal Control

The most popular control algorithm is based on linear optimal control theory which has closed loop structure. In this algorithm, minimization of a Liapunov's quadratic performance index J of the following form is carried out.

$$J = \int_0^{tf} [z^T(t)Qz(t)\ u^T(t)Ru(t)]\ dt \quad (5)$$

where Q and R are called weighting matrices, and t_f is the time duration over which the control force operates. The minimization problem requires the solution of a Riccati matrix equation, leading to the control force vector given as

$$u(t) = -\frac{1}{2}R^{-1}B^T P(t)z(t) = Gz(t) \quad (6)$$

in which G is called the gain matrix. Many studies have been carried out on linear optimal control, such as those by Yang (1975), Abdel-Rohman and Leipholz (1983), Chang and Soong (1980), Chung et al. (1988), Soong (1992), and Sarbjeet and Datta (1998).

2.2 Method of Pole Assignment

Having defined $u(t)$ by Eq. (6) the control equation of motion can be written in the form:

$$\ddot{z}(t) = (A+BG)\ z(t) + Hf(t) \quad (7)$$

The modal damping ratios and frequencies obtained from the modified matrix$(A+BG)$ provide the dynamic characteristics of the system. The gain matrix G can be chosen such that the eigenvalues of the modified matrix take a set of prescribed values. Generally, the eigenvalues corresponding to the first few modes are considered. Therefore, the control scheme is useful for structures having first few modes as the predominant modes of vibration. There have been a few works in this area, like those reported by Abdel-Rohman and Leipholz (1978), Martin and Soong (1976), and Abdel-Rohman and Nayfeh (1987).

2.3 Modal Space Control Algorithm

In this control scheme, the state space equation is written in modal co-ordinates by defining a modal control force $u_j(t)$ and modal load $f_i(t)$. The equation of motion becomes decoupled, if it is assumed that the modal control force $u_j(t)$ depends only on the modal co-ordinate y_j (t). A modal quadratic performance function J_j of the form of Eq. (5) can be constructed, and a total performance function, ΣJ_j (Meirovitch and Oz, 1980; Meirovitch and Baruh, 1983; Meirovitch and Ghosh, 1987) is minimized to obtain the modal control force. Meirovitch and a few other researchers investigated the effectiveness of modal space control.

2.4 Instantaneous Control Technique

In this control algorithm, the latest values of external excitation are utilized in obtaining the improved control algorithm which makes use of the time-dependent performance function $J(t)$. The optimal control force is derived by minimizing $J(t)$ at any instant of time, t. The formulation of the problem is based on writing the state vector $z(t)$ in terms of the state vector and excitation at previous time step, which are supposed to be known by now. The performance function $J(t)$ is minimized subjected to the constraint given by the expression of the evolution of the state vector $z(t)$ subject to the constraint given by the expression of the evolution of the state vector $z(t)$ over the time-interval Δt . Some works on instantaneous control include those by Abdel-Rohman and Leipholz (1979), and Yang et al. (1987). The minimization of the cost function is carried out over the time interval.

2.5 Bounded State Control

In bounded state control, the control force is applied to keep response within an allowable range. All pulse control strategies in the literature fall into this category. The basic idea of pulse control is to apply a train of force pulses to produce responses matching that produced by a continuous loading of arbitrary nature. It is meant to destroy gradual rhythmic building up of the structural response in the case of resonance. The pulse magnitudes are determined analytically so as to minimize non-negative cost function of linear quadratic regulator form. The minimization of the cost function is carried out over the inter-pulse spacing. They may be applied every time, a zero crossing of the response variable is detected. A continuous monitoring of the system state

variable is required in this control scheme. The advantages of the bounded state control are its applicability for inelastic structures and its energy saving. The bounded state control was studied by Abdel-Rohman et al. (1993), Udwadia and Tabai (1981a, 1981b), Masri et al. (1981a, 1981b), Prucz et al. (1985), and by Reinhorn et al. (1987).

2.6 Non-linear Control Theory

In non-linear control, a higher order performance function is minimized, such that the control force becomes a non-linear function of the state variable. The idea behind determining a non-linear control strategy is to obtain a better control of response, with relatively less control force. Wu et al. (1995) developed a non-linear control strategy in the line of LQR problem by using the solution of Riccati equation. The control force was expressed in a convenient form by using a weighted non-linearity feedback parameter. By setting this parameter to zero, the control force becomes same as that of the LQR problem. Other works on non-linear active control include those of Shefer and Beakwell (1987), Suhardijo et al. (1992a), and Wu et al. (1995). Another type of non-linear control scheme is addressed in the literature for response reduction of non-linear structures. The stiffness and damping non-linearities can be included in this algorithm, and the non-linear equation of motion can be solved in time domain, with a control force derived as a non-linear function of state variable. The minimization of the non-linear performance function is achieved through the solution of Matrix-Riccati equation.

2.7 Generalized Feedback Control

In this control scheme, the dynamic equations of controller are also incorporated. As a result, absolute acceleration of the structure also becomes another feedback, apart from the displacement and velocity of the structure. The modified LQR performance function contains the acceleration feed-back vector, and therefore, the control force becomes a function of structural displacement, velocity and acceleration. Studies on active control with acceleration feed-back have been reported by Yang et al. (1991, 1994), Suhardjo et al. (1992b), Spencer et al. (1993), Rofooei and Tadjbakhsh (1993), Dyke et al. (1996a), and by Suneja and Datta (1998).

2.8 Sliding Mode Control (SMC)

Sliding mode control scheme was first developed by Utkin (1978). In the sliding mode control, a sliding surface is generated consisting of a linear combination of state variables. The sliding surface is defined such that the motion of the structure, i.e. structural response, is stable on this surface. The sliding surface is obtained by minimizing a performance function of LQR type, and thus by requiring the solution of Riccati equation. Controllers are designed such that they drive the response trajectory on to the sliding surface. This is accomplished by the Liapunov stability criterion (since the motion of the sliding surface is always stable). From this condition, the control force is estimated. A possible continuous controller which allows the response trajectory to move on to the sliding surface (even if the sliding surface is discontinuous) is obtained by allowing sliding margin. An improvement over the sliding mode control is achieved by designing a controller which provides control force based on linear feed-back system and non-linear feed-back of the state vector. The non-linear feed-back is introduced to take into consideration the uncertainties arising from the excitation. The purpose is to make the control strategy robust against all kinds of uncertainties in the system. Some of the important studies on sliding mode control include those by Yang et al. (1994), Singh and Matheu (1997), Adhikari and Yamaguchi (1997), and by Sarbjeet and Datta (2000).

2.9 Time Delay Compensation

The aforementioned control algorithms are based on the instantaneous effect, i.e. it is assumed that there exists no time delay between the response measurement and the control action. In reality, this is never achieved, and there always exists a time delay between the two. It is somewhat difficult to include the time delay effect in the control scheme and to define control force in terms of delayed state vector. The introduction of time delay parameter makes the system of equations as parametered differential equations and nonlinear. As a consequence, the stability analysis of the system becomes important. In fact, the time delay effect, if not properly compensated, may cause instability of the system. The importance of time delay compensation in structural control has been demonstrated in laboratory (Chung et al., 1988, 1995; McGreevy et al., 1988), and several compensation methods have been proposed (Hammerstrom and Gros, 1980; Abdel-Rohman, 1985; Soliman and Roy, 1992). These include modification of control gain by performing a phase shift of measured state variables in the modal domain and by methods updating the measured quantities dynamically. Some of the important works on the time delay effect were presented by Abdel-Rohman (1985, 1987, 1993), Jun-Ping and Kelly (1991), Jun-PingandDeh-Shiu (1988), Yang et al. (1990), and by Chung et al. (1995).

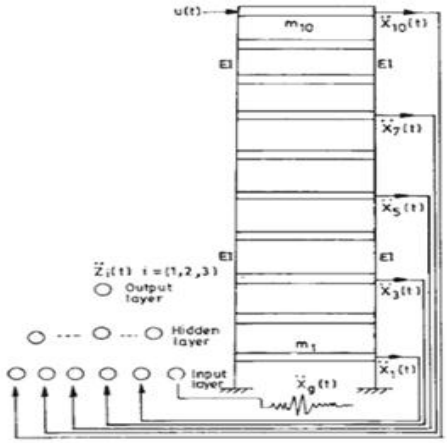

Fig 4: Active neuro fuzzy control.

2.10 Active Control Using Neural Network and Fuzzy Logic

In recent years, there has been growing application of the neural network and the theory of fuzzy logic, for controlling the structural response due to dynamic excitation. The main objective of applying this concept for structural control is to obviate the need for developing a control algorithm analytically. However, in some cases, the neural network or fuzzy logic is used, keeping in view the minimization of some objective function, which tends to reduce the structural response. These control strategies do not strictly optimally control the structural response. They are better in terms of practical applications, and are more versatile. In the active control of structures using neural network, neural nets tend to provide control forces, which would reduce the response of the structure when subjected to unknown future earthquakes. Various types of neuro-controllers have been reported in the literature (Ghaboussi and Joghataei, 1995; Chen etal., 1995; Bani-Hani and Ghaboussi, 1998; Rao and Datta, 1998). A neuro-controller is trained with the help of a trained emulator network. The purpose of emulator network is to aid the learning of the neuro SET controller in establishing the desired relation between the immediate past history of the response of the structure and the adjusted control signals of the actuator. Emulator network is essentially used to determine the error at the output of the neuro-controller, which is minimized during the training of the neuro-controller network. Further, emulator network helps in averaging out the error developed due to the time delay effect. Once the neuro-controller is trained by using the emulator network, it can be independently used for controlling the response of the structure. The neuro-controller is trained via the minimization of certain criterion. Chen et al. (1995) described a criterion in which the instantaneous error function is taken as the summation of errors between the actual and desired responses. Ghaboussi and Joghataie (1995) considered the criterion to be the average of an expected response for the future time steps to be zero. Kim et al. (2000) used the minimization of the cost function (of closed loop control scheme, LQR) as the criterion for training. This control scheme was used to control both linear and nonlinear structures. Rao and Datta (1998) developed a control scheme by using a single neural network, for a predetermined response reduction of the single mode control of building frames. This control scheme explicitly takes into account the time delay effect in the training of the neural network. This concept was further extended to the multi-mode response of building frames in which the use of emulator network was dispensed with. The method first predicts the modal response of the structure, and then obtains the required control force to be applied to the structure. A typical neural net-based control scheme is shown in Fig 4. In recent years, fuzzy control theory has drawn considerable interest of researchers for active and semi-active control of structures subjected to earthquake excitations. The advantage of this approach is its inherent robustness and its ability to handle the non-linear behavior of the structure. Moreover, the computations for driving the controller are quite simple, and can be easily implemented into a fuzzy chip. In the fuzzy control, the control equation of motion is generally solved by using the MATLAB environment with the help of Simulink and Fuzzy tool boxes. Different types of fuzzy rule bases are used to map control forces according to the levels of the structural responses. The rule bases can be constructed by considering feed-back as: (i) only velocity, (ii) velocity and displacement, and (iii) velocity, acceleration, and displacement. Generally, maximum bounds on the control forces/damping coefficients for active/semi-active control schemes are prescribed. Fuzzy control does not provide an optimal control, but has more flexibility compared to the classical control theories. Different applications of fuzzy control theory for active and semi-active control of different types of structures include those by Symansand Kelly (1999), Battaini et al. (1998), Tani et al. (1998), Kurata et al. (1999).

2.11 Other Types of Control Strategies

In line with the concept of active/semi-active control, a few other types of control strategy have been investigated, namely hybrid control, adaptive control, and stochastic control. Hybrid control is a combination of passive control and active control. Various combinations of passive and active systems have been attempted, such as base isolation and actuators, ATMD, visco-elastic dampers and actuators etc. Hybrid control is preferred when more

stringent control of one or more response quantities is desired. It is governed by a control algorithm in which the dynamic characteristics of structural system include those of passive control devices. Formulation of active control problem remains the same, except that the structural system becomes non-classically damped. An adaptive controller is a controller with adjustable parameters, incorporating a mechanism for adjusting these parameters. Adaptive control is generally used to control structures whose parameters are unknown or uncertain. It consists of choice of the controlled structure, choice of a performance function, online evaluation of the performance with respect to some desired behaviour, and online adjustment of the control parameters, to bring the performance closer to the desired behaviour. The adaptive control methods are generally divided into direct and indirect methods. Indirect methods have been experimented, and have been used by considering the direct model. The structure to be controlled is represented by:

$\dot{X}$ (t) = $A_s X_s$ (t) + $B_s u_s$(t) (8)

Y_s (t) = $C_s X_s$ (t) – observer (9)

Here, Y_s is the response of adaptive control.The reference model has the similar structure, and has response with suffix m. The adaptive controller is based on tracking the error, e (t) = Y_m (t) –Y_s(t) Both feed-forward and feed-back control are possible by the least mean-square algorithm. Stochastic active control becomes necessary when (i) uncertainty exists in both inherent nature of the structure and exogenous forces that it sees, (ii) structures are with infinite degrees of freedom, and are not completely observable from sensors located, and (iii) sensors are also contaminated with noise. Responses are modeled as random processes, and may have non-linear transfer relationships with the input. Determination of control force requires minimization of the expected values of the cost function. The problem is mathematically tractable for white noise type of disturbance by using stochastic dynamic programming. Another variation of stochastic control consists of covariance control, such that the state feed-back gain K is determined such that

E [u(t)u^T(t)] = KSK^T (10)

in which S is the covariance matrix of the stationary state.

III. FUTURE DIRECTIONS

Besides the availability of the advanced algorithms, there are a number of problems encountered in the practical implementation of the active control scheme. Because of these problems, active control of structures has not yet been widely applied. Apart from the availability of large power sources for the implementation of control schemes, there are some other real time application problems. They include modeling error, time delay, limited sensor, parameter uncertainties and system identification, reliability, cost-effectiveness and hardware requirement. These problems have gained attention of the researchers, and it is hopeful that control systems will soon be applied to a large number of structures in developing as well as developed countries.

REFERENCES

[1] Yang (1975), Abdel-Rohman and Leipholz (1983), Chang and Soong (1980), Chung et al. (1988), Soong (1992), and Sarbjeet and Datta (1998).

[2] Abdel-Rohman and Leipholz (1978), Martin and Soong (1976), and Abdel-Rohman and Nayfeh (1987).

[3] Meirovitch and Oz, (1980); Meirovitch and Baruh, (1983); Meirovitch and Ghosh, {1987).

[4] Abdel-Rohman and Leipholz (1979), and Yang et al. (1987).

[5] Abdel-Rohman et al. (1993), Udwadia and Tabai (1981a, 1981b), Masri et al. (1981a, 1981b), Prucz et al. (1985), and by Reinhorn et al. (1987).

[6] Shefer and Beakwell (1987), Suhardijo et al. (1992a), and Wu et al. (1995).

[7] Yang et al. (1991, 1994),Suhardjo et al. (1992b), Spencer et al. (1993), Rofooei and Tadjbakhsh (1993), Dyke et al. (1996a), and by Suneja and Datta (1998).

[8] (Chung et al., 1988, 1995; McGreevy et al., 1988),

[9] (Hammerstrom and Gros, 1980; Abdel-Rohman, 1985; Soliman and Roy, 1992Abdel-Rohman (1985, 1987, 1993)

[10] Symansand Kelly (1999), Battaini et al. (1998), Tani et al. (1998), Kurata et al. (1999).

[11] T.K. Datta ,Department of Civil Engineering, Indian Institute of Technology Delhi, Hauz Khas, New Delhi-110016

[12] B.F. Spencer, Jr. Department of Civil Engineering and Geological sciences, University of Notre Dame, Notre Dame, IN 46556, USA

[13] T.T. Soong, Department of Civil, Structural and Environmental Engineering, State University of New York at Buffalo, Buffalo, NY 14260, USA

[14] Michael D. Symans (1996/1997) and Michael C. Constantinou (1996/1997); Washington-University, State University of Newyork (Buffalo).

International Journal of Engineering Research and Applications (IJERA) ISSN: 2248-9622
National Conference on Advances in Engineering and Technology
(AET- 29th March 2014)

RESEARCH ARTICLE OPEN ACCESS

Comparison between Different Methods of Ultrasonic Pulse Velocity Tests on Concrete

K. D. Savaliya*, K. K. Thaker**, U. V. Dave***
*(Department of Civil Engineering, NIRMA University, Ahmedabad-382481
Email: 12mclc27@nirmauni.ac.in)
** (KCT Consultancy Services, Ahmedabad-382481
Email: kctconser@yahoo.com)
*** (Department of Civil Engineering, NIRMA University, Ahmedabad-382481
Email: urmil.dave@nirmauni.ac.in)

ABSTRACT
The relationship between velocities of Ultrasonic waves propagating along direct, semi-direct and indirect method is investigated. Simple cement concrete beams of M 25 grade and fabricated anomalies namely rubber pieces and re-bars are casted for experimentation. The comparisons of UPV results between direct, indirect and semi-direct methods describe.
Keywords **–** Direct, Indirect, Semi-direct, Ultrasonic waves, Velocity.

I. INTRODUCTION

Ultrasonic Pulse Velocity test is used to evaluate the material properties, to detect defects on the concrete structures. In addition to physical deterioration of the concrete structure is also access by UPV test.

Concrete material consist of two separate constitutes i.e. matrix and aggregates which have different dynamic modulus of elasticity and strength properties. Transmitting transducer is used to create Ultrasonic waves and receiving transducer is used to receive this stress waves. And travel time of this stress wave from one point to another point is measured. Distance measured between this points which plays a vital role in case of indirect method of Transmission. Ultrasonic waves are totally independent to geometry of the specimen. It is depends on material property, frequency of the stress wave, dynamic modulus of elasticity and density of the material. In this study, the test on concrete specimens has been carried out with different three methods namely direct, indirect and semi-direct methods.

II. AIM AND OBJECTIVES

Basically, Ultrasonic waves are stress waves which may be shear, compressive or surface waves. The stress wave propagation depends on material properties and frequency of the wave. Effect of different method of UPV on velocity and behavior of the stress wave in concrete specimen are found out.

III. EXPERIMENTAL PROCEDURE AND APPARATUS

Experimental procedure consists of 12 nos. cement concrete beams. M25 grade concrete with Ordinary Portland Cement is used. Locally available 10 and 20 mm aggregates and river sand is used. And the concrete proportions are as follows:

Table 1: Concrete Proportion

Material	**Per m^3 Concrete Quantity**
Cement	340kg
Sand	689kg
CA 20mm	789kg
CA 10mm	526kg
Water	181 liters

3.1 CASTING AND CURING PROCEDURE

Casting of concrete and mortar specimens was done in drum mixture. The purpose of casting of specimens with different anomalies is to know wave behavior in different media having different acoustic medium. From Fig 1 and Fig 2, Total 6 nos. of Concrete beams are casted. And 3 nos. of Concrete mixed with small rubber pieces & rebar mixed with concrete are casted. Size of the Beam element is 150X150X700 mm. All specimens of concrete are

subjected to same condition. Specimens are compacted and cured at ambient temperature until the date of testing.

Fig 1: Rubber anomalies mixed with concrete

Fig 2: 2-8 mm Ø Bar placed at center from all direction of beam

3.2 TESTING APPARATUS AND PROCEDURE

Ultrasonic stress (compression or shear) waves are produced by electro acoustic transducers made up of piezoelectric material. Transducers convert electric energy to the mechanical energy in form of stress wave which may be surface, compressive or shear waves.

PUNDIT 7 is shown in Fig 3 is used for UPV testing of specimens. From Fig 4 Piezoelectric Transducers having 54 kHz frequency are employed. As a coupling agent petroleum gel is used. Gel facilitates an airtight bond between concrete or mortar specimen and Transducers.

The Testing Procedure is consisting of UPV test by Direct, Indirect and Semi-direct method at ages of 7, 28 and days interval.

Fig 3: PUNDIT 7 Equipment

Fig 4: Transducers with 54 kHz frequency

In Direct method, Transmitting and Receiving Transducers are kept on its opposite faces. While in Semi direct method, Transmitting and Receiving Transducers are kept on adjacent faces. And in Indirect method, Transducers are kept on the same face. All three methods are shown in Fig 5. The readings are taken by putting transmitter and receiving transducer on opposite faces in case of direct method. While In semi direct method, the readings are taken by putting transmitter on top and bottom faces sequentially and by varying receiver transducers on adjacent faces. In Indirect method, the receiving and transmitting Transducers are kept on same face with different interval. And it has been varied by 150 mm distance on same face.

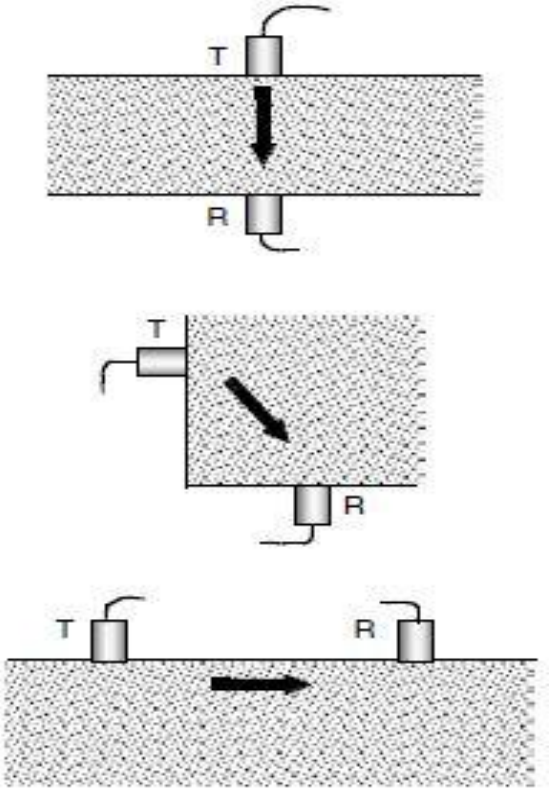

Fig 5: Direct, Semi-direct and Indirect Method.

IV. RESULTS AND DISCUSSION

UPV results by different three methods at different age. The results are taken at 7 and 28 days of different beam specimens with different anomalies.

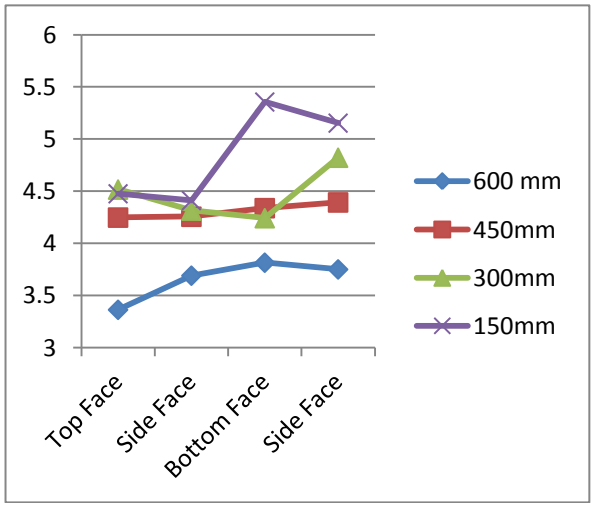

Fig 6: UPV of Indirect method on Beam at different interval vs different faces of the concrete beam.

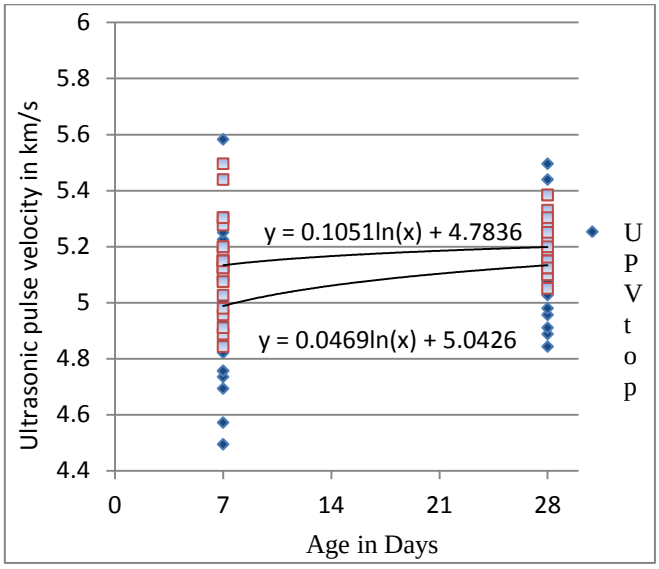

Fig 7: UP velocity of top and bottom surface versus Age of Concrete

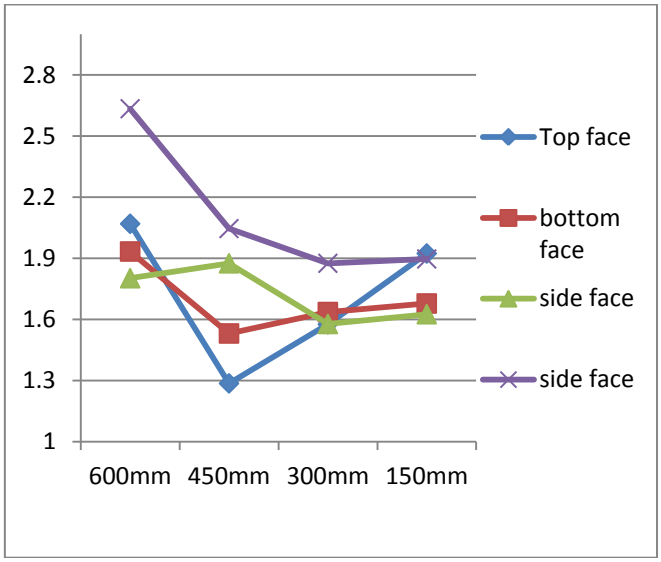

Fig 8: UP velocity of rubber anamolies mixed with concrete versus diff distance

V. CONCLUSION

Ultrasonic Pulse Velocity is observed in Fig 6 that In indirect method velocity increase with decreasing path length. And from Fig 7, the UP Velocity continuously increasing much slower rate which is observed between 7 and 28 days of casting in semi-direct method. In Indirect method when path length is less than its depth than surface wave reaches first on receiver while in direct method compressive wave reaches first on receiver.

Thus, in small path length wave can't go throughout depth so result may be faulty. From Fig 7 different material having different acoustic impedance so rubber having low acoustic impedance

compare to concrete, shows from Fig 6 and Fig 8.while steel having much acoustic impedance compare to concrete so waves can pass much faster rate compare to concrete.

REFERENCES

[1] V.M. Malhotra, N.J. Carino, "Non Destructive Testing of Concrete", *CRC Press*, 2004

[2] J.H. Bungey, S.G. Millard, M.G. Grantham, "Testing of Concrete in Structures",*Taylor and Francis Group*, 2006

[3] T. Voigt, Y. Akkaya, S.P. Shah, **"**Determination of Early Age Mortar and Concrete Strength by Ultrasonic Wave Reflections", *Journal of Materials in Civil Engineering*, 15(3), 2003, 247-254.

[4] J H Kim, S P Shah, Z Sun, and H G Kwak, "Ultrasonic Wave Reflection and Resonant Frequency Measurements for Monitoring Early-Age Concrete", *Journal of Materials in Civil Engineering*, 21(9), 2009, 476-483.

[5] Boyd, A. J. And Ferraro, C. C., "Effect of Curing and Deterioration on Stress Wave Velocities in Concrete", *Journal of Materials in Civil Engineering*, 17(2), 2005, 153-158.

[6] S.A. Kumar, M. Santhanam, "Detection of Concrete Damage Using Ultrasonic Pulse Velocity Method", *Proc. National Seminar on Non-Destructive Evaluation*, 2006, 7 - 9,

International Journal of Engineering Research and Applications (IJERA) ISSN: 2248-9622
National Conference on Advances in Engineering and Technology
(AET- 29th March 2014)

RESEARCH ARTICLE OPEN ACCESS

Hydrological Impacts of Climate Change

Pooja Pandey*, K. C. Patra**
*(Department of Civil Engineering, NIT, Rourkela, India
Email: luck.pooja@gmail.com)
** (Department of Civil Engineering, NIT, Rourkela, India
Email: prof_kcpatra@yahoo.com)

ABSTRACT
The increasing rate of the global surface temperature will have a significant impact on local hydrological regimes and water resources, which leads to the assessment of the climate change impacts. Main parameters that are closely related to the climate change are temperature and precipitation. Therefore, there is a growing need for an integrated analysis that can quantify the impacts of climate change on various aspects of water resources such as precipitation, hydrologic regimes, floods, drought, etc. There have been many studies of climate-change effects on hydrology and water resources which usually include: (a) use of climate models (GCMs), (b) use of downscaling techniques to model the hydrologic variables (e.g., precipitation) at a smaller scale based on large scale GCM outputs and (c) use of hydrological models for assessment of global climate change impacts. This paper reviews the existing methods for assessing the hydrological impact of climate change and discusses the challenges for future studies in this field.
***Key words*:** Climate change, Downscaling, GCM, hydrological models.

I. INTRODUCTION

Climate change can cause significant impacts on water resources by resulting changes in the hydrological cycle. Study of climate change include: (a) use of general circulation models (GCMs) for simulating time series of climate variables globally, accounting for effects of greenhouse gases in the atmosphere, (b) use of downscaling techniques to model the hydrologic variables (e.g., precipitation) at a smaller scale based on large scale GCM outputs, (c) use of hydrological models for assessment of global climate change impacts [1].

General Circulation Models (GCMs) are an important tool for assessing the impact of climate change on a range of human and natural systems. GCMs perform well at continental and large regional scales, but their ability to simulate climate at finer spatial scales is still limited [2]. Simulations at these finer scales are of considerable interest to hydrologists for assessing the possible impact of climate change on water supply and related aspects. This has led to the development of a range of downscaling methods, which uses the coarse scale GCM atmospheric simulations as the basis to produce finer scale variables. Different climate models have been used worldwide for climate impact assessment studies. The International Panel on Climate Change (IPCC) 4th assessment report identified 23 GCMs for assessment of plausible climate change impact on a range of human and natural systems [3].

General Circulation Models or global climate models (GCMs) are among the best available tools to represent the main features of the global distribution of basic climate parameters. But these models are unable to produce the details of regional climate conditions at different temporal and spatial scales. Anthropogenic global climate change would lead to changes in large-scale atmospheric features. However, the effect of large-scale feature changes on local surface climate cannot be resolved in the current generation of GCMs, which introduces the need for downscaling [4]. Hence, there is a great need to develop tools for downscaling GCM predictions of climate change to regional and local or station scales. Downscaling techniques have been designed to bridge the gap between the information that the climate modeling community can currently provide and that required by the impacts research community [5].

Currently general circulation models (GCMs) are considered to be the best tools for investigating the physical and dynamic processes of the earth surface-atmosphere system and they provide plausible patterns of global climate change. However, it is not yet possible to make reliable predictions of regional hydrologic changes directly from climate models due to the coarse resolution of GCMs and the

simplification of hydrologic cycle in climate models [6].

Hydrological modeling is a mathematical representation of natural processes that influence primarily the energy and water balances of a watershed. The main purpose of using hydrological modeling is to provide information for managing water resources in a sustained manner. Some of the hydrologic models used are: SWAT (Soil and Water Assessment Tool), MIKE-SHE, Variable infiltration Capacity (VIC) model [7].

II. DOWNSCALING TECHNIQUES

Downscaling techniques have been designed to bridge the gap between the information that the climate modeling community can currently provide and that required by the impacts research community. There are two broad categories of downscaling procedures: (a) dynamical downscaling techniques, which involves the extraction of regional scale information from large-scale GCM data based on the modeling of regional climate dynamical processes, and (b) statistical downscaling techniques that rely on the empirical relationships between predictors i.e. large-scale atmospheric variables and predictands i.e. surface environment variables [8]. There are many advantages and disadvantages of dynamical downscaling and statistical downscaling techniques for climate change impacts, which indicate that neither technique is better than the other [9]. Based on the assessment of the climate change impacts on the hydrologic regimes of a number of selected basins, it was found that these two techniques could reproduce some general features of the basin climatology, but both displayed systematic biases with respect to observations as well. Further, it was found that the assessment results were dependent on the specific climatology of the basin under consideration. Hence, it is necessary to test different, but physically plausible, downscaling methods to find the most suitable approach for a particular region of interest. A schematic diagram has been shown for illustrating the downscaling approach as shown in Fig 1. Several statistical downscaling techniques have been developed to establish relationships between variables and the large-scale GCMs outputs. Among these techniques, the statistical downscaling method based on the Statistical Downscaling Model (SDSM) and the stochastic weather generators LARS-WG are widely used.

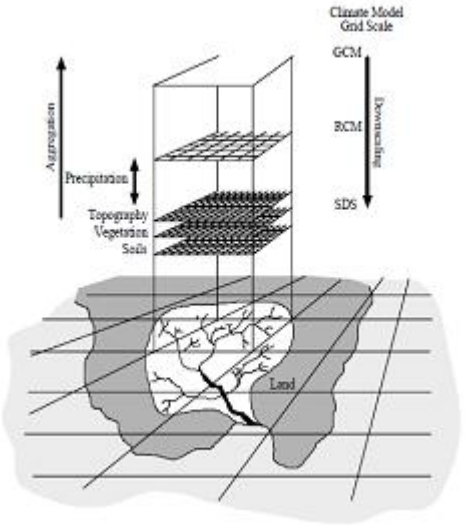

Fig 1: A schematic illustrating the general approach to downscaling [10]

III. CLIMATE CHANGE IMPACTS ON INDIAN WATER RESOURCES

Changes in temperature, precipitation and other climatic variables are likely to influence the amount and distribution of runoff into Indian River systems. The impact of future climatic change is expected to be more severe in developing countries such as India whose economy is largely dependent on the agriculture and is already under stress due to population increase and associated demands for energy, fresh water and food.

The river systems of central, western and southern India are charged by groundwater and their flows are reinforced by the seasonal rainfall. The water potentials of these non- snow and glacier fed rivers are strongly associated with the conditions of monsoons. A poor monsoon rainfall leads to drought conditions and situation is further motivated if monsoon fails for consecutive years and back-to-back drought occurs. Studies carried out on 12 river basins of India using SWAT model indicated that as a result of global warming, the conditions may deteriorate in terms of severity of droughts in some parts of the country and enhanced intensity of floods in other parts [11]. A general overall reduction in the quantity of the available runoff is expected under the GHG scenario.

The water resources of the country are likely to be affected due to climate change. The adaptation strategies have to be considered in the water resources sector in view of these changes. Studies are required to be taken up for developing the modified methodologies for the assessment of water resources, hydrological design practices, flood and drought management, operation policies for the existing as

well as proposed water resources projects and assessment of available water for irrigation including the land uses and cropping patterns.

IV. CLIMATE CHANGE IMPACT ON WATER RESOURCES

Some of the issues concerned with the impacts of climate change on water resources are:

1. Determining extent of current climatic/hydro meteorological variability and future projections due to climate change.
2. Reliable downscaling of GCMs (Global Circulation Models) projections to regional and basin level.
3. Improvement required in hydro-meteorological network design for adaptation.
4. Assessment of impact on surface and ground water interaction.
5. Impact of Climate Change on LandUse/LandCover.

V. CHALLENGES FOR FUTURE

Modeling seems to be the only remedy to address complex environmental and water resources problems. Models will continue to find increasing use in the planning and management of water resources. As the demand placed on hydrologic models for environmental decision making has increased, particularly for problems involving prediction of future hydrologic conditions resulting from changes in land use or climate, the use of distributed models in environmental analysis is becoming more common in recent studies.

For evaluating the effect of climate change at smaller scale and finer resolution, an integrated modeling system that links climate model (GCM/RCM) with hydrological model through statistical downscaling is needed [12]. Previous studies have shown that the existing regionalization methods need to be improved, uncertainty induced from transferring the regionalization scheme based on the sub-catchment scale to basin scale, from basin unit to rectangular grid unit of the similar size, and from one geographic/climatic region to the other need to be evaluated and quantified. The importance to quantify this uncertainty for allowing the use of the predictions and for assessing the value of different model approaches and additional data to reduce the degree of uncertainty is to be emphasized.

VI. CONCLUSION

General Circulation Models (GCMs) are among the best available tools to represent reasonably well the main features of the global distribution of basic climate parameters. Outputs from GCMs are usually at resolution that is too coarse Downscaling of GCM projections of climate variables are therefore necessary. Outputs from climate model integrations are used to drive hydrological models and estimate climate change impacts. The main aim of this paper is to highlight the existing methods for assessing the hydrological impact of climate change at different spatial and temporal scales and discusses the future challenges in this field.

REFERENCES

[1] Xu CY, Widen E, Halldin S, "Modelling hydrological consequences of climate change—progress and challenges", *Adv Atmospheric Sci* 22(6), 2005:789–797.

[2] Xu, C.-Y., and V. P. Singh, "Review on regional water resources assessment under stationary and changing climate", *Water Resources Management, 18(6),* 2004, 591–612.

[3] Solomon, S., D. Qin, M. Manning, Z. Chen, M. Marquis, K.B. Averyt, M. Tignor and H.L. Miller, "Climate Change: The Physical Science Basis", *Cambridge University Press*, 2007, 996.

[4] Anandhi, A., Srinivas, V. V., Nanjundiah, R. S, Kumar, D. N. "Downscaling precipitation to river basin in India for IPCC SRES scenarios using Support Vector Machine", *Int.J Climatol.*, 28, 2008, 401 – 420. doi:10.1002/joc.1529.

[5] Maraun, D., Wetterhall, F., Ireson, A. M. and Chandler, R. E., "Precipitation downscaling under climate change: Recent developments to bridge the gap between dynamical models and the end user", *Rev. Geophys.*, 48, 2010, doi: 10.1029/2009 RG000314.

[6] Arora, V.K. "Streamflow simulations for continental-scale river basins in a global atmospheric general circulation model" *Advances in Water Resources 24*, 2001, 775–791.

[7] Dadhwal, V. K., Aggarwal, S. P. and Misra, N., "Hydrological simulation of Mahanadi River basin and impact of landuse/ landcover change on surface runoff using a macro scale hydrological model", *Proceeding of International Society for Photogrammetry and Remote Sensing (ISPRS) TC VII Symposium*, 38, 2010, 165–170.

[8] Ghosh S, and Misra C**., "**Assessing Hydrological Impacts of Climate Change: Modeling Techniques and Challenges", *The Open Hydrology Journal, 4*, 2010, 115-121.

[9] Wilby, R. L., L. E. Hay, W. J. Gutowski, R. W. Arritt, E. S. Takle, Z. Pan, G. H. Leavesley, and M. P. Clark, "Hydrological responses to dynamically and statistically downscaled climate model output", *Geophys. Res. Lett., 27*, 2000, 1199–1202.

[10] Wilby RL, Dawson CW, "Using SDSM version 4.2—a decision support tool for the assessment of regional climate change impacts. SDSM User Manual, Climate Change Unit", Environment Agency of England and Wales, 2007, 67.

[11] Gosain AK, Rao S, Basuray D., "Climate change impact assessment on hydrology of Indian river basins", *Curr Sci., 90 (3)*, 2006, 346-53.

[12] Fowler, H. J., Blenkinsop, S., Tebaldi, C., "Linking climate change modelling to impact studies: Recent advances in downscaling techniques for hydrological modelling", *Int. J. Climatol.*, 27, 2007, 1547–1578.

International Journal of Engineering Research and Applications (IJERA) ISSN: 2248-9622
National Conference on Advances in Engineering and Technology
(AET- 29th March 2014)

RESEARCH ARTICLE OPEN ACCESS

STUDY OF PROPERTIES OF LIGHT WEIGHT FLY ASH BRICK

Ravi Kumar[1], Vandana Patyal[2], Balwinder Lallotra[3] and Deepankar Kumar Ashish[4]

[1]Department of Civil Engineering, Maharishi Markandeshwar University, Sadopur (Ambala),
Email: ranaraviambala@gmail.com

[2]Department of Civil Engineering, Maharishi Markandeshwar University, Sadopur (Ambala),
Email: vandanapatyal2009@gmail.com

[3]Department of Civil Engineering Maharishi Markandeshwar University, Sadopur (Ambala),
Email: balwinder.com@gmail.com

[4]Department of Civil Engineering, Swami Devi Dayal Institute of Engineering & Technology, Barwala,
Email: deepankar1303@gmail.com

ABSTRACT
In this paper, efforts has been made to study the behavior of fly ash bricks by taking different proportions of fly ash, cement, lime, gypsum and sand. Three types of fly ash bricks in the different percentage of cement such as 3%, 5% and without cement are designed and then various tests such as compressive strength test, water absorption test, efflorescence, weight test, structural test were performed in order to have comparison with conventional bricks. In the experimental study it is found that the compressive strength of fly ash brick containing 5% cement is 152.1 kg/cm2 which is more than that of class I conventional bricks by 40% approximately. Effort has been made by making different proportions of ingredients having composition of fly ash, cement, lime, gypsum, and sand.

Keywords: Cement, Fly ash, Fly ash brick, Fine aggregate.

I. INTRODUCTION

Fly Ash bricks are made of fly ash, lime, gypsum cement and sand. These can be extensively used in all building constructional activities similar to that of common burnt clay bricks. The fly ash bricks are comparatively lighter in weight and stronger than common clay bricks. Since fly ash is being accumulated as waste material in large quantity near thermal power plants and creating serious environmental pollution problems, its utilization as main raw material in the manufacture of bricks will not only create ample opportunities for its proper and useful disposal but also help in environmental pollution control to a greater extent in the surrounding areas of power plants.

Manufacturing of commercial brick produce a lot of air pollution. The technology adopted for making. The fly ash bricks are eco-friendly. It is no need fire operation in production unlike the conventional bricks Among the traditional fossil fuel sources, coal exists in quantities capable of supplying a large portion of nation's energy need. That's why the power sector in India is a major consumer of coal in India and will continue to remain so far many years to come. Combustion of coal in thermal power plant not only produces steam to run electricity-generating turbine but also produces a large quantity of by-products like fly ash etc.

About 80 thermal power plants in India are sources of fly ash, where around millions of tonnes of coal are used annually. India currently generates 100 million tones of fly ash every year. This produces 30-40 million tonnes of fly ash unused every year. This disposal will need thousands hectares of storage land, which may cause further ecological imbalance. In fact, this waste material is simply disposed off in the form aqueous slurry on the adjoining areas. This type of disposal not only converts useful agricultural land to waste ones but also possesses a threat to the quality of environment. The human development of united nation development programme indicates that annually 83-163 million hectares of land is eroded in India causing productivity loss of about 4 to 6.3% of the total agricultural output worth $2.4 billion. Therefore, using fly ash as a building material has assumed great significance like never before. Several investigations have been carried out throughout the world to make an attempt to use fly ash in many civil engineering projects by virtue of its good properties as an ingredient of concrete. The Comparison between Clay brick and Fly ash Brick is shown in Table 1.

Table 1: Comparison between Clay brick and Fly ash Brick

Clay Brick	**Fly Ash Brick**
Varying colour as per soil	Uniform pleasing colour like cement
Uneven shape as hand made	Uniform in shape and smooth in finish
Lightly bonded	Dense composition
Plastering required	No plastering required
Heavier in weight	Lighter in weight
Compressive strength is around 35 Kg/Cm^2	Compressive strength is around 100 Kg/Cm^2
More porous	Less porous
Thermal conductivity 1.25 – 1.35 W/m2ºC	Thermal conductivity 0.90-1.05 W/m2ºC
Water absorption 20-25%	Water absorption 6-12%

II. MARKET DEMAND

The country consumes about 180 billion tones bricks, exhausting approximately 340 billion tones of clay every year and about 5000 acres of top soil land is made unfertile for a long period. The Government is seriously concerned over soil erosion for production of massive quantities of bricks, in the background of enormous housing needs. The excellent engineering property and durability of fly ash brick enlarges its scope for application in building construction and development of infrastructure, construction of pavements, dams, tanks, under water works, canal lining and irrigation work etc. Enormous quantities of fly ash are available in and around thermal power stations in all the states. The demand of bricks could be met by establishing small units near thermal power stations and to meet the local demand with less transportation costs.

III. EXPERIMENTAL INVESTIGATION

In the present study we are making investigation on different percentage of cement such as without cement, 3%, and 5% in the fly ash bricks. And after making these bricks various tests were performed such as compressive strength test, water absorption test, efflorescence, and these results were compared with conventional bricks results.

IV. MATERIALS USED

Materials used are cement, fly ash, gypsum, sand and lime.

4.1 Cement

Ordinary Portland cement of grade 43 was used for making the brick mortar. The quality of cement was checked through various tests and was compared with specifications given IS 269-1976 for OPC. The properties of cement used are given in Table 2.

Table 2: Physical properties of Ordinary Portland Cement Used

Sr. No	Characteristics	Value obtained Experimentally	Value specified in IS :8112-1989
1	Specific Gravity	3.16	3.15
2	Fineness by sieve through IS 90 micron standard sieve	300	225
3	Setting Times (minutes) i. Initial ii. Final	 81 480	 >30 <600
4	Compressive strength(N/mm2) I. At 3 day (Average 6 samples) II. At 7 day (Average 6 samples) III. At 28 day (Average 6 sample	 28.8 38.87 47.94	 >23 >33 >43

4.2 Fine Aggregate

Locally available river sand was used. The sand was cleaned from all inorganic impurities and passed through 2.36 mm size sieve and retained on 150 micron sieve have been used. Particle size and other properties are listed in Table 3.

Table 3: Sieve Analysis of fine Aggregate

Size of Sieve	Weight Retained in IS Sieve (gm)	Cumulative Weight Retained in IS Sieve	Percentage Retained	Percentage passing	Grading Limit according to IS :383-1970
10 mm	0	0	0	100	Zone III
4.75 mm	0	0	0	100	
2.36 mm	11	6	2.1	97.9	
1.18 mm	34	30	4.5	95.5	
600 micron	165	195	21	79	
300 micron	622	832	83.2	16.8	
150 micron	98	930	93	7	

Fineness Modules=496.2/100=4.96
Weight of sample taken=1 KG

V. EXPERIMENTAL PROGRAME

In the present study, fly ash brick is developed with different composition.

- Fly ash (55), Lime (20%), sand (20%), gypsum (5%), Cement (0%)
- Fly ash (52), Lime (20%), sand (20%), gypsum (5%), Cement (3%)
- Fly ash (50) Lime (20%), sand (20%), gypsum (5%), Cement (5%)

The fly ash bricks were tested as per IS 12894-1990 that is coed for fly ash-lime bricks and the conventional bricks were tested as per procedure laid down in IS 3495-1973 for the following test:

- Compressive Strength
- Water absorption
- Efflorescence

1. Compressive Strength test

The red and fly ash bricks were tested on the compressive testing machine of capacity 100 tones which read to the nearest 0.5 tonne. The load was applied steadily and uniformly. 6 bricks of each type were tested for compressive strength. The average compressive strength was calculated.

2. Water absorption test

The red and fly ash bricks were dried and weighted. These were then immersed in water for 24 hours and then weighted again. The bricks were tested in accordance with procedure laid down in IS 3495 (Part-II) 1976 (36).

3. Efflorescence test

Red and fly ash bricks 5 number each were selected at random out of the samples of red and fly ash bricks. Then each bricks was placed on edge in dish containing distilled water, the depth of immersion of the brick was not less than 2.5 cm. The whole arrangement was placed to in a ventilated room at 20 to 30 C until whole of water in the dish evaporated .when the water has been absorbed and bricks appeared to be dried, a similar quantity of distilled water was put in the dish and same was allowed to evaporate as before. At the end of this period, the brick was examined for efflorescence.

VI. EXPERIMENTAL RESULT & DISCUSSION

6.1 Compressive Strength Test

As per the Table 4 & Fig 1 the compressive strength of conventional brick is found to be 92.85 kg/cm^2, for fly ash brick without cement is found to be 125.9 kg/cm^2, fly ash brick with 3% cement is found to be 141 kg/cm^2 and fly ash brick with 5% cement is found to be 152 kg/cm^2.

Table 4: Compressive strength

Type of specimen	Mean load at failure	Average compressive Strength (kg/cm^2)	% Increase Average compressive strength
Conventional brick	208.3	92.85	-
Fly ash brick (0%)	281.8	125.9	35%
Fly ash brick (3%)	314.7	141	51.8%
Fly ash brick (5%)	342.2	152.1	63.3%

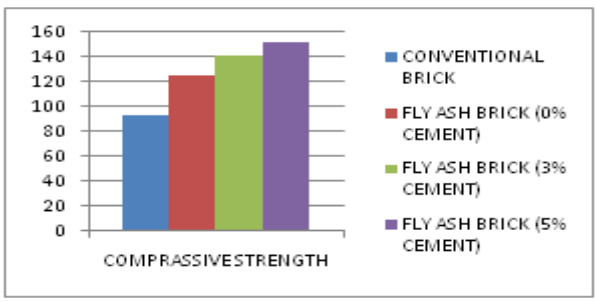

Fig 1: Compressive Strength graph

6.2 Water absorption test

As per the Table 5 & Fig 2 the average absorbed moister content of conventional brick is found to be 10.45% , for fly ash brick without cement is found to be 7.63%, fly ash brick with 3% cement is found to be 6.06% and fly ash brick with 5% cement is found to be 5.41%.

Table 5: Water Absorption Test

Type of specimen	Mean Dry Weight (Kg)	Mean Moist Weight (Kg)	Average Water Absorption %	% Decrease in Water Absorption
Conventional brick	3.12	3.45	10.45	-
Fly ash brick (0%)	2.57	2.77	7.63	27%
Fly ash brick (3%)	2.66	2.85	6.06	42%
Fly ash brick (5%)	2.83	2.99	5.41	48%

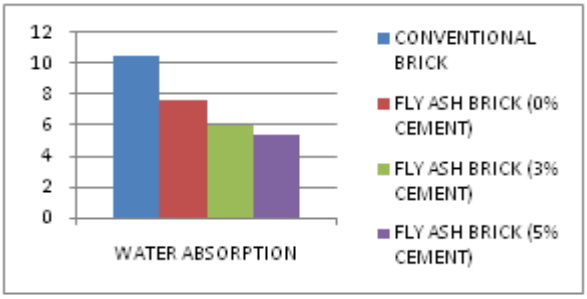

Fig 2: Water Absorption test graph in percentage

6.3 Efflorescence test

Table 6 shows the details of efflorescence test. The Efflorescence test of conventional brick, fly ash brick without cement, fly ash brick with 3% cement & fly ash brick with 5% cement and the result were compared in which grey or white deposits are slight to moderate in conventional brick, less than 10% on surface area in fly ash brick without cement, less than 8% on surface area in fly ash brick with 3% cement and less than 7% on surface area in fly ash brick with 5% cement.

Table 6: Efflorescence test

Conventional brick	Slight to moderate
Fly ash brick (0%)	The grey deposit are less than 10%
Fly ash brick (3%)	The grey deposit are less than 8%
Fly ash brick (5%)	The grey deposit are less than 7%

VII. CONCLUSION & FUTURE WORK

On the basis of the experimental work it is concluded that the compressive strength of fly ash brick with 0% cement is 27% more than that of class I conventional brick but when 3% cement is added in the fly ash brick then compressive strength is 51.8% more than that of class I conventional brick and also when 5% cement added in fly ash brick then the compressive strength is more than 63%. It is also analyzed that water absorption of fly ash brick with 0% cement is 27% less as compared to that of conventional bricks and 42% less as compared to conventional brick when 3% cement is added and 48% less as compared to conventional brick when 5% cement is added. The Efflorescence test of conventional brick, fly ash brick without cement, fly ash brick with 3% cement & fly ash brick with 5% cement and the result were compared in which grey or white deposits are slight to moderate in conventional brick, less than 10% on surface area in fly ash brick without cement, less than 8% on surface area in fly ash brick with 3% cement and less than 7% on surface area in fly ash brick with 5% cement. Fly-Ash bricks are eco friendly as it protects environment though conservation of top soil and utilization of waste products of coal or lignite used in thermal power plants. It is three times stronger than the conventional burnt clay bricks. It plays a vital role in the abatement of carbon dioxide a harmful green house gas mass emission of which is threatening to throw the earth's atmosphere out of balance. Being lighter in weight as compared to conventional bricks, dead load on the structure is reduced and hence saving is overall cost of construction.

The possibility of using innovative building materials and eco-friendly technologies, more so covering waste material like fly ash is the need of the hour. Fly ash affects the plastic properties of concrete by improving workability, reducing water demand, reducing segregation and bleeding, and lowering heat of hydration. It also increases strength, reduces permeability, reduces corrosion of reinforcing steel, increases sulphate, resistance, and reduces alkali-aggregate reaction.

REFERENCES

[1] Gupta P.C, Ray S. C. ," Commercialization of Fly ash", *The Indian Concrete Journal*, 167, 1993, 554-560.

[2] Sengupta J. , "Availability of Fly ash and its Application in Construction Industry", *NBO Journal, XXXIX*, 1984, 17-22.

[3] Thorne , D.L. , Watt , J.D. , "Composition and Properties of pulverized fuel ashes",

Part II, *Journal of Applied Chemistry, London,*15 ,1965, 595-604.

[4] Arya D. S., "Steel and Masonry Structure", ISBN 086186168X.

[5] Butterworth B., "Bricks made with pulverized Fuel Ash.", *Trans. Brit. Ceram.Soc*' ENGLAND, 53 (5), 1954, 293-313.

[6] Gupta, R.L. , Bhagwan, Gautam, D.K., Garg, S.P., "A Press for Sand Lime Bricks Research and Industry", 22(40), 1977, 246-249.

[7] Parul, R. Patel, "Use of Fly ash in Brick Manufacturing", *National Conference On Advances in Construction Materials*, " *AICM*-India, 2004, 53-56.

[8] Peter George Kenneth Kingth, "Pulverized fuel ash as a construction material", *proceedings of institution of Civil Engineers*, 16, 1960, 419-432.

[9] Rai, Mohan, Gupta, R. L., "Energy Conservation in the Manufacture of sand Lime Bricks", Proc. of National Seminar on Energy Conservation in Process Industries, *Institution of Engineers India*, 1985.

[10] I.S Code 12894-1990 for Fly ash – Lime Bricks- Specification.

[11] I.S Code: 8112-1989, Ordinary Portland Cement, 43 Grade- Specification

[12] IS: 3495(P-I)-1976, Determination of Compressive Strength (Second Revision).

[13] IS: 3495 (P-II) -1976, Determination of Water Absorption (Second Revision).

[14] IS: 3495 (P-II)-1976, Determination of Effloresce (Second Revision).

[15] S.C Rangwala, "Engineering Material", *Charotar Publications*, 15th Edition, 1991, 72-112.

[16] Bhanumathidas, N., "Fly ash in precast products- The Indian Scenario*"*, 1999, 31-35.